

STUDY OF BIOMEDICAL SIGNAL MEASUREMENT & ANALYSIS TECHNIQUES

**A THESIS
SUBMITTED TO THE DELHI TECHNOLOGICAL UNIVERSITY
FOR THE AWARD OF THE DEGREE OF
DOCTOR OF PHILOSOPHY
IN
ELECTRONICS & COMMUNICATION ENGINEERING**

SUBMITTED BY

**RAJESH BIROK
(Roll No: 2K12/PhD/EC/01)**



Under the Supervision
of
Prof. RAJIV KAPOOR

**DEPARTMENT OF ELECTRONICS & COMMUNICATION ENGINEERING
DELHI TECHNOLOGICAL UNIVERSITY
(Formerly Delhi College of Engineering)
DELHI- 110042 (INDIA)
MAY-2022**



©DELHI TECHNOLOGICAL UNIVERSITY-2022
ALL RIGHTS RESERVED

CERTIFICATE

This is to certify that the thesis entitled “*Study of Biomedical Signal Measurement & Analysis Techniques*” submitted by **Mr. RAJESH BIROK (Roll No: 2K12/PhD/EC/01)** for the award of degree of Doctor of Philosophy to the Delhi Technological University is based on the original work carried out by him. He has worked under my supervision and has fulfilled the requirements, which to my knowledge & belief have reached the requisite standard for the submission of this thesis. It is further certified that the work embodied in this thesis has neither partially nor fully submitted to any other university or institution for the award of any degree or diploma.

Prof. Rajiv Kapoor
(Supervisor)
Department of Electronics & Communication Engineering
Delhi Technological University, Delhi.

ACKNOWLEDGMENT

I'm highly indebted and would like to express a great feeling of gratitude towards several persons who guided and supported me throughout the completion of my research program.

First and foremost, I would like to thank my supervisor **Prof. RAJIV KAPOOR**, for his constant support and reposing faith in me during the course of my Ph.D. Studies. My research work couldn't be turned into a prodigious experience without his substantial and thorough approach, together with his unpretentious interest in the research subject.

Above all, my deepest thanks go to my parents, brother & sister for their absolute affection and support. Also, my wholehearted recognition to my wife **Mrs SUMAN LATA**, my son **Mr. VIPRANJAL** and my daughter **Ms VARNIKA** for their inspiration & patience as they had to bear the loss of my time and efforts at home. Moreover, I would like to record their contribution towards the competition of proposed research work and preparation of this thesis.

Finally, I would also like to express my sincere thanks to all those who supported me directly and indirectly along with my colleagues, friends and of course my teachers and HoD (especially **Prof. RAJESH ROHILA, Prof. M. S. CHOUDHRY, Prof. N. S. RAGHAVA, Prof. DINESH KUMAR, Prof. NEETA PANDEY, Prof. D. K. VISHWAKARMA, Prof. MUKHTIAR SINGH, Prof. RAJESHWARI PANDEY, Prof. S. INDU, Prof. O. P. VERMA, Prof. J. PANDA, Prof. MANOJ KUMAR, Prof. VINOD KUMAR, Prof. A. K. SINGH, Prof. KAPIL SHARMA, Dr. DEVANAND & Dr. R. K. YADAV**) for their continuous encouragement and advices, which they provided me during this research journey.

Last but not the least, thanks are also due to **Mr. RAHUL** and **Mr. NIKHIL** PhD scholars in ECE department of DTU for their support and kind help as and when required.

RAJESH BIROK
(Roll No: 2K12/PhD/EC/01)

ABSTRACT

Biomedical signal is a summarizing term for all kinds of signals that can be continually measured and monitored from living creatures including human beings. Electrocardiogram (ECG), perhaps is the most common and popular 1-D biomedical signals as it is directly associated with one of the most important organs of human body that is activities of the heart. ECG has a wide range of applications in cardiac diagnostics and is preferred over other methods as it is largely non-invasive, safe to the patient, easy to obtain, provides instantaneous results with highest level of accuracy.

The appropriate analysis of the ECG signals using suitable means is of utmost importance, before any diagnostics. Therefore, to fulfill this requirement the higher order cumulants are an effective mathematical tool for the analysis of nonlinear and non-stationary ECG signals. The proposed method in this thesis, classifies dataset of ECG signals based upon higher order statistics i.e., using cumulants. It provides a quality detection technique in comparison to the other methods used earlier in this research domain.

However, ECG very easily gets contaminated by various types of noises and artefacts during the process of its acquisition. Therefore, this contaminated ECG must be “cleaned” to the appropriate level, it means to minimize the counter-productive effects of embedded noise and artefacts so as to enhance the required information, before using it for any further processing for diagnosis or interpretation. There are different types of noises or artefacts present in any ECG signal, but baseline wander is considered as severest one. This research work is mainly focused on proposing novel methods for removal of baseline wander and other types of noises from ECG signal.

Accordingly, a new method is proposed for baseline wander artefact denoising from ECG using cascaded combination of Complete Ensemble Empirical Mode Decomposition (CEEMD) and Artificial Neural Networks [ANN]. The proposed method maintains morphology of ECG signal during denoising and thus there is no loss of vital information from the ECG signal. The denoising of ECG signal is further enhanced by another novel approach making use of Genetic Particle filter improved fuzzy-AEEMD, which has been proposed in this thesis. The performance of proposed methods is tested with different types of readily available ECG datasets and compared with other state-of-the-art methods and these proposed methods proved to be more effective and efficient denoising methods.

Biomedical signal measurement is one of the most important aspects of biomedical signal analysis and interpretation to support scientific hypotheses and medical diagnoses. Biomedical signal measurement aims at appropriately acquiring and measuring biomedical signals for accurate and improved diagnosis and proper medicine management. Extensive research is going on in the field of Bio-Medical Measurements and Instrumentation to find out new non-invasive ways and methods for diagnosis and measurement of health parameters for the welfare of the mankind. Non-invasive techniques are more suitable than the invasive ones if sufficient accuracy can be achieved using them. Among the available non-invasive medical devices and techniques, perhaps bioimpedance based diagnostics is still highly unexplored and underrated owing to insufficient research efforts.

Keeping above scenario in mind accordingly, an efficient low-cost bioelectrical impedance measuring instrument was developed, implemented, and tested in this study. Primarily, it is based upon the low-cost component-level approach so that it can be easily used by researchers and investigators in the specific domain. The measurement setup of instrument was tested on adult human subjects to obtain the impedance signal of the forearm which is under investigation in this case. However, depending on the illness or activity under examination, the instrument can be used on any other part of the body. The technique is easy and user-friendly, and it does not necessitate any special training, therefore it can be effectively used to collect bioimpedance data and interpret the findings for medical diagnostics.

LIST OF PUBLICATIONS

JOURNALS

- 1] Rajiv Kapoor & **Rajesh Birok** “Genetic particle filter improved fuzzy-AEEMD For ECG signal denoising.” Computer Methods in Biomechanics and Biomedical Engineering, ISSN: 14768259, 10255842 DOI: 10.1080/10255842.2021.1892659 [SJR-0.354]. [Published in SCIE]
- 2] **Rajesh Birok** & Rajiv Kapoor “Design of Low Cost Bioimpedance Measuring Instrument” International Journal of Advanced Computer Science and Applications, ISSN: 21565570, 2158107X in Volume 13, No. 1 (2022). [SJR-0.193] [Published in ESCI]
- 3] **Rajesh Birok** & Rajiv Kapoor “ECG Signal Analysis Using Higher-order Cumulants” [Communicated in SCIE/ESCI Journal]
- 4] **Rajesh Birok**, Rajiv Kapoor & Mahipal Singh Choudhry “ECG Denoising Using Artificial Neural Networks and Complete Ensemble Empirical Mode Decomposition” Turkish Journal of Computer and Mathematics Education [TURCOMAT], ISSN: 2382 - 2389 in Volume 12, No. 2 (2021). [SJR - 0.218] [Published in SCOPUS INDEXED JOURNAL]

PATENT AWARDED

BIOELECTRICAL IMPEDANCE METER DESIGN to 1. RAJIV KAPOOR 2. ABHISHEK GROVER 3. **RAJESH BIROK** 4. PADMA BATRA et al Vide Patent No.: 354875 [SL No: 011129756]; Application No.: 2169/DEL/2015

INTERNATIONAL CONFERENCES

- 1] Satyam Mishra & **Rajesh Birok** “Sleep Classification using CNN and RNN on raw EEG Single-Channel” 2020 International Conference on Computational Performance Evaluation (ComPE) North-Eastern Hill University, Shillong, Meghalaya, India. Jul 2-4, 2020
- 2] Shubham Kaushik & **Rajesh Birok** “Heart Failure Prediction using Voting Ensemble Classifier” August 2021 Asian Conference on Innovation in Technology (ASIANCON) Pune, India.
- 3] Shubham Kaushik & **Rajesh Birok** “Heart Failure prediction using Xgboost algorithm and feature selection using feature permutation” September 2021 Fourth IEEE International Conference on Electrical, Computer and Communication Technologies (ICECCT 2021)

TABLE OF CONTENTS	
DESCRIPTION	PAGE NO.
CERTIFICATE	iii
ACKNOWLEDGMENT	iv
ABSTRACT	v
LIST OF PUBLICATIONS	vii
TABLE OF CONTENTS	viii
LIST OF FIGURES	xi
LIST OF TABLES	xiii
Bio-Medical Signal Analysis Techniques [PART-I]	
CHAPTER 1 INTRODUCTION TO BIOMEDICAL SIGNALS WITH SPECIAL REFERENCE TO ECG & BIOIMPEDANCE	1-23
1.1 Introduction to Human Body	1
1.2 Types of Biomedical Signals	3
1.3 Behavior of Biomedical Signals	4
1.4 Objectives of Biomedical Signal Analysis	4
1.5 Origin of Bioelectrical Signals	5
1.5.1 Action Potential	6
1.6 Types of Bioelectrical Signals	9
1.6.1 Electroneurogram (ENG)	10
1.6.2 Electromyogram (EMG)	11
1.6.3 Electroencephalogram (EEG)	13
1.6.4 Electrogastrogram (EGG)	15
1.6.5 Vectorcardiography [VCG]	16
1.6.6 Electrocardiogram (ECG)	17
1.6.7.1 The Heart	17
1.6.7.2 Heart's Electrical Signal Generation System	17
1.6.7.3 ECG Signal Acquisition	21
1.7 Bioimpedance	21
1.7.1 Basics and Origin of Bioimpedance	21
CHAPTER 2 LITERATURE REVIEW	24-39
2.1 ECG Signal Analysis Techniques	24
2.1.1 Higher Order Statistics Analysis	25
2.1.2 Neural Networks	26
2.1.3 Type-2 Fuzzy Logic System	26
2.1.4 Miscellaneous Methods	27
2.2 ECG Denoising Techniques	27
2.2.1 Digital Window-Based Filters	28
2.2.2 Adaptive Filters	29
2.2.3 Wavelets	30
2.2.4 Empirical Mode Decomposition	30
2.2.4.1 Ensemble Empirical Mode Decomposition (EEMD)	30
2.2.5 Miscellaneous Methods	33
2.3. Research Gaps	33
Bio-Medical Signal Measurement [PART-II]	
2.4 Bioimpedance Measurement	

2.4.1 Cole parameters	34
2.4.2 Stepped-Sine Excitations	
2.4.3 Transfer Function Approach	
2.4.4 Voltage Sensing Circuit	
2.4.5 Non-Invasively Tracking Blood Glucose Levels	
2.5 Miscellaneous Methods	36
2.6 Research Gaps	39
2.7 Research Objectives	
CHAPTER 3: ECG SIGNAL ANALYSIS USING HIGHER ORDER CUMULANTS	40-61
3.1 Introduction	40
3.2 Theoretical Background	41
3.2.1 Cumulants	
3.2.2 Classifiers	45
3.2.2.1. Support Vector Machine [SVM]	
3.2.2.2. Fuzzy-2	46
3.2.2.3. Deep Structured Neural Network [DSNN]	47
3.3 Proposed Methodology	48
3.3.1 Block Diagram	49
3.3.2 Dataset Used	
3.3.3 Taking the ECG Datasets	51
3.3.4 Calculating the Cumulants for the ECG Signals	
3.3.5 Classification Using SVM, Fuzzy-2 and DSNN Classifiers	
3.4 Results	61
3.5 Significant Findings	
CHAPTER 4: ECG DENOISING USING ANN AND CEEMD	62-72
4.1 Introduction	62
4.2 Theoretical Background	63
4.2.1 Complete Ensemble Empirical Mode Decomposition [CEEMD]	
4.2.2 Artificial Neural Network [ANN]	64
4.3 Proposed Methodology	65
4.4 Results	67
4.5 Significant Findings	72
CHAPTER 5: GENETIC PARTICLE-FILTER IMPROVED FUZZY-AEEMD FOR ECG SIGNAL DE-NOISING	73-89
5.1 Introduction	73
5.2 Theoretical Background	
5.2.1 Ensemble EMD	74
5.2.2 Adaptive EEMD	76
5.2.3 Fuzzy Thresholding	77
5.2.4 Genetic Particle Filter	
5.3 Proposed Methodology	79
5.4 Results	80
5.5 Significant Findings	88
CHAPTER 6: DESIGN OF LOW COST BIOIMPEDANCE MEASURING INSTRUMENT	90-111
6.1 Introduction	90
6.2 The Human-Instrument System	
6.3 Important Factors for the Design of Biomedical Instruments	91
6.4 General Constraints in the Design of Medical Instrumentation Systems, Biomedical Signal Acquisition and Analysis	
6.5 Basic Medical Instrumentation System	93
6.6 Performance Requirements of Medical Instrumentation Systems	94

6.7 Non-Invasive Biomedical Techniques	95
6.8 Theoretical Background: Bioimpedance	
6.8.1 Frequency Response of Bioimpedance	96
6.8.2 Types of Electrode Configurations	97
6.9 Proposed Methodology	99
6.9.1 Waveform Generation	100
6.9.2 V to I Convertor	101
6.9.3 Instrumentation Amplifier	102
6.9.4 Demodulator	103
6.9.5 Low Pass Filter	106
6.9.6 Assumptions, Measurement Protocol and Data Acquisition	
6.4 Results	108
6.5 Significant Findings	109
CHAPTER 7 CONCLUSIONS & FUTURE SCOPE	112-115
7.1 Conclusions	112
7.2 Future Research Scope	114
REFERENCES	116
AUTHOR's BIOGRAPHY	120

LIST OF FIGURES	
DESCRIPTION	PAGE NO.
Fig.1.1 Different levels of structural organization of human body	1
Fig.1.2 Different levels of structural complexity of human body	2
Fig.1.3 Process for the generation of cell potential waveform and its recorded signal.	6
Fig.1.4 Electrical activity associated with one contraction in a muscle.	8
Fig.1.5 Types and Sources of Bioelectrical Signals	9
Fig.1.6 Acquisition of Electroneurogram (ENG) signal	10
Fig.1.7 Generation and Processing of Electromyogram (EMG) signal	11
Fig.1.8 10-20 System of electrode placement for EEG recording	12
Fig.1.9 EEG signal frequency bands and associated brain activities	13
Fig.1.10 Generation and output signals of Electrogastragram [EGG]	14
Fig.1.11 3D cardiac electrical vector loops in frontal, horizontal, and sagittal planes	15
Fig.1.12 Conventional Vectorcardiography scheme	16
Fig.1.13 Electrocardiogram (ECoG) setup and signal output	17
Fig.1.14 Schematic for cardiac conduction system	18
Fig.1.15 Typical ECG signal waveform	19
Fig.1.16 Wilson's central terminal and Einthoven's triangle for ECG measurement	20
Fig.1.17 ECG signal acquisition process	22
Fig.1.18 Typical normal ECG signal and distorted ECG signals due to various cardiac ailments	23
Fig.1.19 Five component model for human body	46
Fig.1.20 Representation of Total Body Water (TBW) in human body	47
Fig.3.1 Fuzzy-2 flowchart	49
Fig.3.2 Fuzzy-2 membership function	50
Fig.3.3 Block diagram of the proposed method	52
Fig.3.4 ECG Signal Waveforms	54
Fig.3.5 Third order cumulant obtained for dataset used	55
Fig.3.6 Third order cumulant for dataset used in frequency domain (Bi-spectrum)	56
Fig.3.7 Fourth order cumulant obtained for dataset used	57
Fig.3.8 Fourth order cumulant for dataset used in frequency domain (Tri-spectrum)	58
Fig.3.9 Neural Network Scheme for Proposed Method	60
Fig.3.10 Regression plots for ANN	65
Fig.3.11 Regression plot for DSNN	68
Fig.4.1 Flowchart of proposed method	69
Fig.4.2 (a) Noisy signal (Recording-1) (b) Denoised signal using EMD and Neural Network (c) Denoised signal using EEMD and Neural network (d) Denoised signal using CEEMD and Neural network	70
Fig.4.3 (a) Noisy signal (Recording-2) (b) Denoised signal using EMD and Neural Network (c) Denoised signal using EEMD and Neural Network (d) Denoised signal using CEEMD and Neural Network	71
Fig.4.4 (a) Noisy signal (Recording-3) (b) Denoised signal using EMD and Neural network (c) Denoised signal using EEMD and Neural Network (d) Denoised signal using CEEMD and Neural Network	75
Fig.4.5 (a) Noisy signal (Recording-1) (b) Denoised signal using EMD and Morphological Operator (c) Denoised signal using Neural Network (d) Denoised signal using CEEMD and Neural Network	76
Fig.5.1 Flow chart of EEMD method	75
Fig.5.2 Noisy ECG signal	76

Fig.5.3 Block diagram of the proposed GA-PF method	77
Fig.5.4 Membership function for Fuzzy-2	78
Fig.5.5 Block diagram of the proposed ECG de-noising method	80
Fig.5.6 IMFs components obtained by AEEMD method	81
Fig.5.7 Noisy ECG signal and residual signal	82
Fig.5.8 Performance of Genetic Algorithm (o: each individual)	
Fig.5.9 Best solution by Genetic Algorithm (: o) and RS (: *) in each generation	83
Fig.5.10 Best solution by Genetic Algorithm (: o) and RS (: *) for overall	
Fig.5.11 De-noised ECG signal	84
Fig.5.12 SNR vs different database with different method and proposed method	85
Fig.5.13 RMSE vs different database with different method and proposed method	86
Fig.5.14 Original signal and added random noise	87
Fig.5.15 Original signal multiplied by std (0.3), AEEMD with SNR 10	
Fig.5.16 The effect of using constant amplitude 0.3 std and the AEEMD process	
Fig.5.17 DSO output acquired through proposed algorithm (AEEMD)	88
<hr/>	
Fig.6.1 Generalized Medical Instrumentation System	93
Fig.6.2 Bioimpedance measurement using: (a) two-electrode method, (b) four-electrode method.	98
Fig.6.3 General block diagram of Measuring Instrument	99
Fig.6.4 Schematic diagram of ICL8038	100
Fig.6.5 Circuit diagram for Voltage to Current converter	101
Fig.6.6 Variation of current through {R} with respect to change in value of load resistance, y-axis is the current through the load and x-axis is the impedance of the load connected to the V to I converter.	102
Fig.6.7 Circuit Diagram for Instrumentation Amplifier	102
Fig.6.8 Frequency response analysis of the Instrumentation Amplifier	103
Fig.6.9 Circuit Diagram of simple envelope detector	104
Fig.6.10 Precision Detector	
Fig.6.11 Precision Envelope Detector	105
Fig.6.12 Final version of designed Bioimpedance Measuring Instrument	106
Fig.6.13 The human body's impedance when modelled as a homogeneous cylindrical volume conductor	107
Fig.6.14 General test setup for BIA	
Fig.6.15 Output voltage signals measured using the instrument. (a) is the output signal of volunteer set-A (b) being the output signal of volunteer set-B and (c) is the output signal of volunteer set-C. The y-axis in each figure is the output voltage amplitude value and the x-axis represents number of samples.	109

LIST OF TABLES		
DESCRIPTION		PAGE NO.
Table 1.1: Most common bioelectric signals with their primary characteristics		8
Table 1.2: EEG frequency bands		12
Table 3.1: Used dataset description		50
Table 3.2: Description of dataset used for classification		51
Table 3.3: SVM Confusion Matrix		57
Table 3.4: ANN Confusion Matrix		59
Table 3.5: FUZZY-2 Confusion Matrix		
Table 3.6: DSNN Confusion Matrix		
Table 3.7: Comparison of four classifiers		60
Table 3.8: Comparison of proposed method of ECG classification with other methods used		61
Table 4.1: Recording-1	<i>Input SNR & Input MSE calculated for methods (a) EMD and ANN (b) EEMD and ANN, and (c) CEEMD and ANN</i>	68
Table 4.1: Recording-2		69
Table 4.1: Recording-3		70
Table 4.1: Recording-1 (<i>Input SNR & Input MSE calculated for methods (a) EMD and Morphological Operator (b) ANN, and (c) CEEMD and ANN</i>)		71
Table 5.1: SNR values comparison of proposed approach with other known techniques		84
Table 5.2: Comparison of RMSE values for different database of existing methods with proposed method		85
TABLE 6.1: BASAL IMPEDANCE (FOREARM)		108
PATENT AWARDED		111

CHAPTER 1

INTRODUCTION TO BIOMEDICAL SIGNALS WITH SPECIAL REFERENCE TO ECG & BIOIMPEDANCE

1.1 INTRODUCTION TO HUMAN BODY

All living creatures whether they are animals or plants are always made up of three-dimensional arrangement of cells and tissues. The human body is likewise a complicated biological structure and system, as it is made up of billions of cells and tissues organized in three dimensions. The human body functions like a highly complicated and sophisticated system. It functions as a single entity, yet it is made up of a number of interconnected operating subparts. Each portion is linked to a specific, and sometimes related function that is critical to the individual's well-being. The individual components do not work in isolation, but rather in tandem with one another. The ability of an individual to survive is dependent on the integrated functioning of their physical parts. As a result, both the structure and function of the human body are complicated. As demonstrated in fig. 1.1 below the different levels of structural organisation in the human body are:

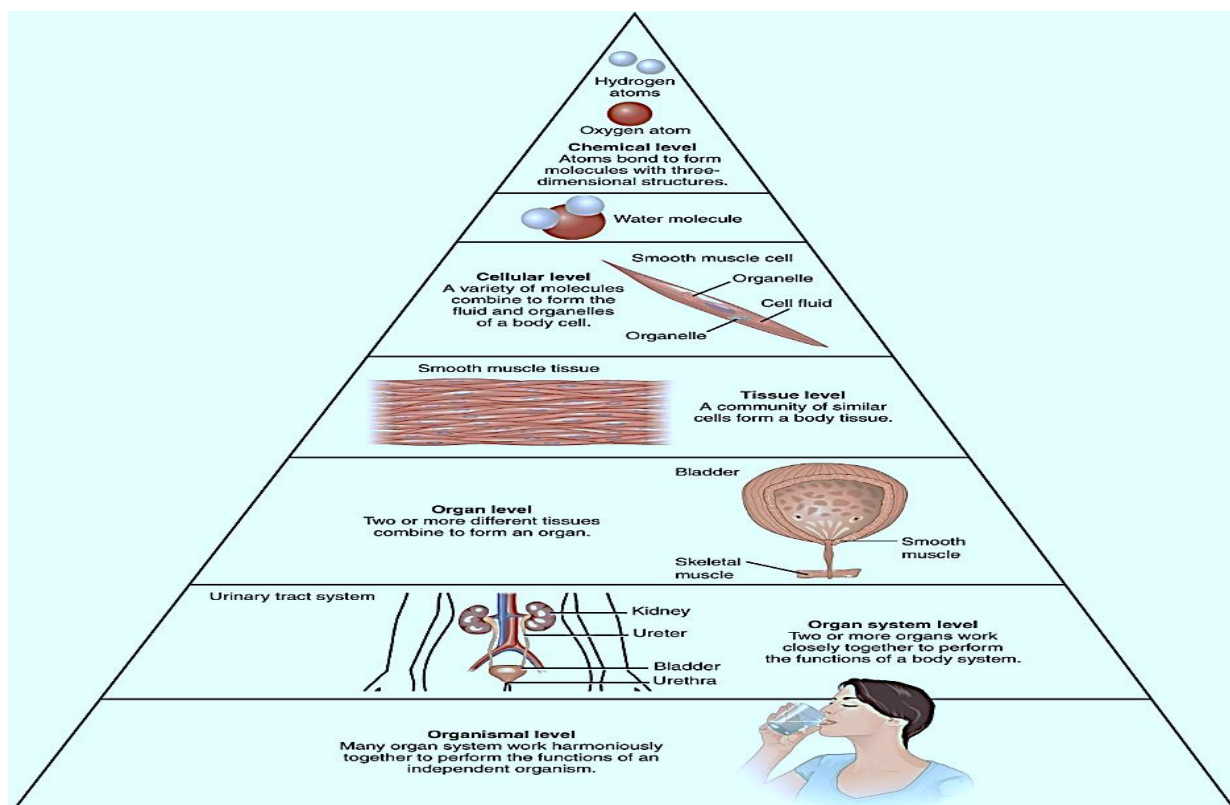


Fig.1.1 Different levels of structural organisation of human body

These levels shown in fig.1.2 are broadly classified as:

- Chemical, Cellular, Tissue, Organ, Organ system & Organismal level

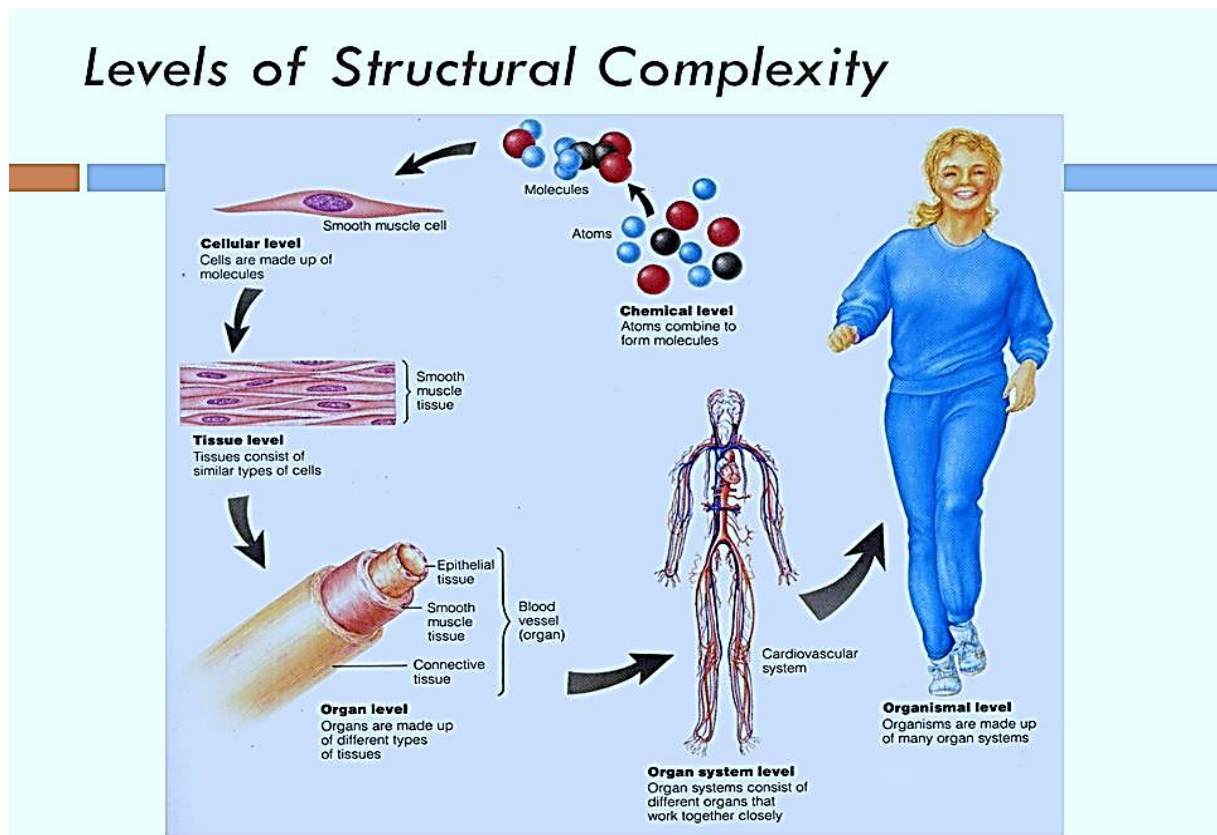


Fig.1.2 Different levels of structural complexity of human body

Chemical is the lowest level. Atoms combine to form molecules, of which the human body has a wide variety. The body contains billions of cells, which are the smallest autonomous units of living matter. Each cell type has grown specialised, performing a specific role that aids the body's demands. Cells with similar structures and functions are found together in complex organisms like the human body, forming tissues. Organs are made up of a variety of tissue types and perform a specific function. A system is made up of a group of organs and tissues that work together to meet one or more of the body's survival needs. The human body is made up of various systems that work together to perform certain functions and are all necessary for good health.

The external environment surrounds the body and supplies all of the body's cells with oxygen and nutrition. The skin acts as a barrier between the dry outside world and the wet inside world of most bodily cells. The water-based medium in which body cells dwell is known as the internal environment. The fluid that surrounds cells is known as tissue fluid. To reach them,

oxygen and other substances must travel via the interstitial fluid from the internal transport networks.

Chapter 1: Introduction to Biomedical Signals with Special Reference to ECG & Bioimpedance

The cell membrane surrounds each cell and acts as a possible barrier to substances entering or leaving the cell. Membrane structure confers permeability which can be semi or selective. Large molecules can't move between the cell and the tissue fluid because of this. Smaller particles can normally flow through the membrane, albeit some do so more easily than others, and the chemical makeup of the fluid inside the cell differs from that outside.

1.2 TYPES OF BIOMEDICAL SIGNALS

Biomedical signal is a collective term used for all types of physiological signals that can be measured from different parts of the living creatures or specifically human beings. Biomedical signals are broadly classified into following major categories;

I) Biochemical: - Mostly, these are in the form of pH changes, Hormones and Neurotransmitters, Level of glucose, Blood oxygen level;

II) Bioelectrical: -Electrocardiogram (ECG), Electroencephalogram (EEG), Electromyogram (EMG), Electrooculography (EOG), Electrogastragram (EGG);

III) Biomechanical: - Blood Pressure, Accelerometer signals describing human movements, gait, balance and posture (used for Parkinson disease, mobile applications, fitness);

IIIA) Bio-acoustic: -Subset of mechanical signals that describe the acoustic sound produced by the body (vibrations and motions). Examples includes: Phonocardiography for cardiac sounds, Obstructive Sleep Apnea detection or snoring, sounds related to respiration process;

IV) Biothermal: - Generally in the form of body temperature maps to describe the temperature distribution over the body surface;

V) Bio-optical: These signals are formed as a result of biological system's optical functions, which might occur spontaneously or be caused by the measuring procedure, for example- blood oxygenation levels;

VI) Bio-magnetic: Few organs, generate exceptionally low magnetic fields. The obtained signals can be measured to provide information not accessible in other forms of bio-signals, such as bio-electric signals. The magneto-encephalograph signal from the brain is a such an example;

VII) Bio-impedance: The tissue's impedance provides vital information on its composition, blood distribution, and blood volume, among other things. A common example of this sort of signal is the measurement of galvanic skin resistance. The bio-impedance signal may also be acquired by administering the tissue with ac current and detecting the drop in voltage caused

by the impedance of tissue. This sort of signal includes the measuring of respiration rate using the bio-impedance approach.

Chapter 1: Introduction to Biomedical Signals with Special Reference to ECG & Bioimpedance

1.3 BEHAVIOUR OF BIOMEDICAL SIGNALS

Living things are made up of many different component systems, such as the circulatory and nervous systems. Subsystems that perform a range of physiological tasks make up each system. For instance, the cardiac system is in charge of the body's regular, oxygenated blood pumping. The phenomena of physiological processes, which include the activation and control of the nervous system, are extremely complex. A biological system's diseases or faults frequently alter the regular physiological processes, leading to pathological processes that have an effect on the system's performance, health, and general well-being. Signals that are associated with a diseased process typically differ in some manner from their equivalent normal signals.

For instance, most illnesses cause an increase in body temperature that is simple to spot. A scalar quantity that describes the thermal condition of the human body is the single or one-time measurement of temperature. When the temperature is recorded constantly, then the obtained signal can be described as continuous-time analog signal $x(t)$, it can be written as $x(nT)$ or $x(n)$ when it is discrete in nature. If this discrete signal is further encoded it becomes digital signal. In another example; the monitoring of blood pressure (BP), is indicated by two pressures namely systolic and diastolic, which can be written as a vector $\mathbf{x} = [x_1, x_2]^T$, where x_1 is systolic pressure & x_2 is diastolic pressure. In clinical practise, blood pressure is measured in millimetres of mercury (mm of Hg).

1.4 OBJECTIVES OF BIOMEDICAL SIGNAL ANALYSIS

Following are the major objectives of biomedical instrumentation and signal analysis:

- Gathering of Information**
- Diagnostics**
- Monitoring and supervision**
- Control and Therapy** and finally, an evaluation is performed, which is an objective examination used to assess a system's capacity to satisfy functional criteria, get evidence of performance, perform quality control, or measure a treatment's effect.

1.5 ORIGIN OF BIOELECTRICAL SIGNALS

Animal electricity was discovered by renowned Italian physician and biologist Luigi Galvani in the 18th century, and it became the foundation for explaining the behaviour of living tissues in terms of bioelectric potentials. The human body, generates various types of electrical signals mainly by nerves and muscles. Ion migration is related with normal muscle contraction, resulting in potential changes that can be measured with appropriately placed electrodes. The heart and brain, for example, produce distinct patterns of voltage variations that may be recorded and analysed for use in clinical treatment and research.

Electrochemical alterations accompanying the transmission of signals via nerves to or from the brain also cause potential variations. When these impulses, which are in the order of a few microvolts, are recorded, they produce a complex pattern of electrical activity. A cell is made up of an ionic conductor that is isolated by a membrane which is semipermeable in behaviour. All biological substances are made up of different sorts of cells. The body fluids, which surrounds the cells of the body are ionic in nature and supports electric potentials through its conducting medium. The main ions involved in the phenomenon of creating cell potentials are Na^+ , K^+ , and Cl^- .

The semi-permeable cell membrane impedes the Na^+ ions movement, but easily allows the entry of K^+ and Cl^- . As a result, the Na^+ ion concentration is higher on the outer of the cell than on the inside it. Due to this a cell's membrane its resting state has more +ve charge on its outside. At this time the potential measured is known as resting potential, which has basically generated due to the unbalanced charge distribution. Now the cell is in its polarised state. The cell potential changes to around +20 mV as a result of this process, which is known as depolarization. Repolarization occurs after a brief period of time, when the cell returns to its usual condition, with the interior of the membrane being negative in relation to the outside. To re-establish the resting potential, repolarization is required. The voltage waveforms produced by this discharging and recharging of the cell can be recorded using appropriate microelectrode methods. The process for the generation of cell potential waveform and its recorded signal is shown in fig. 1.3.

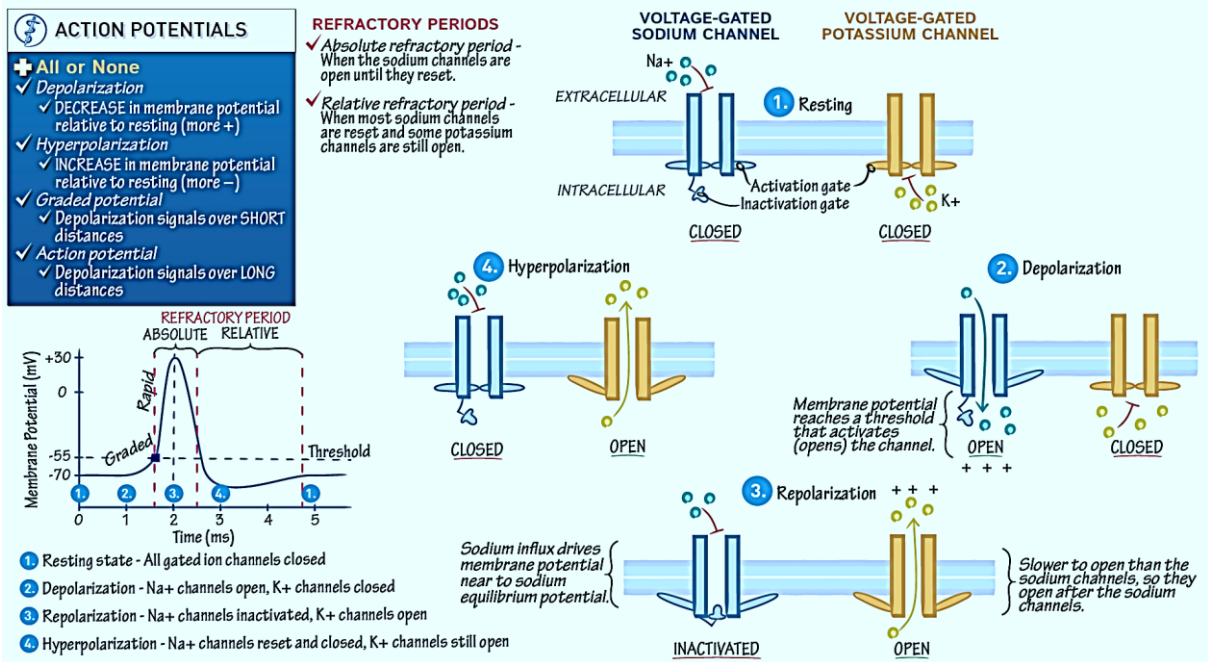


Fig.1.3 Process for the generation of cell potential waveform and its recorded signal

1.5.1 ACTION POTENTIAL

When a single cell is activated by an electrical current, the Action Potential (AP) is the electrical signal that accompanies the mechanical contraction (neural or external). A minimum threshold current is always required for the depolarization of the cell. Owing to finite mass and restricted speeds of the ions, they are offered resistance while their movement through the fluid. It results in finite rise and fall time for the cell action potential. To record an action potential, a single cell must be isolated and microelectrodes with tips of a few micrometres must be used to stimulate the cell and record the response. The various steps involved in the generation of cell action potential as shown in fig.1.4 are:

1. Resting Potential & Stimulus: A semi-permeable membrane surrounds nerve and muscle cells, allowing certain molecules to flow through while keeping others out. Excitable cell membranes readily accept the admission of K⁺ and Cl⁻ ions in their resting state, but effectively restrict the entry of Na⁺ ions. According to the phenomenon of charge concentration, various ions strive to achieve a balance between the interior and outside of a cell. A polarised cell is one that is in its resting state with some resting potential.

Until a disruption or stimulus breaks the equilibrium, most cells retain a resting potential of -60 to -100 mV. The stimulus threshold is the name given to the minimum value of applied stimulus for depolarization. After a cell has been stimulated, it takes a certain amount of time for it to recover to its pre-stimulus state. This is due to the fact that the energy associated with

Chapter 1: Introduction to Biomedical Signals with Special Reference to ECG & Bioimpedance

the action potential is generated by metabolic processes that require time to complete within the cell. This is referred to as the refractory period.

2. Depolarization: When a cell is stimulated by another external stimulus, the membrane changes its properties and allows Na^+ ions to enter. The flow of Na^+ ions create an ionic current, which lowers the membrane barrier to Na^+ ions even further. This causes an avalanche effect, in which Na^+ ions flood the cell. Because K^+ ions were in higher concentration inside the cell in the previous resting state, they try to escape the cell, but they can't move as quickly as Na^+ ions. As a result of the imbalance of K^+ ions, the inside of the cell becomes positive in comparison to the exterior. After the surge of Na^+ ions stop, a new state of equilibrium is attained. For most cells, this change marks the start of the action potential, which has a peak value of around +20 mV. Hence, depolarization is the process of an excited cell displaying an action potential and becoming depolarized.

3. Repolarization: It is the process by which a depolarized cell becomes polarised again and returns to its resting potential after a period of depolarization. Repolarization happens through processes similar to depolarization, although the main ions involved in repolarization are K^+ ions rather than Na^+ ions. Because the permeability of K^+ ions varies far more slowly than that of Na^+ ions during depolarization, the initial depolarization is produced by an inrush of Na^+ ions. However, around the apex of the depolarization, the membrane permeability changes for Na^+ ions begin to diminish spontaneously, whilst those for K^+ ions continue to rise. As a result, during repolarization, K^+ ions have the highest membrane permeability. Because the quantity of K^+ within the cell is significantly larger than outside, there is a net outflow of K^+ from the cell, causing the interior to become more negative, causing repolarization to the resting potential.

4. Hyperpolarization: It is a condition when the membrane potential is a reduced by the

- outflow of potassium ions and
- potassium channels cessation.

5. Resting state: This state occurs before the next stimulus is applied and it happens due to returning of the membrane potential back to its resting potential.

The all-or-none or all-or-nothing phenomenon describes how the action potential of a cell remains constant independent of the manner of excitation or the strength of the stimulus beyond a threshold.

Chapter 1: Introduction to Biomedical Signals with Special Reference to ECG & Bioimpedance

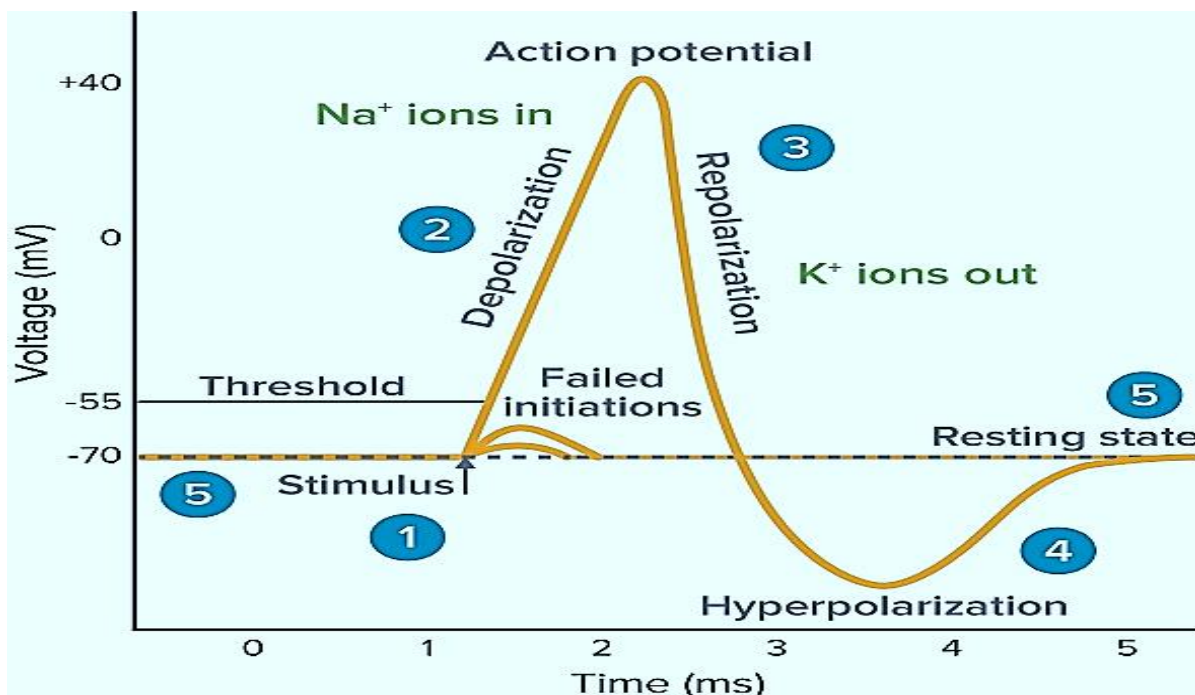


Fig.1.4 Electrical activity associated with one contraction in a muscle.

The absolute refractory phase occurs after an action potential, during which a cell is unable to respond to any fresh stimulation. The refractory period follows it, during which a significantly greater stimulus can elicit another action potential. The coordinated activity of large groups of cells produces the bioelectric signals of clinical interest, which are frequently recorded. The table 1.1. shows the most common bioelectric signals with their primary characteristics:

Table 1.1: Most common bioelectric signals with their primary characteristics

Bioelectric signal	Biological Source	Amplitude	Frequency
Electrocardiogram (ECG)	Heart	0.5 – 4 mV	0.05 – 150 Hz
Electroencephalogram (EEG)	Brain	5 – 300 μ V	0.5 – 150 Hz
Electromyogram (EMG)	Muscles	1 – 10 mV	0 – 10 kHz
Electrooculogram (EOG)	Eye dipole field	10 – 100 μ V	0 – 10 Hz
Electroretinogram (ERG)	Eye retina	0 – 900 μ V	0 – 50 Hz
Electrocortigram (ECoG)	Exposed surface Brain	-	100 Hz – 5kHz
Electroneurogram (ENG)	Nerve blunder	5 μ V – 10 mV	100 Hz – 1kHz
Evoked potentials	Brain	0.1 – 20 μ V	-
Action potentials	Nerves and muscles	-80 – 80 mV	10 – 10 kHz

Chapter 1: Introduction to Biomedical Signals with Special Reference to ECG & Bioimpedance

1.6 TYPES OF BIOELECTRICAL SIGNALS

The various types and sources of bioelectric Signals has been shown in fig.1.5.

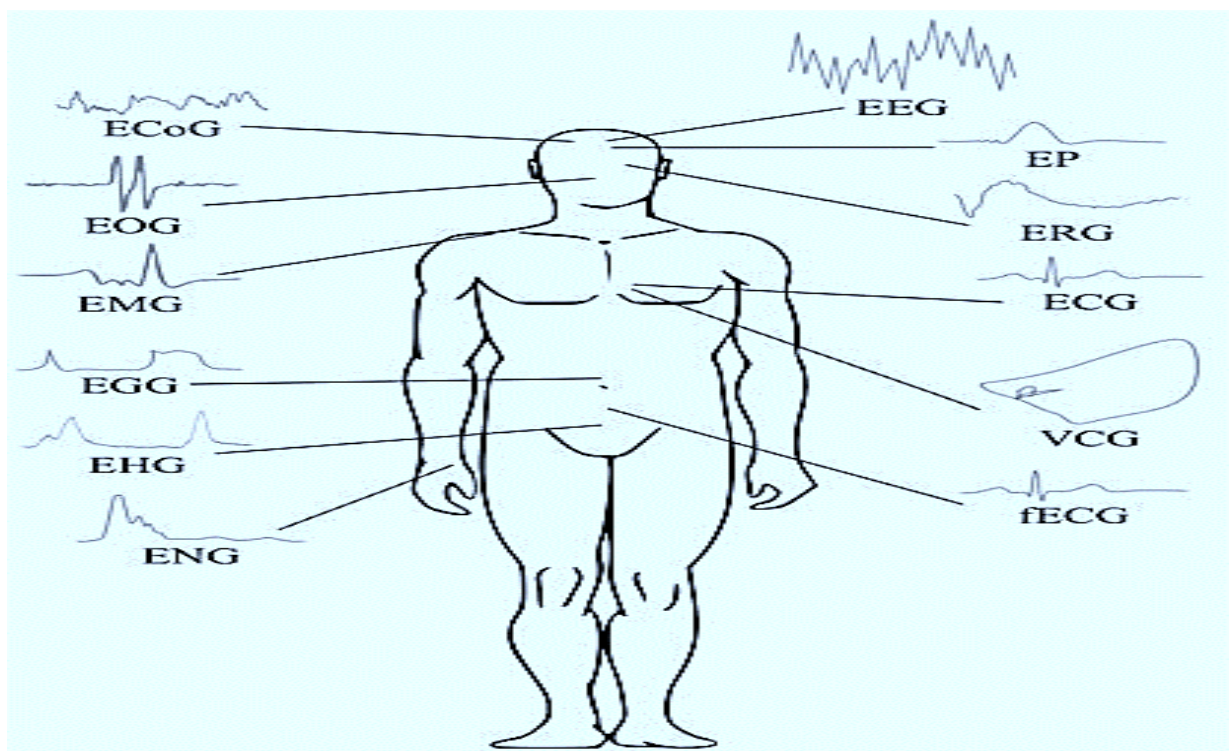


Fig.1.5 Types and Sources of Bioelectrical Signals

The brief description of few important bioelectrical signals is as follows:

1.6.1 ELECTRONEUROGRAM (ENG)

The ENG is an electrical signal that is detected as a stimulus and propagates along the length of a neuron as a nerve action potential. It may be used to determine the speed at which a stimulus or action potential propagates across a nerve (also known as conduction velocity). A peripheral nerve's conduction velocity can be assessed by activating a motor nerve and monitoring the corresponding activity at two places along its route that are a known distance apart.

To reduce muscular contraction and other undesirable consequences, the limb is kept in a relaxed position while a powerful but brief stimulation is administered in the form of a pulse with an amplitude of around 100 V and a duration of 100 - 300 μ s. The conduction velocity in the nerve may be calculated using the separation distance between the stimulus locations. The conduction velocity decreases due to the presence of neural diseases. The ENGs recorded in a nerve conduction velocity investigation are shown in fig. 1.6.

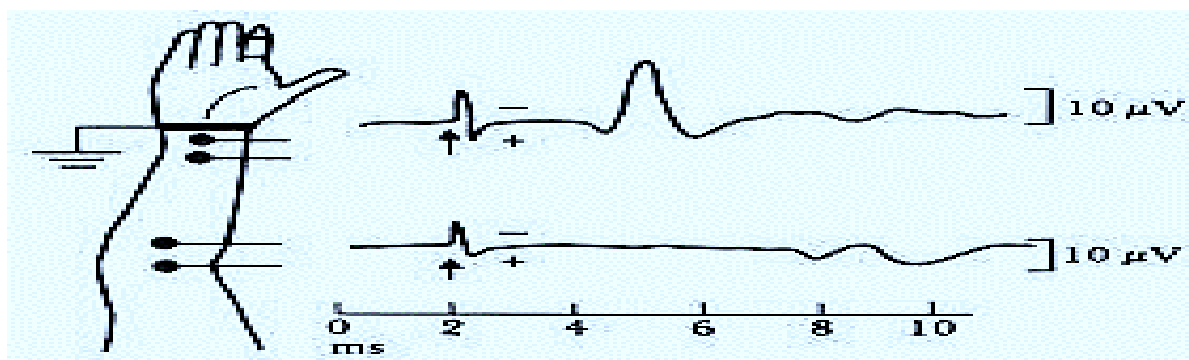


Fig.1.6 Acquisition of Electroneurogram (ENG) signal

1.6.2 ELECTROMYOGRAM (EMG)

Twitch fibres are skeletal muscle fibres that produce a mechanical twitch reaction in response to a single stimulus and create a propagated action potential. The Motor Units (MUs) are grouped together to form skeletal muscles. A motor unit's component fibres are triggered in a synchronous manner. A motor unit's component fibres run longitudinally in loose bundles along the muscle. The fibres of one motor unit are intermingled with the fibres of other motor units in cross-section. A schematic for the generation and processing of EMG signal is shown in fig.1.7.

Large muscles with hundreds of fibres per motor unit are used for general movement; smaller muscles with fewer fibres per motor unit are used for precision movement. The innervation ratio is the number of muscle fibres per motor nerve fibre. The cumulative outcome of numerous

motor unit's activation and contraction is the mechanical output (contraction) of a muscle. When each motor unit is triggered by a brain signal, it contracts and produces an electrical signal that is the total of all of its component cell's action potentials. The Single Motor Unit Action Potential (SMUAP, or simply MUAP) is a kind of action potential that may be recorded using needle electrodes put into the muscle of interest.

SMUAPs are commonly biphasic or triphasic, with a length of 3-15 ms, an amplitude of 100- 300 μV , and a frequency of 6-30 Hz. Disease has an impact on the form of SMUAPs. Slow conduction and/or desynchronized activation of fibres, as well as a polyphasic SMUAP with a higher amplitude, are all symptoms of neuropathy. Myopathy is characterised by the loss of muscle fibres in motor units while the neurons remain intact. Asynchronous contraction occurs when motor units fire at various times and at distinct frequencies. Motor units fire at around 5-15 pulses/second due to a lack of volitional effort. The EMG of the muscle is generated by

Chapter 1: Introduction to Biomedical Signals with Special Reference to ECG & Bioimpedance

adding the MUAPs of all activated motor units in a spatial-temporal manner.

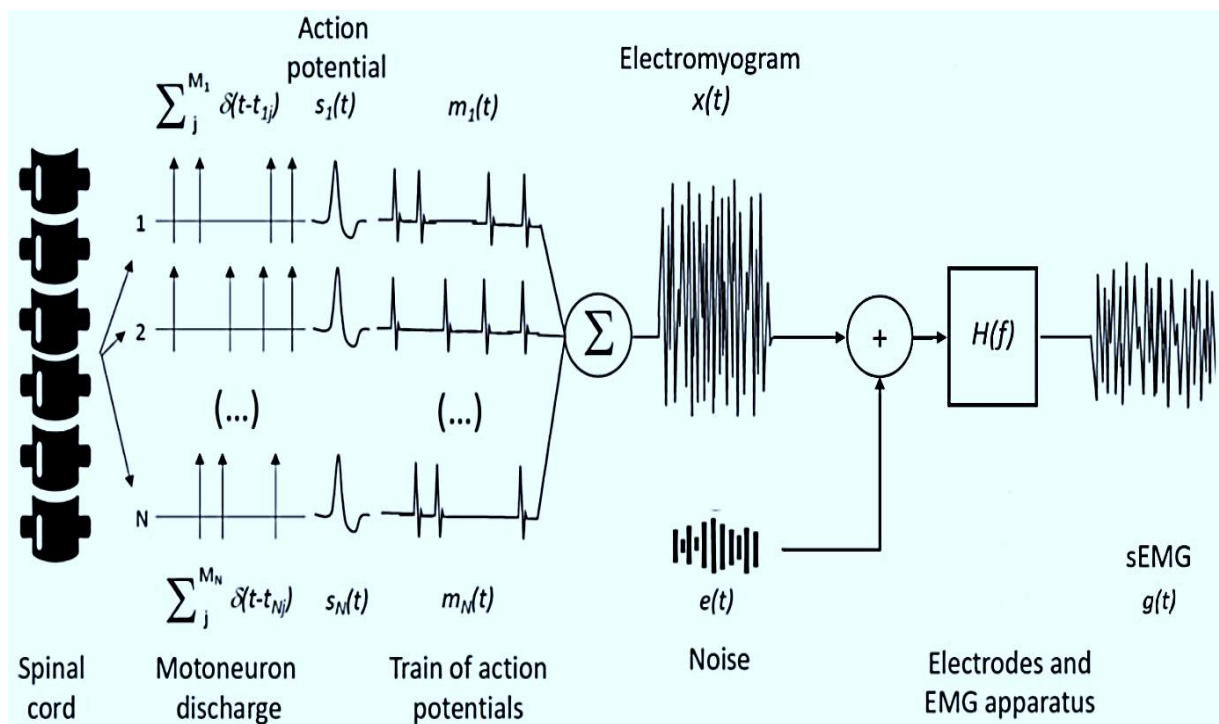


Fig.1.7 Generation and Processing of Electromyogram (EMG) signal

1.6.3 ELECTROENCEPHALOGRAPH (EEG)

The EEG (also known as brain waves) is a measurement of the brain's electrical activity. Physiological control systems, mental processes, and external stimuli all create signals in the

brain that may be recorded using surface electrodes on the scalp. The scalp EEG is an average of the numerous different activities of many tiny zones underneath the electrode on the cortical surface. Several channels of the EEG are recorded concurrently from several points on the scalp in clinical practise for comparative examination of activity in different brain areas. The 10-20 scheme of electrode placement for clinical EEG recording is the most common and popular method as shown schematically in fig.1.8.

The designation 10-20 refers to the fact that the electrodes along the midline are arranged at fractional distances of the respective reference distances of 10,20,20,20,20 and 10% of the total nasion-inion distance. EEG signals may be used to investigate the neural system, track sleep stages, provide biofeedback & control, and diagnose disorders like epilepsy. Monitoring sleep EEG and detecting epileptic seizure transients may need multichannel EEG recording over

Chapter 1: Introduction to Biomedical Signals with Special Reference to ECG & Bioimpedance

several hours. The use of needle electrodes, naso-pharyngeal electrodes, and other specialised EEG methods are among the most often used.

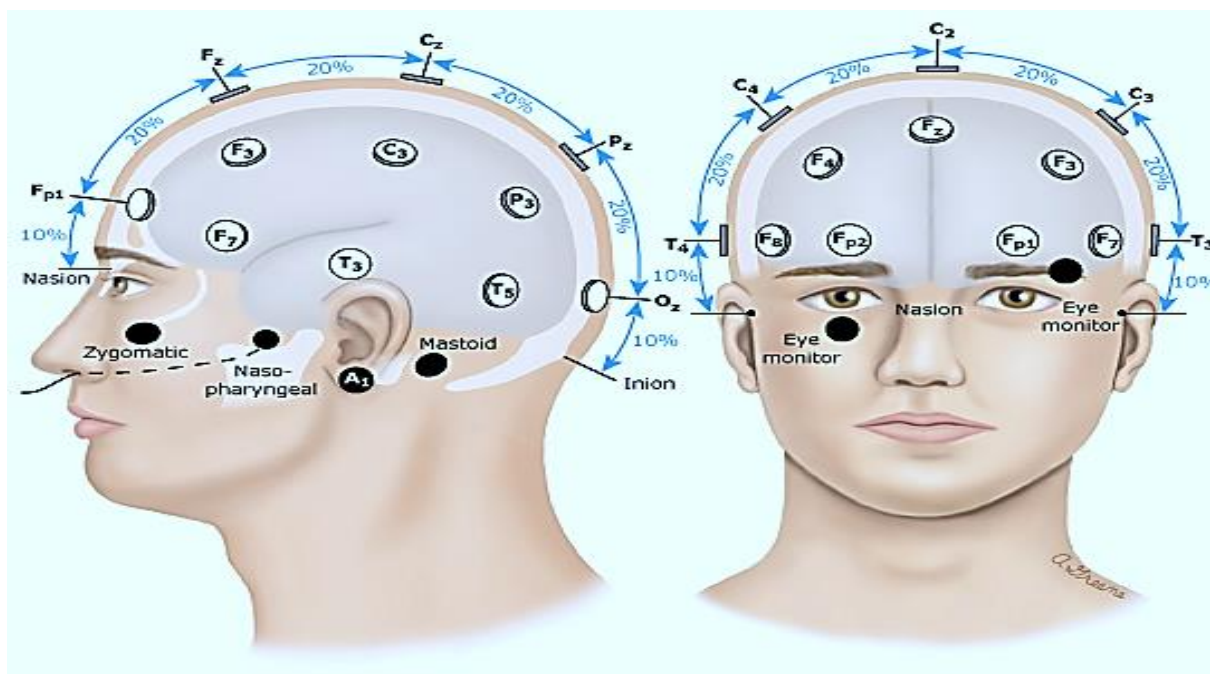


Fig.1.8 10-20 System of electrode placement for EEG recording

The different EEG frequency bands are shown in table 1.2.

Table 1.2: EEG frequency bands

S. No	Frequency Band Name	Frequency Range
1	Delta (δ)	0.5- 4 Hz
2	Theta (θ)	4 - 8 Hz
3	Alpha (α)	8 - 13 Hz
4	Beta (β)	> 13 Hz.

The fig.1.9 shows EEG signal frequency bands and associated brain activities. Various physiological and mental functions are linked to EEG rhythms. The alpha rhythm is the brain's primary resting rhythm, and it's frequent in awake, resting adults, particularly in the occipital region with bilateral synchronisation. With the eyes closed, auditory and mental arithmetic activities produce significant alpha waves, which are inhibited when the eyes are opened. Theta waves emerge at the start of sleep, whereas delta waves appear during profound sleep. In tense and worried people, high-frequency beta waves seem as background activity.

Chapter 1: Introduction to Biomedical Signals with Special Reference to ECG & Bioimpedance

In a certain state of the individual, depression or the lack of the normal rhythm might suggest abnormalities. In a wakeful adult, the occurrence of delta or theta (slow) waves would be regarded aberrant. Abnormal slow waves in the corresponding areas are caused by focal brain damage and tumours. The existence of epileptogenic areas in the corresponding portions of the brain might be indicated by spikes and sharp waves. All of the channels have a lot of alpha activity. Spikes, transients, and other waves and patterns linked with various neurological illnesses can also be found in EEG readings.

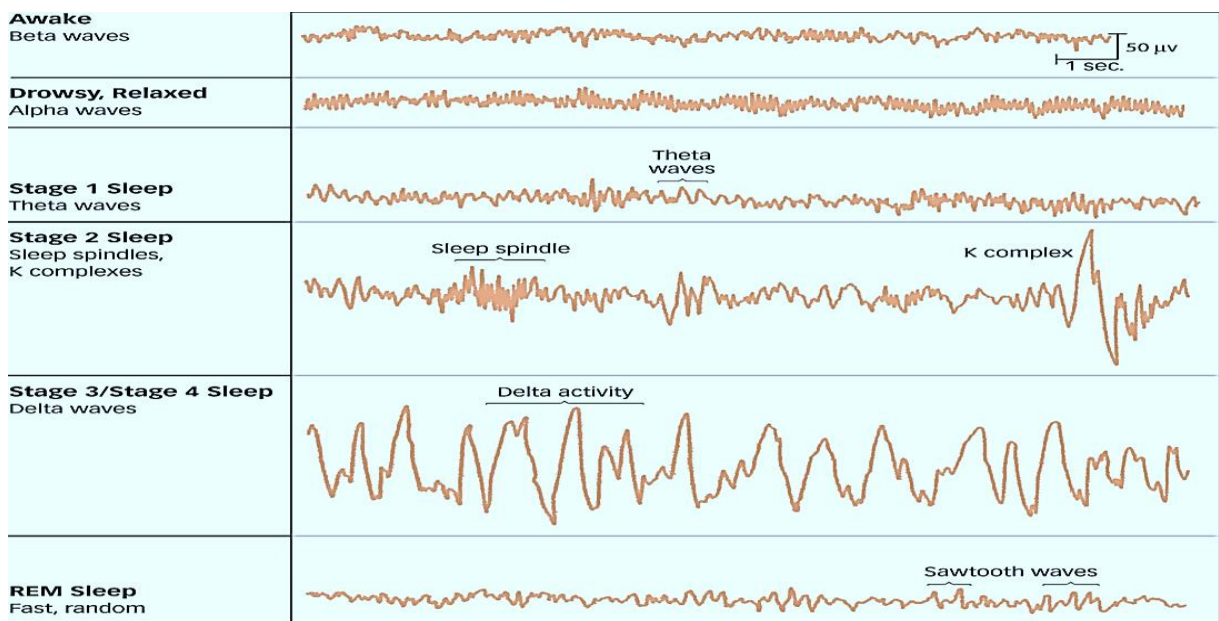


Fig.1.9 EEG signal frequency bands and associated brain activities

1.6.4 ELECTROGASTROGRAM (EGG)

An EGG can be recorded with the help of external (cutaneous) electrodes as depicted in fig.1.10. The surface EGG is believed to reflect the overall stomach activity, which includes the both electrical control activity and the electrical response activity. The analysis of the EGG provides the details of gastric dysrhythmia or arrhythmia. However, accurate and reliable measurement using EGG requires implanting of electrodes in the stomach, which limits its practical applicability.

1.6.5 VECTORCARDIOGRAPH [VCG]

A vectorcardiogram is the name for the display known as Vectorcardiography [VCG] which is a procedure that involves plotting and analysing the 3D cardiac electrical vector loops in three mutually orthogonal planes, which are frontal, horizontal, and sagittal planes as shown in fig.1.11. In contrast to an ECG, which shows the electrical potential on a single axis, a

Chapter 1: Introduction to Biomedical Signals with Special Reference to ECG & Bioimpedance

vectorcardiogram shows the same electrical events on two perpendicular axes at the same time. This creates loop type patterns on the CRT screen as shown in fig.1.12. Each cardiac cycle is usually documented with a picture. The amplitude and direction of the P, Q, R, S, and T vector loops may be calculated using such images.

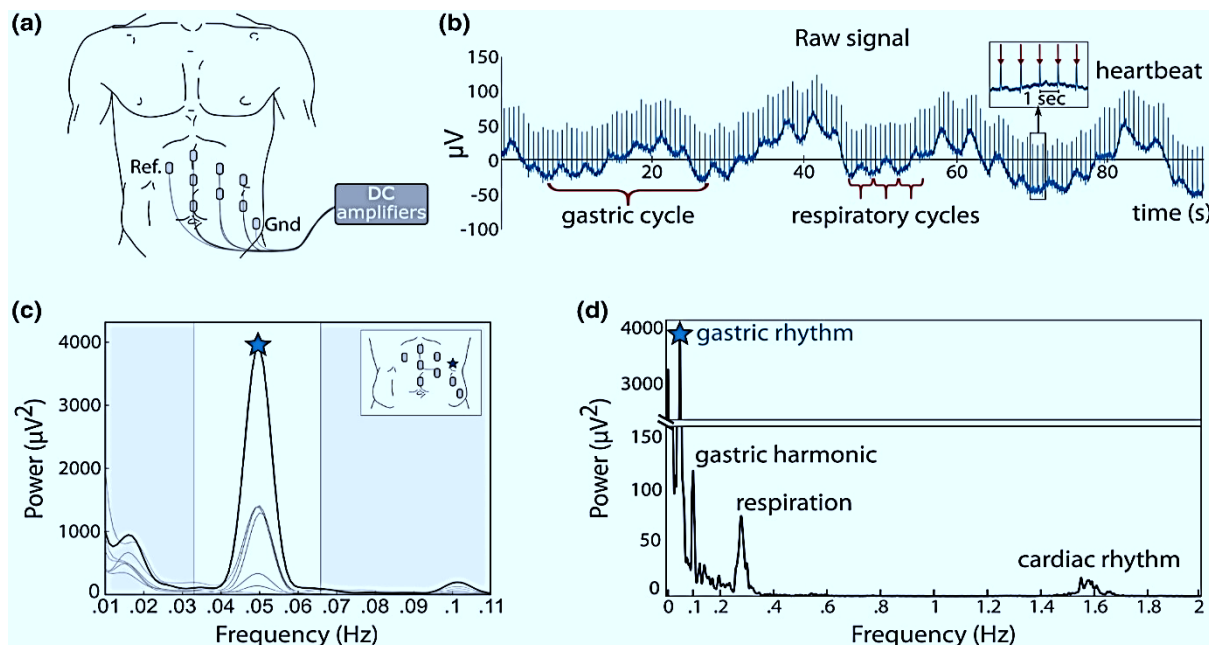


Fig.1.10 Generation and output signals of Electrogastragram [EGG]

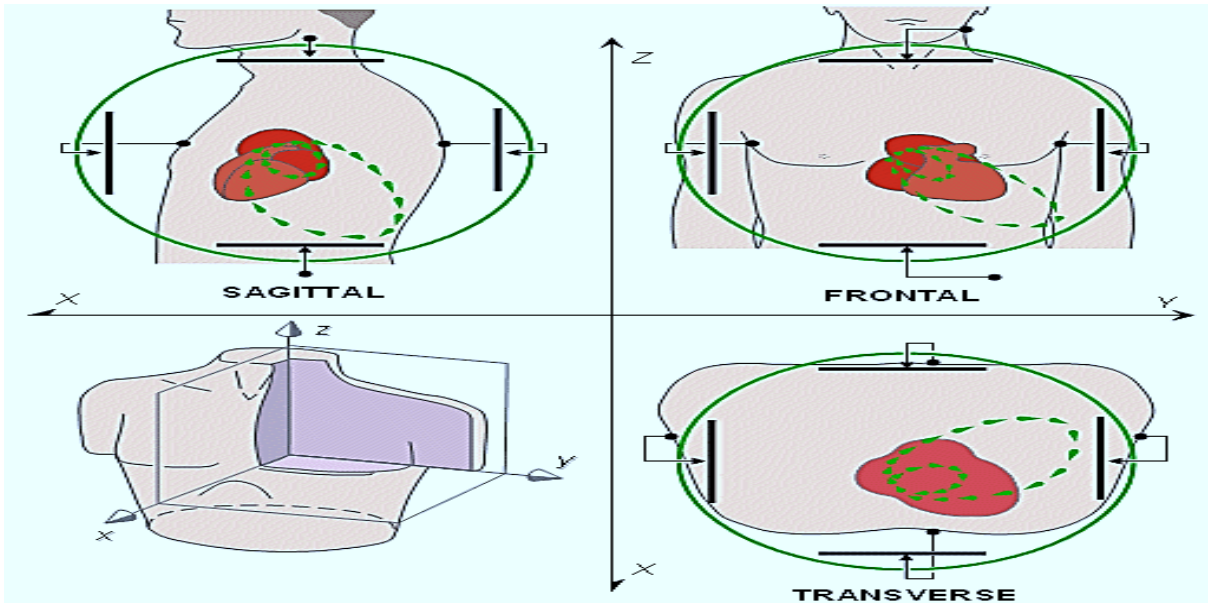


Fig.1.11 3D cardiac electrical vector loops in frontal, horizontal, and sagittal planes

VCG depicts the phase differences between voltages as well as the different leads from which it is formed. Each vectorcardiogram has three loops, one for the P wave, one for the QRS axis, and one for the T wave. Loops from the QRS complex prevail due to the high amplitude associated with QRS. To fully depict the loops caused by the P wave and T wave, an increase in horizontal and vertical deflection sensitivity is usually necessary.

Chapter 1: Introduction to Biomedical Signals with Special Reference to ECG & Bioimpedance

and one for the T wave. Loops from the QRS complex prevail due to the high amplitude associated with QRS. To fully depict the loops caused by the P wave and T wave, an increase in horizontal and vertical deflection sensitivity is usually necessary.

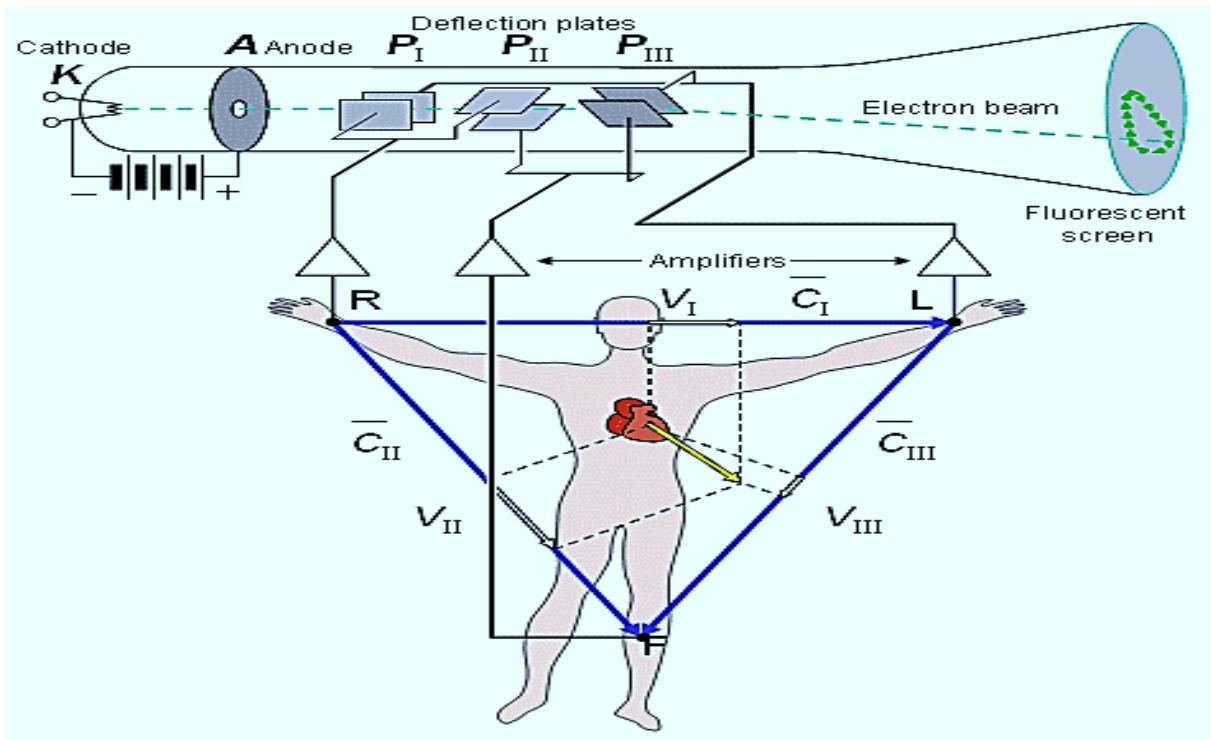


Fig.1.12 Conventional Vectorcardiography scheme

1.6.6 ELECTROCORTICOGRAM (ECoG)

In Electrocorticography (ECoG) procedure, neurosurgeons place macroelectrodes (usually 2–3 mm in diameter) on the exposed surface of the cortex to determine the cause of seizures in drug-resistant epileptic patients. The part of the brain that causes seizures is then surgically removed. The intra-operative recording of cortical potentials has played an essential role in the surgical therapy of patients with medically resistant epilepsy. It's been utilised to: 1) locate epileptogenic tissue; 2) map out brain functions; and 3) forecast surgical outcome. Thus, the traditional electroencephalography (EEG) electrodes, measures the brain activities from outside the skull, whereas ECoG can be done in the operating theatre during surgery (intraoperative ECoG) or outside of surgery (extra operative ECoG) as depicted in fig.1.13. However, the ECoG technique is invasive in nature.

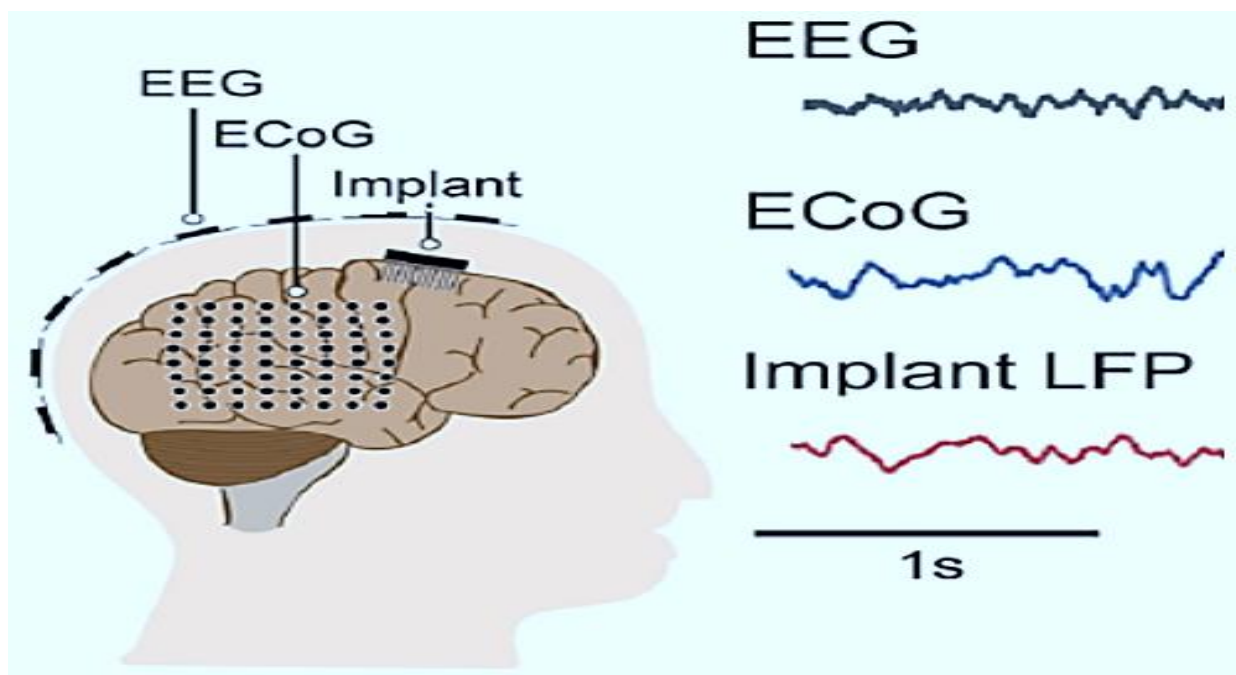


Fig.1.13 *Electrocorticogram (ECoG) setup and signal output*

1.6.7 ELECTROCARDIOGRAM (ECG)

The ECG is the electrical representation of the heart's contractile activity, and it may be easily recorded using surface electrodes on the limbs or chest. Perhaps the most well-known, recognised, and used biological signal is the ECG. The important aspects of ECG are as follows:

1.6.7.1 THE HEART

The heart is a four-chambered pump that has two atria for blood collecting and two ventricles for blood pumping out. The four chambers and the main arteries that link to the heart is shown schematically in fig.1.14. Diastole refers to the resting or filling phase of a heart chamber, whereas systole refers to the contracting or pumping phase. The superior and inferior vena-cavae send impure blood to the right atrium (or auricle, RA). The largest and most significant heart chamber is the left ventricle. Because it needs to pump oxygenated blood, the left ventricle contracts the hardest of the heart chambers. The names systole and diastole are used to the ventricles by default due to the greater significance of ventricle contraction.

The Sino-Atrial (SA) node is the specialized pacemaker of the heart. The average (resting) heart rate is around 70 beats per minute. Although the heart rate drops during sleep, unusually low heart rates of less than 60 beats per minute during exercise may suggest bradycardia. During strenuous exercise or sports activity, the instantaneous heart rate can approach 200 beats per minute; a high resting heart rate, known as tachycardia, can be caused by sickness, disease, or cardiac anomalies.

Chapter 1: Introduction to Biomedical Signals with Special Reference to ECG & Bioimpedance

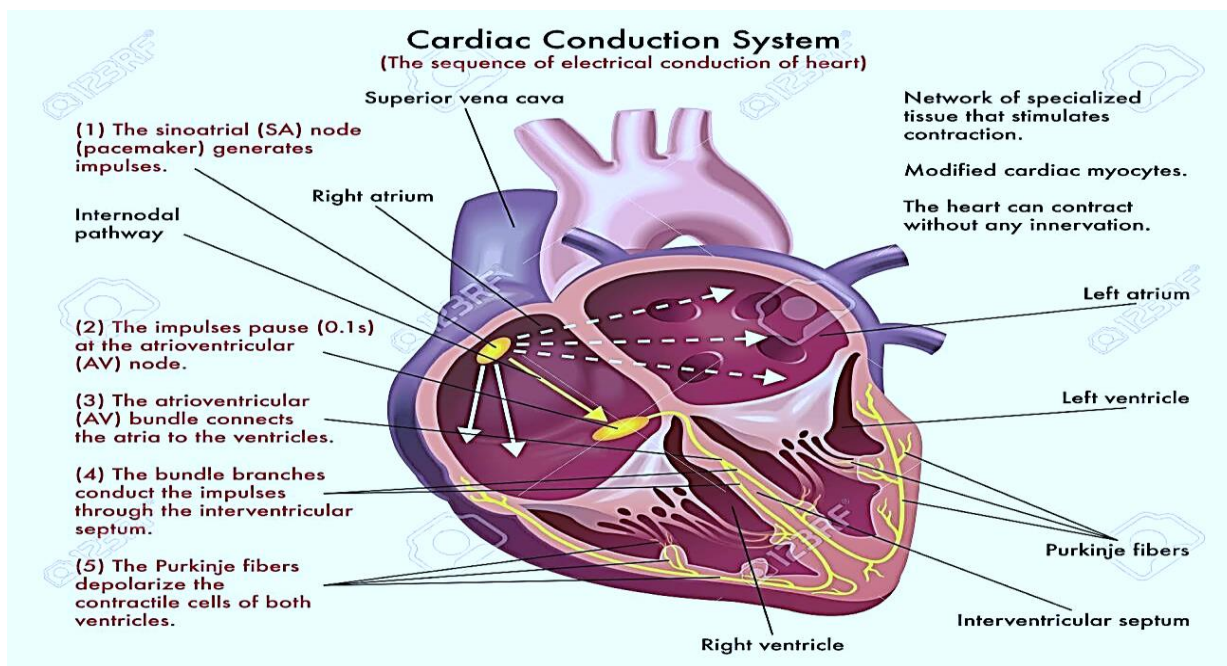


Fig.1.14 Schematic for cardiac conduction system

1.6.7.2 HEART'S ELECTRICAL SIGNAL GENERATION SYSTEM

The SA node is a simple, natural cardiac pacemaker that initiates a series of action potentials on its own. The SA node's action potential travels across the remainder of the heart, creating a specific pattern of excitation and contraction as shown in fig.1.15.

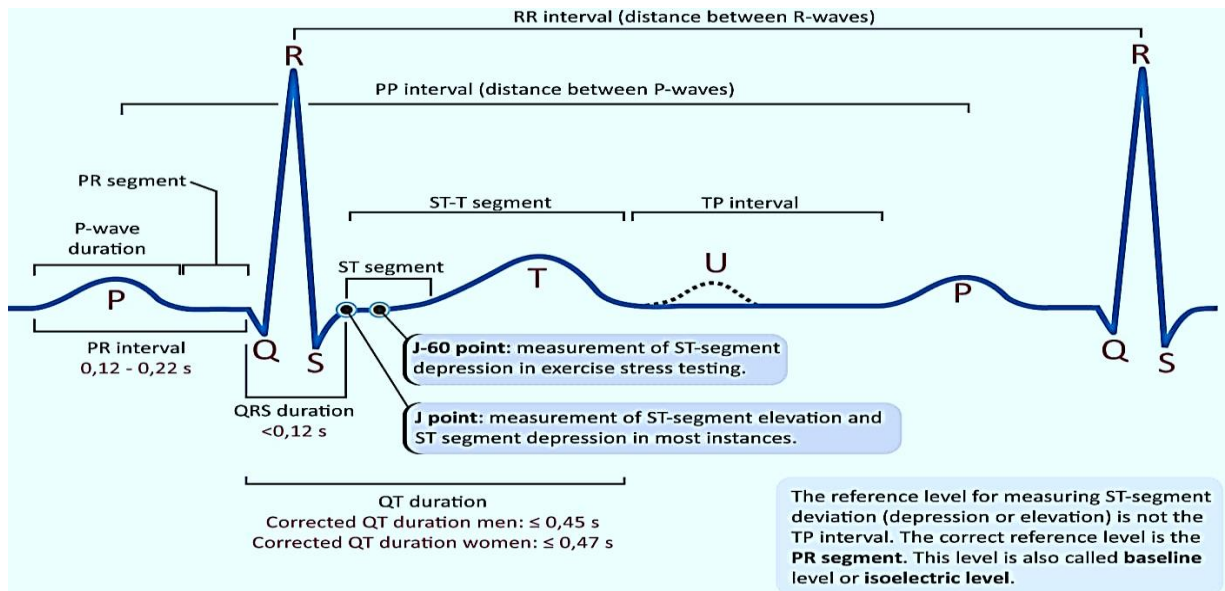


Fig.1.15 Typical ECG signal waveform

1.6.7.3 ECG SIGNAL ACQUISITION

The conventional 12-channel ECG is acquired in clinical practise utilising four limb leads and six chest leads in six places. The reference electrode is placed on the right leg. Leads I, II, and III are obtained via the left arm, right arm, and left leg. Wilson's central terminal is a

Chapter 1: Introduction to Biomedical Signals with Special Reference to ECG & Bioimpedance

composite reference made up of the left arm, right arm, and left leg leads that is used as a reference for chest leads. Einthoven's triangle is a hypothetical equilateral triangle formed of leads I, II, and III. Wilson's central terminal is represented by the triangle's centre as shown in fig.1.16. The heart is supposed to be at the centre of the triangle in this arrangement or diagram.

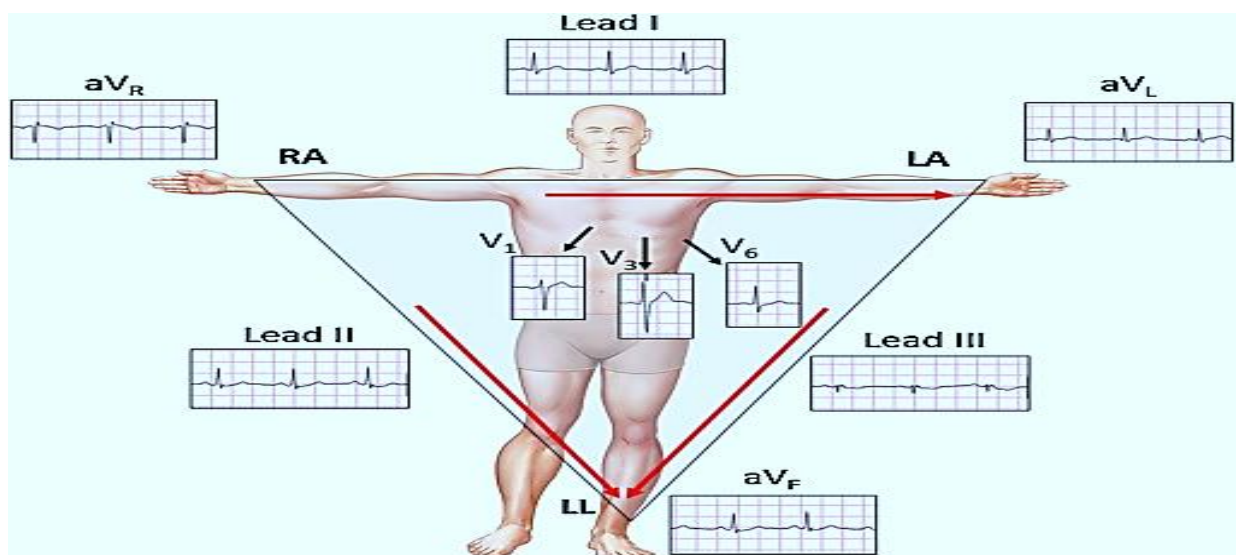


Fig.1.16 Wilson's central terminal and Einthoven's triangle for ECG measurement

The six leads measure 3D cardiac electrical vector projections onto the axes which are sampled in the 0° - 180° range in around 30° increments. The projections make it easier to see and analyse

the electrical activity of the heart from various angles in the frontal plane. The V1 and V2 leads are located immediately to the right and left of the sternum, respectively, in the fourth intercostal gap as shown in fig.1.17. The fifth intercostal gap on the left midclavicular line is where V4 is recorded. Similarly, V3, V5 & V6 are also recorded. Despite the fact that it is redundant, the 12-lead method is the foundation of the conventional clinical ECG. The majority of clinical ECG interpretation is empirical, depending on prior experience. Regardless, in clinical practise, the 12-lead scalar ECG is the most often employed method.

External ECG recordings are not unique since they are a projection of the interior 3D cardiac electrical vector. The following are some of the most important inter-relationships:

$$\square \quad \text{II} = \text{I} + \text{III}$$

$$\square \quad aV_L = (\text{I} - \text{III})/2.$$

where aV_L is augmented lead for left arm.

The 12-lead ECG of a healthy male adult along with distorted ECG signals due to various cardiac ailments is shown in fig.1.18. By analysing the waveshapes in the six limb leads, a well-trained cardiologist may derive the 3D direction of the heart electrical vector. The waveshapes in the six chest leads can be used to locate any cardiac abnormalities.

Chapter 1: Introduction to Biomedical Signals with Special Reference to ECG & Bioimpedance

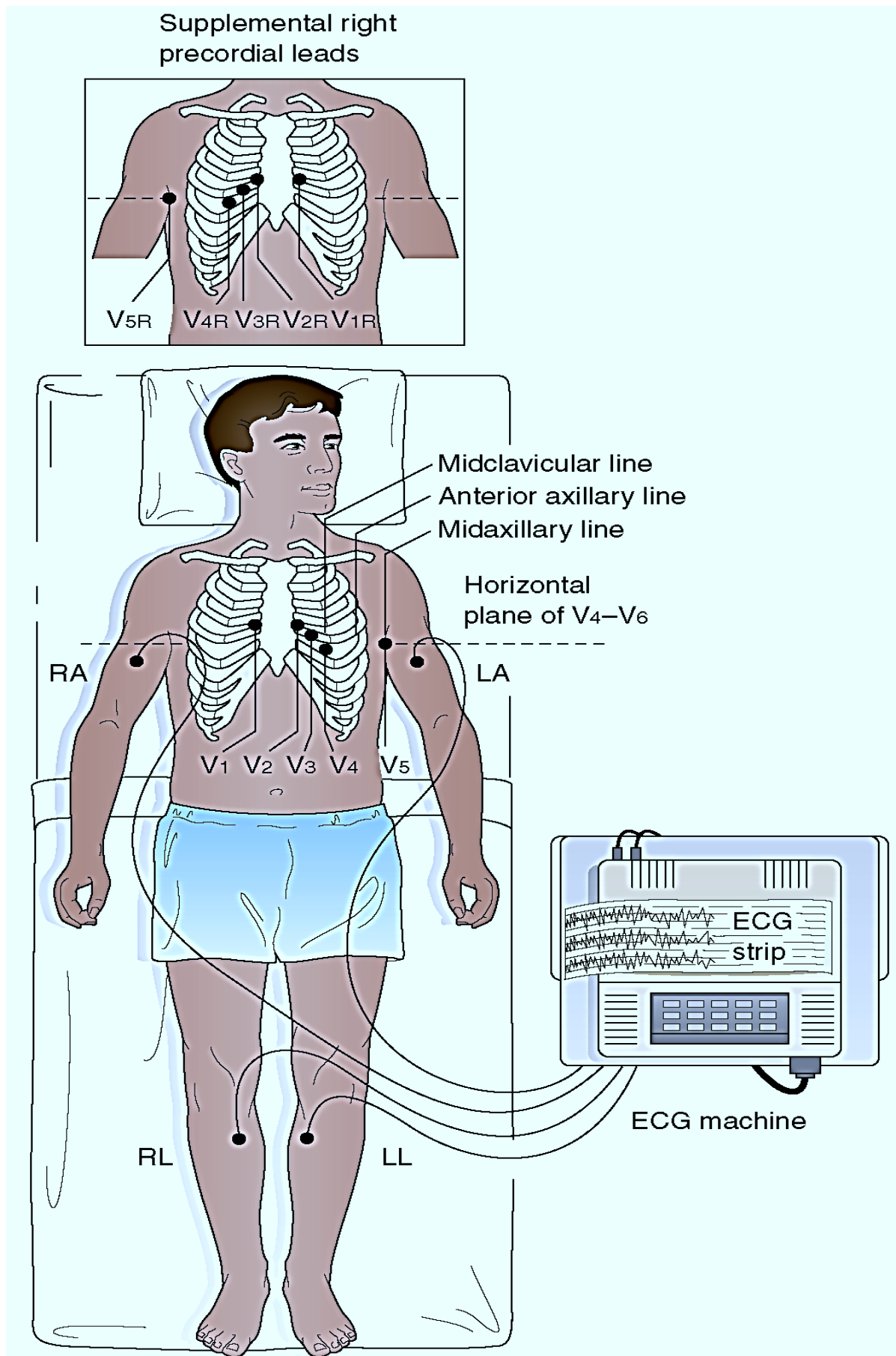


Fig.1.17 ECG signal acquisition process

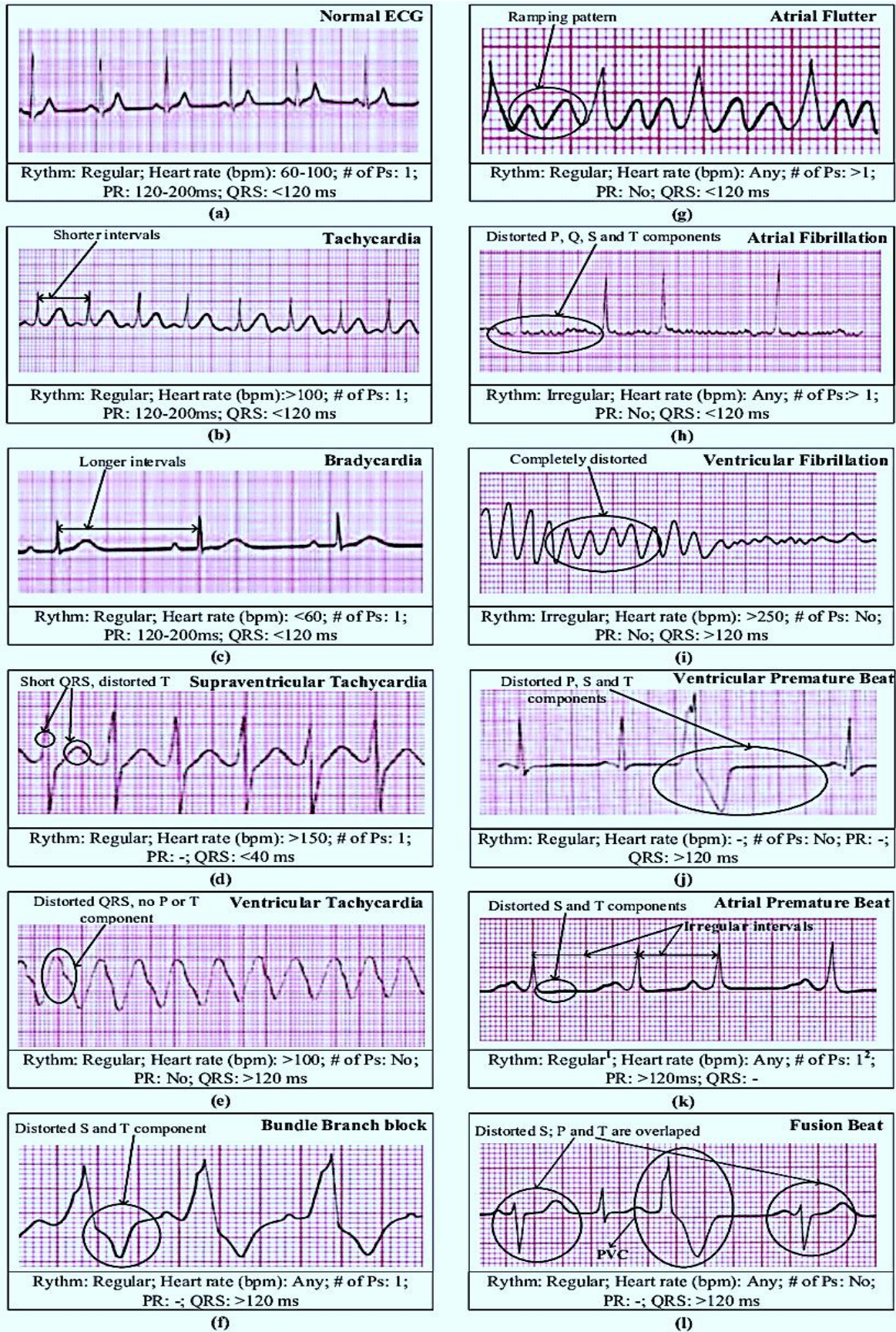


Fig.1.18 Typical normal ECG signal and distorted ECG signals due to various cardiac ailments

1.7 BIOIMPEDANCE

Simply, impedance offered by a living tissue is known as bioimpedance. Whether, it is animal and plant cells or tissues, these are always made up of three-dimensional arrangement of cells and tissues. Therefore, human body is a complex biological structure and system, which is also made up of billions of cells and tissues arranged in 3-D formation [1]. The biological cells and tissues of both animals and plants floats in ECF which is known as Extra-Cellular Fluids. This ECF comprises Intra-Cellular Fluids (ICF) and Cell Membranes (CM) which may be with or without cell wall. When biological cells and tissues are subjected to the external electrical stimulus they respond and produces a complex bioelectrical impedance or simply known as bioimpedance. This bioimpedance is highly frequency-dependent [2, 3].

Accordingly, frequency response of bioimpedance of cells and tissues of humans is greatly affected by physiological and physiochemical composition and structure of these cells and tissues. Moreover, it also changes from person to person. As a result, learning about cell and tissue anatomy and physiology through biological cell and tissue bioimpedance analysis will be a valuable resource. Therefore, it has been found that studying complex bioimpedance of biological cell and tissues is a useful method for non-invasive physiological and pathological investigations. As we know that the bioelectrical impedance of a biological cells or tissues is dependent on the signal frequency, however, multifrequency application may also be used for non-invasive diagnostics and medical investigations, so as to determine their physiological or pathological behavior or even properties. There are numerous Non-invasive bioimpedance techniques such as BIA (Bio-Impedance Analysis), EIT (Electrical Impedance Tomography), IPG (Impedance Plethysmography), ICG (Impedance Cardiography) etc. The bioimpedance measurement technique proposed in this study, is a low-cost, efficient, and effective non-invasive diagnostic technique.

1.7.1 BASICS AND ORIGIN OF BIOIMPEDANCE

Bioimpedance is a passive electrical property that describes a biological tissue's ability to obstruct (oppose) electrical current flow. The reaction to electrical excitation (current or potential) applied to biological tissue is used to determine bioimpedance. The same or other electrodes apply the excitation signal and pick up the reaction in bioimpedance measurements, converting the electronic charge to ionic charge and vice versa [4]. Simply, the ratio of voltage (V) to alternating current (I) is known as electrical impedance (Z). Since, Direct Current (DC) is quite hazardous to humans, therefore, it is never used for any experimentation on humans. In fact, Alternating Current (AC) is more preferable choice for such type of applications. The

calculated or observed bioimpedance (Z) is highly influenced by the Resistive (R), Capacitive (C), and Inductive (L) components of the cells and tissues. The bioimpedance (Z) can be given by using the modulus $|Z|$ and the phase change. Since, bioimpedance (Z) is a complex function or parameter, therefore its real part is Resistance (R) and whereas, the imaginary part is Capacitance Reactance (X_c). As the ICF, CM, and ECF are made of dissimilar materials with nonidentical electrical properties, therefore every cell and tissue components react differently to the applied AC signal.

As we know that ICF and ECF are made up of ionic solution which are highly conducting in nature, thus it provides highly conducting or low resistive path to the applied AC signal [5]. The Cell membranes are composed of lipid bilayers which are electrically nonconducting and sandwiched between two conducting protein layers. This sandwiched structure, produces a capacitive reactance (X_c) to the applied AC signal [6, 7]. Due to this, biological cells and tissues produces a complex bioimpedance (Z) which can be considered as overall response to an applied AC signal [2, 3]. Thus, bioimpedance (Z) is a complex function depends upon cell and tissue composition and structure, health of person and applied AC signal frequency. Moreover, it also changes with measurement direction, varies from subject to subject and even tissue to tissue. The human body composition comprises, water (64%), protein (20%), fat (10%), and minerals (5%) and starch (1%) as shown in fig.1.19 through the concept of five component model for human body.

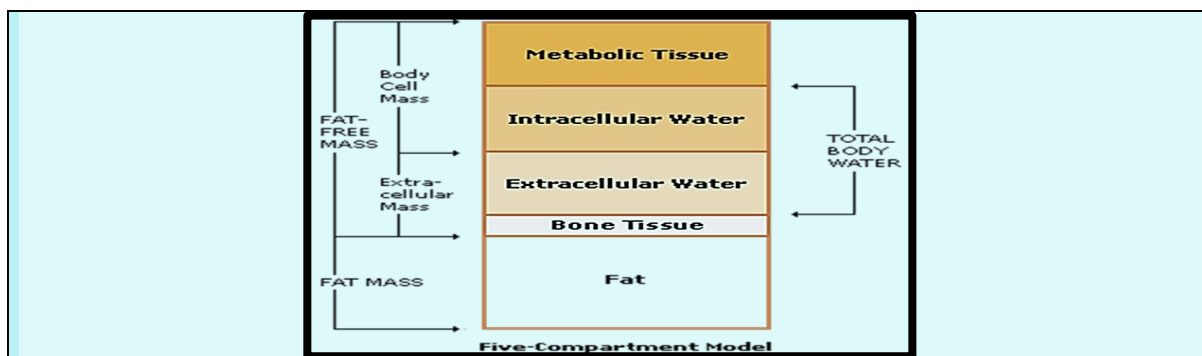


Fig.1.19 Five component model for human body

The mass of the human body is mainly due to oxygen (65%), carbon (18%), and hydrogen (8%). The majority of muscles are made up of protein whereas, majority of bones are made up of minerals [1]. The bioimpedance is proportional to Total Body Water (TBW), which contains Intra-Cellular Water (ICW) and Extra-Cellular Water (ECW) as shown in fig.1.20. Body water, body fat, and body muscle have different impedance values according to the amount of presence of water in these. Thus applied AC signal pass through paths that contain more water as it

it provides high conductivity [8].

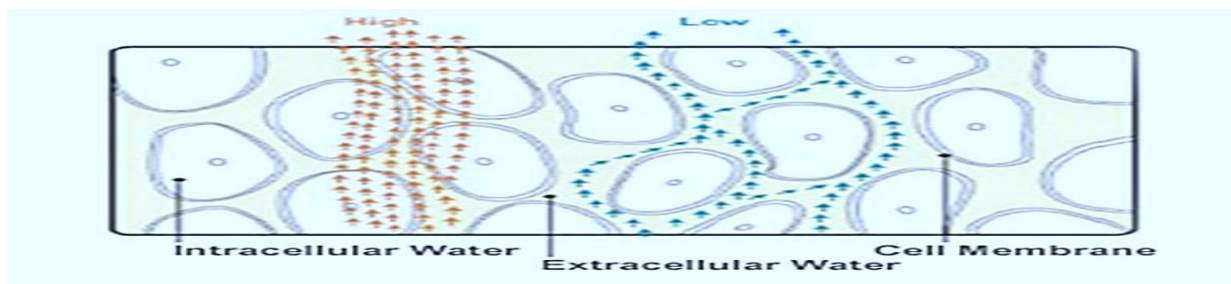


Fig.1.20 Representation of Total Body Water (TBW) in human body

The physiological, morphological, and pathological settings, as well as the frequency of the applied electrical signal, all affect and influence the electrical properties of biological cells and tissues [7, 9]. The biological cells and tissues may have active (endogenous) or passive (exogenous) electrical properties, depending on the type of source of applied AC signal. The electrocardiograph (ECG) signals from the heart, electroencephalograph (EEG) signals from the brain, electromyograph (EMG) signals from the muscles are few examples of active properties (bioelectricity) produced by ionic activities within cells and tissues (typical of nerve cells). Passive properties are generated by simulating them with an external electrical excitation source [4].

The extracellular fluids surround all cells with membranes in biological tissues. The main constituents of Extra-Cellular Fluid (ECF) are fluid component of the blood known as plasma and the other one is Interstitial Fluid (IF) which surrounds all cells that are not in blood. The extracellular space is the part of a multicellular organism outside the cells, whereas intracellular space is within the organism's cells. The cell membranes separate extracellular spaces and intracellular space thus producing two electrically conducting compartments known as extracellular media and intracellular media. These intracellular and extracellular fluids provide resistive pathways. Due to its insulating design and structure, the lipid bilayer cell membrane is very-very thin measuring approximately 6-7 nm. This lipid bilayer cell membrane is semi-permeable, due to which it has a high capacitance and which produces capacitive reactance [10, 11, 12]. Although biological cells and tissues may have inductive properties, inductance is much lower at low frequencies than resistance and capacitive reactance, so it is often overlooked [13]. Thus, biological cells or tissue's complex bioimpedance is the contributions from both frequency-dependent capacitance and conductance. Bioelectrical impedance often differs from one tissue to the next, as well as from one subject to the next. The complex bioelectrical impedance is affected by changes in cell and tissue composition and structure, and even health condition or status of the subject [4, 5].

CHAPTER 2

LITERATURE REVIEW

Bio-Medical Signal Analysis Techniques [PART-I]

The Electrocardiogram (ECG) is one of the several kinds of bioelectrical impulses and is extremely significant. The ECG, a technique for monitoring the bioelectric impulses generated by the heart, is used by cardiologists and doctors to evaluate a patient's heart health. Recent years have seen an increase in the importance of the ECG signal in the initial diagnosis, prognosis, and survival analysis of cardiac illnesses, however all this heavily rely on the quality of ECG. Overall, ECG has a considerable impact on medical practise. Doctors use top quality ECGs to spot pathological and physiological phenomenas. Therefore, thorough ECG analysis is crucial for medical signal processing and analysis in order to control and monitor further medicine management.

2.1 ECG SIGNAL ANALYSIS TECHNIQUES

In the past, several researchers have employed a wide range of techniques to increase the diagnostic precision and ECG signal categorization. To name a few of these initiatives:

2.1.1 HIGHER ORDER STATISTICAL ANALYSIS: Many statistical techniques are available to extract information from random signals, such as the ECG. Higher Order Spectra (HOS) cumulants are a powerful tool for the investigation of nonlinear and non-stationary signals, such as the electrocardiogram (ECG). Most often, first and second order statistics are utilised. However, when nonlinearity in systems is present, many signals cannot be fully investigated using second order statistical techniques. As a result, more advanced statistical approaches have been developed. These methods are very useful when non-Gaussian, non-minimum phase, phase coupling, nonlinear behaviour, and resistance to additive noise are required. Higher Order Statistics and Spectra in Communication Systems were studied by Sanaullah [14], for application in communication and pattern recognition, higher level statistical and spectral approaches for detection and classification have been developed. Singoreto et al., [15] suggested a kernel function that makes use of the fourth-order cross-cumulant tensor spectral data that is connected to each multichannel signal. However, relevant connections to the system dynamics can be developed under specific modelling hypotheses.

Kernel functions for unstructured data do not make use of the underlying dynamism of multichannel signals. In addition to the above, Classification of Multichannel Signals using Cumulant-Based Kernels was carried out by Dah-Chung Chang et al. [16]. When the modulation type is adaptive, Automatic Modulation Classification (AMC), a classical topic in the field of signal classification, is frequently used. The fourth-order cumulant statistics are frequently used for modulation classification for typical modulation methods such as M-PSK & M-QAM. An association between the cumulants of the received signal and the multipath fading effects is created to address the channel impulse response.

2.1.2 NEURAL NETWORKS: Shivajirao M. Jadhav et al. [17] conducted ECG Arrhythmia Classification using Modular Neural Network Model; They divided arrhythmia into normal and pathological groups using the Modular Neural Network (MNN) model. The MNN model was built using one to three hidden layers, and it was trained using different training percentages in various data set divisions. However, the primary goal of this study was to produce accurate data for the categorization of arrhythmias only. Manab Kumar Das et al. [18] carried out Electrocardiogram (ECG) Signal Classification using S-transform, Genetic Algorithm and Neural Network; Argyro Kampouraki et al. [19] used Support Vector Machines (SVM) for Heartbeat Time Series Classification; In this work, SVM were used to classify heartbeat time series. With a very little amount of data, few characteristics were extracted from the signals of long-term ECG recordings of healthy patients and subjects with coronary artery disease using statistical approaches and signal processing techniques.

Shwetha Edla et al. [20] performed ECG Signal Modelling with Adaptive Parameter Estimation Using Sequential Bayesian Methods; In this article, authors suggested sequential Bayesian approaches for modelling and adaptively choosing ECG signal parameters. However, when real ECG data was used it provided limited success to illustrate the performance of the suggested algorithms. Kartik Audhkhshi et al., [21] studied Noise Benefits in Backpropagation; They made an effort to demonstrate how noise may hasten the backpropagation algorithm's convergence. The training data are directly increased by the noise. Both the neural network's backpropagation training and its deep bidirectional pre-training have a marginal advantage against noise. The probability structure of the neurons at each layer, determines how the noise benefit is shaped. A prohibited noise area created by logical sigmoidal neurons is located beneath a hyperplane. Kaiming He et al. [22] used Spatial Pyramid Pooling in Deep Convolutional Networks for Visual Recognition.

2.1.3 TYPE-2 FUZZY LOGIC SYSTEM: With the use of a straightforward Genetic Type-2 Fuzzy Logic System, I.A. Hameed et al. [23]; demonstrated that the high computational cost of type-2 fuzzy systems (T2FS) is a significant issue that prevents their widespread adoption in real-time applications, despite the benefits they provide in addressing uncertainty in control applications. A Genetic Algorithm (GA) gives the system a tool to identify and display the level of uncertainty it has assimilated, in addition to its role in offering flexibility to deal with changing situations. Researchers have discovered that T1FLS have trouble in modelling and reducing the impact of uncertainty. It takes a lot of computing power to type-reduce T2FS into T1FS so that the defuzzifier can process them and provide a clean result, especially when there are a lot of Membership Functions and a lot of rules. The General and Interval Type-2 Fuzzy Face-Space Approach to Emotion Recognition was used by Anisha Halder et al. [24] and Chia-Feng Juang et al. [25] studied-An Interval Type-2 Neural Fuzzy Classifier; In this study, an interval type-2 neural fuzzy classifier (IT2NFC-SMM) that learns through soft margin reduction is proposed and used to classify human body position with highly limited success.

2.1.4 MISCELLANEOUS METHODS: In addition to the approaches listed above, other techniques have occasionally been employed by various researchers for the delineation, modelling, and detection of ECG waveforms for biomedical signal analysis in general, including: In [26], the use of a Hidden Markov Tree model in a new ECG delineation technique is suggested. The two main goals of this method are to classify the various ECG waves using wavelet coefficients and to link these coefficients using a tree structure in order to identify wave changes. In Hermitian Function [27], to approximate the ECG signal, a piecewise modelling is provided. The majority of modelling techniques tried to produce the accurate representation of the whole ECG signal. This results in weighting each segment's approximation inaccuracy according to how significant it is over the whole ECG complex. As the outcome demonstrates, this approach's overall error is practically cut in half when compared to a comparable non-segmented method. Autoregressive (AR) modelling of cumulants is presented in [28] for improving ECG signals.

The fundamental idea behind the Wavelet Transforms approach [29] is to utilize the same data for Ventricular Premature Contraction (VPC) identification that was used for QRS detection, a step that is required by the majority of ECG classification algorithms. It is discovered that the computation of the proposed distinctive characteristics is significantly influenced by the R wave amplitude. This normalizing procedure enables accurate VPC identification while minimizing the impact of alternating R wave amplitude. However, using the same wavelet for QRS detection and VPC classification has two main drawbacks: it requires additional calculation and

implementation complexity. According to [83], a nonlinear approach may be used to recover the ECG signal's hidden information. In this study, they used Wavelet Packet Decomposition (WPD) of Higher Order Spectra (HOS) cumulants to automatically classify normal and pathological beats. Ventricular Premature Contractions (VPC) and Atrial Premature Contractions (APC) are the aberrant beats. To reduce the number of features, Principal Component Analysis (PCA) is applied to these Wavelet Packet Decomposition (WPD) with HOS cumulant features.

2.2 ECG DENOISING TECHNIQUES

The quality of the ECG signal is always lowered by noise [71]. Because the ECG signal changes over time, removing ECG noise is challenging. A high-quality ECG signal is required since it is utilized as the primary tool for diagnosing and analyzing cardiac problems. The cardiac irregularities can be seen in the ECG signal's minor amplitude and duration changes. It is challenging to identify cardiac problems due to aberrations in the ECG signal, such as Baseline Wander, Electromyogram (EMG), and Power Line Interference (PLI) at 50/60 Hz. Moreover, high-frequency disturbances, and equipment noise frequently damage ECG recordings. Several techniques for ECG signal denoising have been proposed in the literature, particularly for the elimination of low frequency noise, such as:

2.2.1 DIGITAL WINDOW-BASED FILTERS were first proposed by [30][31]. In the processing of low frequency signals, digital filters are crucial. These filters may be utilized in a variety of applications due to their adaptability, including isolating a QRS complex in an ECG signal, removing certain powerline frequencies, and simply reducing aliasing artefacts [30]. The three elliptic approximation filters are made and used on the live ECG data. With different limits, it is found that the newly introduced elliptic filter outperforms Butterworth, Chebyshev type I & type II [31]. The issue with them is that when a severe cut-off is employed, they generate ripples in the pass band. These ripples cause the shape of the ECG signal to change, which is improper from a diagnostic standpoint. Furthermore, the inaccuracy of the precise frequency cut-offs required for a window-based filter is demonstrated by the failure to apply Fourier Transforms to an ECG signal because of its non-stationary and non-linear characteristics.

2.2.2 ADAPTIVE FILTERS: The ability to distinguish the desired signal from disturbances brought on by power line interference, external electromagnetic fields, random body movements, and breathing is a major challenge in the processing of biological data such as ECG. In [32][33] [34], (LMS, NLMS, BLMS, and so on) were proposed as an upgrade over window-based filters. To exclude signal components from undesirable frequency bands,

several digital filters are utilized [32]. Filters with fixed coefficients are challenging to use to minimize biomedical signal noise. This issue needs to be solved using adaptive filtering techniques. The cancellation of noise in ECG data uses normalized adaptive filters [33], which are computationally better and have multiplier free weight update loops. These methods outperform previous Least Mean Square (LMS)-based realizations in terms of speed by primarily using basic addition and shift operations.

Before subtracting noise from the noisy ECG, it is necessary to estimate the noise from an external reference when using adaptive filters to minimize noise [34]. This is typically unhelpful because of the reference signal's weak correlation with the noise in the primary input. These strategies include active signal monitoring and noise prediction based on the difference between predicted and observed signals. Starting with the requirement for pure input signals in order to approximate how the signal differs, problems arise when using these for ECG filtering. Additional issues arise from the reference signals' poor match to the original data and the adaptive filter's minimal Mean Square Error [MSE] requirement.

2.2.3 WAVELETS: Although window-based filtering is preferable to adaptive filtering, there is still room for improvement. Due to recent developments in wavelet-based nonlinear signal processing, wavelets are being employed more and more in ECG denoising. A number of algorithms [36] [37] [38] have been developed on top of the Donoho et al. [35] as given in his thesis in the domain of ECG denoising. This work [36] proposes a unique approach based on the threshold value of ECG signal determination using Wavelet Transform coefficients. This study sought to examine the efficiency of wavelet denoising in multichannel high resolution ECG signal noise reduction [37], in particular, the effects of the wavelet function and decomposition level selections. This work used to suppress parasite electromyographic (EMG) signals (myopotentials) present in electrocardiogram (ECG) signals using the Wiener filtering in the shift-invariant wavelet domain with signal pilot estimate [38]. For pilot estimate, wavelet filtering with hybrid thresholding was utilized.

According to Luong et al. [39], the conventional wavelet method is ineffective in eliminating baseline wander noise. This issue was addressed by a fuzzy rule-based multi wavelet technique that helped to optimize pre and post filtering choices for a specific data collection [40]. The approach for weak ECG signal denoising presented in this work uses wavelet packet analysis and fuzzy thresholding. First, a wavelet packet transform is used to divide the faint ECG signal into several levels. After that, the fuzzy S-function is used to calculate the threshold value. The inverse wavelet packet transform is used to rebuild the ECG signal from the preserved coefficients [94].

2.2.4 EMPIRICAL MODE DECOMPOSITION (EMD): Huang suggested Empirical Mode Decomposition (EMD) as a cutting-edge technique for the analysis of non-linear non-stationary signals in his publication [41]. This is utilized in several algorithms and has been demonstrated to be highly successful in ECG filtering [42]. The majority of EMD research has, however, concentrated on reducing high-frequency noises. Denoising of ECG signals with the use of linear filtering (Butterworth Low Pass Filter) [43] produces superior results as compared to direct denoising by EMD method. Results from the combination of EMD and adaptive filters are better than those from the combination of EMD and linear filters. Combining EMD and wavelets can also be used to achieve ECG denoising [44]. This was modified even more by Zhang et al. [45]. This study investigated the energy of each Intrinsic Mode Function (IMF), and the noisy IMFs were found. The noisy IMFs were the only ones denoised using the Wavelet Soft Thresholding Technique. This speeds up calculation and is currently the most effective approach. All of these methods have the drawback of being unable to handle Baseline Wander noise since they are developed to handle signals with lower IMFs or high frequency components.

In a study by Zhi-Dong Zhao et al. [46], EMD was utilized for baseline wander denoising for the first time. The residual signal, which was used to approximate baseline wander, was left out in order to account for noise in the ECG signal. In order to advance this field, Na Pan et al. [47] divided the signal into 15 IMFs, assuming that the final three IMFs primarily consisted of noise components. Thus, the baseline drift was adjusted by removing the latest three IMFs. These initiatives have limitations as a result of the limited signals they were tested on and the lack of an appropriate mechanism to work with various IMFs. Additionally, it has been shown that the EMD's inherent ability to denoise is inadequate [48] [49]. To get the best possible outcomes, it should be used in conjunction with another strategy. The two primary drawbacks of the EMD are its susceptibility to noise and its mode mixing feature, which introduces inaccuracy into the recorded signal [50].

Empirical Mode Decomposition was the foundation for the de-noising method for ECG data developed by Anil Chacko* et al. [66]. The noisy ECG signal is broken down using the EMD approach into sequences of Intrinsic Mode Functions (IMFs). The IMFs controlled by noise are spontaneously determined by Spectral Flatness (SF). These noisy IMF's noise is filtered out using Butterworth filters. Its Signal to Noise Ratio (SNR) is greater and its Root Mean Square Error is less than Wavelet Transform de-noising (RMSE). The most significant weakness of EMD is the mode mixing consequence. When oscillations of different time scales coexist in one IMF or when oscillations of different time scales are allocated to different IMFs,

this is referred to as mode-mixing. All of these techniques have drawbacks, including mode mixing, oscillation in reconstructed signals, decreased ECG signal amplitude, and degeneracy, to name a few.

2.2.4.1 ENSEMBLE EMPIRICAL MODE DECOMPOSITION (EEMD): To address the above-mentioned issues related with EMD, Huang suggested an Ensemble Empirical Mode Decomposition (EEMD) system [51], which was later improved [52], resulting in a numerically negligible error. Although EEMD has been used to denoise ECG [53], it has had some of the same issues with inadequate denoising strength on its own. With the help of averaging, this solves the problem of mode mixing and oscillations. However, this has a few drawbacks: it is computationally expensive, and the final amplitudes associated with the IMFs are greatly reduced due to the uneven number of modes across the ensemble [54]. An enhanced Ensemble Empirical Mode Decomposition (EEMD) based methodology called Complete Ensemble Empirical Mode Decomposition (CEEMD) requires fewer iterations than the EEMD method, making it computationally more efficient. Additionally, CEEMD appropriately reconstructs the input signal from the extracted modes after decomposing the signal up to the lowest or final level.

2.2.5 MISCELLANEOUS METHODS: The following have been attempted and tested by a number of researchers and scientists in the past:

Artificial Neural Networks [ANN]; are a type of data processing based on how the human brain works. Their efficiency has been diminished by the fact that their application for filtering has been restricted to PLI and electrode motion noise [55] and is reliant on signal reconstruction utilizing pre-existing biological signals. Additional studies, like that of [56], solely utilized the direct noisy values of the ECG signals as input and discovered that networks trained on the direct values were overfit and had a reduced capacity to filter fresh ECG signals. EMD in conjunction with neural networks has been widely employed for the prediction of non-linear non-stationary signals [57] [58]. In Cascade Combination of EMD and Morphological Functions; Mahipal Singh Choudhry et al. suggested employing a cascade combination of the EMD and Morphological function to remove low frequency artefacts from ECG readings. In a another publication, Mahipal Singh Choudhry and Rajiv Kapoor recommended the use of CEEMD and Adaptive Morphological Function [59] for ECG denoising.

Combined Empirical Mode Decomposition and Wavelet Thresholding; Wavelet thresholding and Empirical Mode Decomposition were used in a hybrid technique proposed by B. Pradeep Kumar et al. [61]. Intrinsic Mode Function (IMF) sequences are created using an EMD to separate noisy ECG signals. With wavelet thresholding, noise in a decomposed signal may be

removed. Thus, the hybrid approach has improved the de-noising signal's performance. The hybrid technique is also better than the wavelet transform method in terms of SNR. Noise from the power lines and baseline drift noise are both eliminated.

Un-Decimated Wavelet Transform; In their de-noising technique, V. Naga et al. [62] included an un-decimated wavelet transform. Using this method, the raw ECG signal is deconstructed. This method uses the shrinking process to clean up an unsteady ECG signal. The shrinkage phase makes use of semi-soft and stein block thresholding in addition to conventional soft and hard thresholding. It verified that multiple wavelets might be used to de-noise ECG data. It provided smoother, more stable, and more precise results as compared to the Discrete Wavelet Transform (DWT). The wavelet transform methodology has the following shortcomings as a denoising method for ECG signals: (i) The reconstructed ECG signal may oscillate due to hard thresholding. (ii) Soft thresholding may reduce the ECG waveform amplitudes, especially the R waves, which are more important for identifying cardiac diseases.

Morphological Methodology; A morphological method was recommended by Zhongguo Liu et al. [63] to reduce noise in ECG data. The structural components are available in a wide range of sizes. The different ECG signals and noise environments are processed using these structural elements. Although this filter does a decent job at lowering noise, but it only corrects the baseline drift issue.

Hilbert-Huang Transform; Changnian Zhang et al. [64] suggested a Hilbert-Huang Transform-based technique for de-noising electrocardiogram (ECG) signals. For signal processing, this transform contains two stages. The original dataset is first converted into 'n' number of IMFs using the EMD technique, and then the components of these IMFs are transformed using Hilbert transforms. In comparison to the wavelet de-noising method, it is a simpler approach.

Grid Search Approach; Grid search was used by Dong, Dai, et al. [65] to identify the optimal parameters that resulted in the least amount of multi-scale complexity, but the multi-scale complexity calculation was difficult and not appropriate for small sample data. Based on the recently developed noise invalidation approach, an ECG denoising strategy is presented in this study [67]. By excluding coefficients that are less than the suggested threshold, the approach offers an adaptive data dependent threshold that may be used to denoise ECG signals in an orthogonal basis of choice. By denoising a collection of ECG signals that have been tainted by various sources of noise, the performance of the noise invalidation approach is assessed using mean square error.

In the realm of image processing, patch-based techniques have received a lot of attention recently addressing a number of issues including denoising, inpainting, and super-resolution

interpolation [68]. Investigated the use of the Non-Local Means (NLM) approach, one such technique, for the denoising of biological data. Metrics measuring the denoised waveform's distortion are reduced more significantly, for the ECG as an example. Baseline drift, powerline interference, and other electromagnetic interferences are the three main causes of noise in ECG signals [69]. Frequency transformation techniques are becoming increasingly important for removing noise from ECG signals as a result of the Wavelet transform's recent success in recognizing and removing noise from a wide range of signals. This study uses the S-transform to remove baseline wander from ECG data, and the suggested strategy is then contrasted with one based on the wavelet transform.

There has been another two-stage ECG signal denoising method suggested in [70]. In the translation-invariant wavelet domain, it combines wavelet shrinkage with Wiener filtering. To achieve a more precise signal estimate in the first phase of the approach, a time-frequency dependent thresholding has been created and used. It performs better than other thresholding methods in this region since it is connected to the shape of the ECG signal. This study presents an overview of several sorts of disturbances that damage ECG signals.

It can be difficult to suppress electromyographic (EMG) noise in electrocardiogram (ECG) signals because it typically has an impulsive character and a broad-spectrum content that overlaps the ECG as in [95]. Gaussian noise modelling has been used to suppress EMG signals in the majority of prior attempts. Due to the high-level EMG noise that commonly couples with the ECG signals during exercise, their approaches are largely insensitive to this noise. A particle filter (P) based technique is created for the denoising of non-Gaussian and non-linear ECG data in order to get around this restriction, but with the problem of PF sample degeneracy. In order to address the above-mentioned issue and as well as the parameters selection issue in the Ensemble Empirical Mode Decomposition (EEMD) algorithm, [96] suggested an improved EEMD method based on genetic algorithm better known as GAEEMD, however results were not so promising.

2.3 RESEARCH GAPS

- The Higher Order Spectra (HOS) using Cumulants (HOC) have only recently been employed in the field of biomedicine, specifically for the classification of ECG waveforms. The application of Higher Order Spectra (HOS) using cumulants in the domain of ECG signal analysis and classification is still highly insufficient. Therefore, the extensive research using Higher Order Spectra (HOS) in the domain of ECG signal
- analysis and classification is still highly insufficient. As a result, this analysis and classification method can also be used effectively and efficiently for the analysis and classification of ECGs with the appropriate level of accuracy.
- In addition to the above, the motivation for using cumulants for ECG analysis are: a) ECG signals are largely non-linear & non-Gaussian signals & they are easily ratified by 3rd and 4th order statistics as they manifest quadratic and other higher-order non-linearities; b) ECG signals are comparatively easy to detect and classify either using the bi-spectral or tri-spectrum contours; c) ECG signal can be easily processed in Gaussian noise-free domains.
- The majority of available ECG denoising techniques tend to filter out most of the noises, but causing information loss. One of the most typical ECG artefacts is the baseline drift. Especially when the patient's breathing rate increases, this artefact is commonly observed during stress ECGs. All of these morphological alterations are typical and required for diagnosis, though the majority of available denoising techniques tend to reduce these but again at the cost of distorted ECG signal. Therefore, in this thesis, it is proposed that baseline drift be corrected.
- The fact that baseline wander hasn't received as much attention in the literature as PLI and other forms of noises for which there are plenty of effective denoising techniques are available. Therefore, it is another factor in our decision to use baseline wander for denoising. Accordingly, a combination of CEEMD and Artificial Neural Network [ANN] in our proposed algorithm is used to remove low frequency artefacts from ECG signals. The use of CEEMD eliminates the intrinsic flaws in EMD while also ensuring that the Neural Network does not overfitted.
- The use of a genetic particle filter lowers the degeneracy of particle filter samples. AEEMD is used in this thesis instead of EMD since it solves the mode-mixing issue with EMD. AEEMD offers more adaptation and robustness in the noisy ECG signal filtering field.

Bio-Medical Signal Measurement [PART-II]

2.4 BIOIMPEDANCE MEASUREMENT

Bioimpedance is the resistance provided by a living tissue. Bioimpedance assessment is a non-invasive, low-cost, and popular method for determining body composition measures as well as for evaluating nutrition and health. Engineers and scientists have periodically made a great deal of attempts to build and create devices, components, and systems to measure bioimpedance non-invasively. A few of these endeavors include:

2.4.1 COLE PARAMETERS: It is challenging to identify between plant and animal tissues using bioimpedance due to the wide variation of Cole parameters. A unique electronic method for identifying fruit or vegetable tissue is described in [72]. In order to calculate bioimpedance and Cole parameters in the frequency range of 1 Hz to 1 MHz, this system employs a pair of specially made electrodes [72]. In-depth data analysis is done after measuring bioimpedance in the above-mentioned frequency range for apple and potato tissues. The parameters of bioimpedance and the characteristics of cellular structure exhibit a strong association. The voltage output across the cell and tissue is measured after an alternating current injection to ascertain it. However, resistive and capacitive components make up the impedance of human cell and tissue [5, 6] that creates the perceptible variability of Cole parameters that with of plant tissues.

2.4.2 STEPPED-SINE EXCITATIONS: According to [73], Linear Time-Varying (LTV) bioimpedance is measured with a specific degree of precision using stepped-sine excitations. The temporal distortions impacting the data rely on the experimental time, which in turn establishes the data accuracy and restricts the temporal bandwidth of the system that has to be evaluated when measuring linear time-varying (LTV) bioimpedance using stepped-sine excitations. However, due to temporal distortions that might damage the data, the device's temporal bandwidth is constrained and the data accuracy is undermined.

2.4.3 TRANSFER FUNCTION APPROACH: The fundamental building parts of an bioimpedance measuring instrument are the current source and voltage sensor circuit. Numerous researchers have fabricated current sources that operate up to a few hundred kHz with success [74]. The basic component of the system is a monolithic operational amplifier, and the signal current is recovered from the amplifier's power supply leads using a modified current mirror. In order to achieve high drive capability with low amounts of quiescent current,

the entire circuit runs in class-AB mode. In order to quantify the load impedance, Paul Annus et al. [75] used a load-in-loop configuration and a transfer function methodology to systematically assess the design of a current source. The analysis is carried out for the aforementioned load-in-loop current source circuit topology and is generalized to include the grounded load impedance. But it is applicable for comparing the observed data with the theoretical and simulated outcomes only.

2.4.4 VOLTAGE SENSING CIRCUIT consists of amplifier, demodulator and low pass filter. Areny and Webster [76] have examined the usage of instrumentation amplifier for bioimpedance measurements. The measurement method has been applied in a variety of contexts, including the estimation of Total Body Water (TBW), Intra-Cellular Fluid (ICF), and Extra-Cellular Fluid (ECF) [5], Electrical Cardiometry [77], Skin Water Content, Impedance Imaging (Tomography), Ablation Monitoring, and measurement of Respiration Rate [78]. Additionally, the method may be used to biometrics [79]. Examples of bioimpedance applications that are discussed and analyzed in [80] include skin conductance, Electrical Impedance Tomography (EIT), skin composition assessment, and transthoracic impedance pneumography. In-depth analysis of bioimpedance systems for medical applications is developed in this study. Applications of bioimpedance such as Electrical Impedance Tomography (EIT), Impedance Cardiography (ICG), Transthoracic Impedance Pneumography, and skin conductance are described and studied.

2.4.5 NON-INVASIVELY TRACKING BLOOD GLUCOSE LEVELS: [81] examined the potential for monitoring blood glucose levels non-invasively utilising bioimpedance data, which would enable more frequent testing and improved diabetes treatment and monitoring. The measurement of resistance (R) and capacitive reactance (X_c), which is carried out using an analogue instrument, is made possible by the passage of a small amplitude electrical current with a certain frequency delivered through leads attached to electrodes placed on the human body. Current may flow through extracellular fluids at low frequencies, but at high frequencies, it can enter cells and intracellular fluid. The efforts are focused on examining the potential for non-invasively monitoring blood glucose levels using bioimpedance data, which would enable more frequent testing and more stringent management of diabetes. Using ANFIS, an adaptive estimating method, the bioimpedance values obtained from various individuals are evaluated for various other subjects after being trained against the real value of blood glucose obtained using the standard clinical procedure.

2.5 MISCELLANEOUS METHODS: In addition to the above following effort were also made to design and develop the non-invasive bioimpedance based measurements:

Bioimpedance analysis is a non-invasive, affordable, and frequently employed method for determining body composition and evaluating clinical status. There are several approaches used to analyse measured bioimpedance data, and bioimpedance is widely used to estimate body composition and assess clinical state. Bioelectrical impedance techniques can be used for non-invasive tissue characterisation since living tissues create a complex electrical impedance under alternating electrical stimulation that is dependent on tissue composition, architecture, health condition, and applied signal frequency.

In bioimpedance spectroscopy, the complex impedance of living tissues is measured across a wide frequency range [97]. For physiological investigations or health monitoring systems, this strategy is very practical. Devices need to be portable, wearable, or even implanted for a variety of purposes. Thus, the implementation of the next generation of bioimpedance sensing systems must take into account resource and power reductions. Impedance measuring techniques may be categorised into two groups. While others rely on "multi-tone" signals, some are based on "single-tone" signals. However, both strategies are rarely appropriate for embedded applications. Moreover, both strategies are quite noise sensitive.

The required frequency range for bioimpedance measurements depends on the object's dielectric characteristics and is normally between 3 and 4 decades in the kHz to MHz region [98]. The number of frequency components employed determines how accurately the equivalent circuit-based impedance model fits the test findings. In general, using higher frequencies makes fitting more accurate but makes measurements more challenging. However, the signal to noise ratio (SNR) of the measurement signals also affects the accuracy of the fitting. It follows that the number of frequency components employed has two opposing effects on how well the comparable circuit model's parameters are estimated. The essential principles of bioimpedance measuring methods, such as frequency-based, allocation-based, bioimpedance vector analysis, and real-time bioimpedance analysis systems, were reviewed in [99]. The effect of anthropometric measures, gender, ethnicity, ethnic groups, postures, measuring techniques, and electrode artefacts on predicted results is also explored, as well as commonly used prediction equations for body composition evaluation.

In order to reduce the electrode-skin impedance that naturally occurs, gel electrodes are used for the majority of bioimpedance tests. The usefulness of dry electrodes is examined in [100] since this type of electrode is frequently inappropriate in measuring conditions. The electrode-skin impedances are measured when signal frequency, contact time, contact pressure,

placement location, and subjects were changed in order to compare the properties of the electrodes. Additionally, for comparison, all tests were carried out using hydrogel electrodes made of silver and silver chloride (Ag/AgCl). The electrode-skin impedance of dry electrodes can be reduced to ranges of hydrogel electrodes and even lower by wisely setting these parameters. However, when converting scientific measuring techniques to clinical settings or commercial products, using dry electrodes is one of the most challenging tasks.

Electrical impedance measurements can be distinguished between tissues with various electrical characteristics as discussed in [100]. The kind of tissue in which the needle tip is located can be determined using a measuring instrument with sufficient spatial resolution focused on a volume around the tip. Generally, Electrode Polarisation Impedance (EPI) have an impact on small electrode impedance values at low frequencies. [102] proposes a different technique for measuring impedances that uses voltage excitation with a fixed amplitude. The technique, which may be easily applied to bioimpedance measurement with electrode sensors, uses the feedback principle to adjust the measurement parameters to the load being tested.

[103] focused on cell coverage and other significant parameters, such as the cell-electrode gap, that may be determined by observing impedance changes brought on by cell development on microelectrodes. The measured bioimpedance immediately reflects the presence and movement of the cells as they adhere to the electrodes [104]. The tetrapolar electrode arrangement is used in the bulk of investigations regarding bioimpedance measurement. However, the measuring current spreads from the current-carrying electrodes in a multi-layered tissue volume, causing unforeseen issues that are addressed as a negative sensitivity issue as demonstrated in [105]. It compared the outcomes obtained by bipolar and tetrapolar bioimpedance devices in order to explore this issue on the bioimpedance measurements of the upper and lower limbs.

[106] suggested that when selecting a material for an implanted electrode, the following five factors must be taken into account: (i) Radiographic visibility, (ii) Tissue Response, (iii) Allergy Response, (iv) Electrode-Tissue Impedance, and (v) Tissue Response. In [107], authors demonstrated that Electrode Polarisation Impedance (EPI), which is generally shown as a distinct dispersion, can be distinguished from measured tissue impedance provided that the characteristic frequencies of the tissue and EPI are not too near to one another. In a clinical context, it is crucial to continually and non-invasively monitor the heart pumping performance as discussed in [108]. In order to evaluate the changes in stroke volume, the study investigated a regional impedance plethysmography approach.

The current driver, which can work across a wide range of impedance and frequency, is a crucial element in bioimpedance studies as elaborated in [113]. High output impedance, little phase delay, and little harmonic distortion are crucial characteristics for current drivers. Based on whether they are open loop or closed loop designs, the analogue current drivers are divided into two types in this study. Historically, only low frequencies, typically below 100 kHz, have been employed to evaluate electrical bioimpedance for medical diagnostic reasons [114]. However, this research only looked at the resistive portion of the impedance; neglected the reactive portion treating it as highly insignificant at low frequencies. The output current from a source must be practically continuous across the desired frequency range and irrespective of the load at the output. Over the years, a number of designs have been put forth, however their performance all significantly declined at frequencies below 1 MHz [116] modified impedance cardiography, for the purpose of measuring cardiac output during stress testing.

Impedance Plethysmography (IPG) is a straightforward, inexpensive, and non-invasive method for evaluating the flow of blood throughout the body's core and periphery [118]. [119] provided the better understand of the morphology, physiology, and pathology of biological tissues by conducting an impedance study over a broad frequency range, since the impedance responses of various tissue characteristics change with the frequencies of the applied signal. Electrical Impedance Spectroscopy (EIS), Impedance Plethysmography (IPG), Impedance Cardiography (ICG), and Electrical Impedance Tomography (EIT) are a few of the impedance-based non-invasive tissue characterization techniques that have been proposed over the past few decades.

[120] Implemented the monitoring techniques for real-time, non-invasive, non-destructive evaluation of the viability and properties of the cell cultures. A non-invasive, label-free, and real-time approach for monitoring tissue engineered structures is provided by the bioimpedance measuring technique, which capitalises on measurements of the electrical characteristics of living tissues.

2.6 RESEARCH GAPS

- There is utter lack of non-invasive method for medical diagnostics, therefore in this scenario bio-impedance based low-cost method can be of immense help for medical diagnosis. Although the bioimpedance measurement is not a brand-new method for biomedical diagnosis, research is currently being done to turn this non-invasive method into a norm for a particular disease's diagnosis.
- For proper prognosis, a significant quantity of data must be gathered for each disease, for each environmental society, and analysis must be performed to link the disease to the signal captured. In order to achieve this goal, we designed and developed a low-cost apparatus that accurately records the bioimpedance signal using conventional analogue signal processing blocks.

2.7 OVERALL RESEARCH OBJECTIVES

This research is focussed on development of accurate and reliable analysis of ECG signal and its appropriate denoising. Moreover, a serious attempt has been made to design and develop a state of art, low-cost bioimpedance measuring instrument. Overall, following objectives have been considered for analysis and investigation in the present study.

RESEARCH OBJECTIVE-1

- The main research objective of ECG analysis using Higher Order Cumulants is to increase the precision with which ECG waveform classification is performed since it offers a thorough assessment of non-linearity and produces superior outcomes in terms of time complexity. Additionally, in contrast to the other techniques previously employed in this study domain, it offers a quality analysis and detection tool.

RESEARCH OBJECTIVE-2

- It's always crucial to clean up or denoise the ECG signal so that the patient's cardiac activity is not misunderstood. Here, it's carried out utilizing:

ANN and CEEMD

GP-F Improved fuzzy-AEEMD

RESEARCH OBJECTIVE-3

- In this work, a reliable and affordable bioelectrical impedance measurement device was designed, developed and evaluated. It is primarily built on the low-cost component-level approach to make it simple for researchers and investigators in the specific domain to utilise.

CHAPTER 3

ECG SIGNAL ANALYSIS USING HIGHER ORDER CUMULANTS

3.1 INTRODUCTION

In general, ECG provides indicative information for most of the cardiac ailments such as heart attack, angina, myocardial infarction, cirrhosis, or sudden cardiac arrest etc. The doctors especially cardiologist uses ECG to acquire first-hand knowledge about the well-being of human heart. However, higher level of radio diagnostic tests such as TMT (Tread-Mill Test) Echocardiography etc. are required to establish a particular type of heart problem so as to carry out subsequent cardiac treatment and proper medicine management. Though, an early diagnosis through ECG allows to select the appropriate cardiovascular medicine management for the time being, which can prove effective and timely relief to heart patients. The domain of electrocardiogram analysis has been explored by many researchers previously as a part of the electrocardiogram based symptomatic treatment and classification. These studies were conducted using both experimental and non-experimental measurements.

The main purpose of ECG analysis is to improve the accuracy of ECG waveform classification. With the aid of appropriate analysis methods, the ECG classification can be more accurate and quicker during the study. Therefore, evaluation of previous ECG analysis algorithms is a significant aspect; however, it still needs in-depth research as on date. According to an analysis by the PubMed Central Journal Report 2021 by Population Studies Center, heart disease is the foremost cause of death in both urbanized and developing countries. Therefore, ECG-based cardiac signal acquisition and classification is always quite effective in early diagnosis and treatment of heart ailments. Thereafter, in addition to this, ECG can also be used effectively for other non-medical applications such as biometrics, person identification etc., but in such cases large amount of ECG data is required to be processed and classified to obtain desired results. This process is quite complicated, tedious and time consuming.

The appropriate analysis of the ECG signals using suitable means is of utmost importance, before any diagnostics. Therefore, to fulfill this requirement the higher order cumulants are an effective mathematical tool for the analysis of nonlinear and non-stationary ECG signals. When

studying non-linear data, the motivation for utilizing cumulants is to attenuate Gaussian noise processes with uncertain spectral properties. Till recently higher order cumulants haven't been used much in the field of biomedicine, especially for ECG waveform analysis, accordingly this classification method can also be used effectively and efficiently for ECG analysis and classification with appropriate level of accuracy.

The proposed method classifies dataset of ECG signals based upon higher order statistics i.e., using cumulants. This method is a comprehensive measure of non-linearity and gives better results in terms of time complexity. It provides a quality detection technique in comparison to the other methods used earlier in this research domain. Few of these methods are Principal Component Analysis (PCA), Hermitian function, Hidden Markov Tree model etc. The proposed method also compares this higher order statistics classification obtained using different classifiers such as SVM, Fuzzy-2 and DSNM to find the best classifier.

3.2 THEORETICAL BACKGROUND

3.2.1 CUMULANTS

The cumulants Q_n of a probability distribution are a set of values that give an alternative to the distribution's moments in probability theory and statistics. The cumulants determine the moments in the same way that the moments do. Any two probability distributions with identical moments will have identical cumulants, and vice versa. The first cumulant is the mean, the second cumulant is the variance, and the third cumulant is the same as the third central moment. Fourth and higher-order cumulants, on the other hand, are not equivalent to central moments. In some circumstances, theoretical solutions based on cumulants are easier to understand than solutions based on moments. The n th-order cumulant of the sum of two or more random variables is equal to the sum of their n th-order cumulants when they are statistically independent. A normal distribution's third and higher-order cumulants are also zero, and it is the only distribution that has this property. It is feasible to define joint cumulants in the same way that joint moments are used for collections of random variables.

In measurement hypothesis and applied math, the cumulants Q_n is the sum of the values that change according to the moment of distribution. The cumulants of a random variable X are calculated using the cumulant-generating function $g(t)$, which is written as

$$g(t) = \log E[e^{tX}] \quad (3.1)$$

Here $E[e^{tX}]$ represents statistical expectation.

Chapter 3: ECG Signal Analysis Using Higher Order Cumulants

The cumulants Q_n are generated from a power series expansion of the cumulant generating function:

$$g(t) = \sum_{n=1}^{\infty} Q_n \frac{t^n}{n!} \quad (3.2)$$

$$= Q_1 \frac{t}{1!} + Q_2 \frac{t^2}{2!} + Q_3 \frac{t^3}{3!} + \dots \quad (3.3)$$

$$= \mu t + \sigma^2 \frac{t^2}{2} \quad (3.4)$$

This expansion is a Maclaurin series, to get the nth cumulant, differentiate this extension n times and calculate the result at $t = 0$ as given below:

$$Q_n = \frac{\partial^n}{\partial t^n} g(t) |_{t=0} \quad (3.5)$$

The two-stage statistical analysis, such as autocorrelation, uses random data as a model, but suppresses phase information, thus allowing only low-level signal analysis. To evaluate low phase signals, such as ECG signals, a high-phase spectrum is required. Therefore, this high-quality spectrum can be defined in terms of moments and cumulants. In general, the relationship between the first few moments and cumulants can be easily obtained by extracting coefficients from the equations as follows:

$$Q_1 = \mu_1 \quad (3.6)$$

$$Q_2 = \mu_2 - \mu_1^2 \quad (3.7)$$

$$Q_3 = \mu_3 - 3\mu_2\mu_1 + 2\mu_1^3 \quad (3.8)$$

$$Q_4 = \mu_4 - 4\mu_3\mu_1 - 3\mu_2^2 + 12\mu_2\mu_1^2 - 6\mu_1^4 \quad (3.9)$$

or conversely,

$$\mu_2 = Q_2 + Q_1^2 \quad (3.10)$$

$$\mu_3 = Q_3 + 3Q_2 Q_1 + Q_1^3 \quad (3.11)$$

$$\mu_4 = Q_4 + 4Q_3 Q_1 + 3Q_2^2 + 6Q_2 Q_1^2 + Q_1^4 \quad (3.12)$$

where,

$Q_1 = \mu_1$ is the mean of some random variable X and Q_2 is the variance or second central moment. However, higher order cumulants are not the same as moments about the mean. If $x(n)$, $n = 0, \pm 1, \pm 2, \pm 3, \dots$ is a real stationary discrete-time signal and its moments up to order p exist, then:

$$p_p(\tau_1, \tau_2, \dots, \tau_{p-1}) = E[x(n) \cdot x(n+\tau_1) \dots x(n+\tau_{p-1})] \quad (3.13)$$

Chapter 3: ECG Signal Analysis Using Higher Order Cumulants

Here, $E[.]$ signifies statistical expectation, which reflects the stationary signal's p th order moment function, which is exclusively dependent on time differences $\tau_1, \tau_2, \dots, \tau_{p-1}$. $T_i = 0, \pm 1, \pm 2, \dots$ for all ' i '. The first order cumulant, which yields the distribution's mean value, may now be defined as:

$$Q_1 = p_1 = E[x(n)] \quad (3.14)$$

where p_1 is the first order moment of the first order cumulant of a real stationary discrete-time signal. The equation for the second order cumulant is:

$$Q_2(\tau) = p_2(\tau) - p_1^2 \quad (3.15)$$

$p_2(\tau)$ stands for second order moment, also known as autocorrelation, while $Q_2(\tau)$ stands for second order cumulant, also known as variance. Then there's the third order cumulant, which is denoted by

$$Q_3(\tau_1, \tau_2) = p_3(\tau_1, \tau_2) - p_1[p_2(\tau_1) + p_2(\tau_2) - p_2(\tau_1 - \tau_2)] + 2p_1^3 \quad (3.16)$$

where $p_3(\tau_1, \tau_2)$ is the third order moment. The third-order cumulants are identically zero when the input signal has a symmetrical probability density function. Bernoulli-Gaussian random variables and signals with Laplace distribution are examples of such situations. In such cases, it is vital to make full use of the fourth order cumulant's non-Gaussian features. The equation for the fourth order cumulant is:

$$Q_4(\tau_1, \tau_2, \tau_3) = p_4(\tau_1, \tau_2, \tau_3) - p_2(\tau_1) \cdot p_2(\tau_3 - \tau_2) - p_2(\tau_2) \cdot p_2(\tau_3 - \tau_1) - p_2(\tau_2 - \tau_1) \cdot p_2(\tau_3) - p_1[p_3(\tau_2 - \tau_1, \tau_3 - \tau_2) + p_3(\tau_2, \tau_3) + p_3(\tau_2, \tau_4) + p_3(\tau_1, \tau_2)] - (p_1)^2[p_2(\tau_1) + p_2(\tau_2) + p_2(\tau_3) + p_2(\tau_3 - \tau_1) + p_2(\tau_3 - \tau_2) + p_2(\tau_2 - \tau_1)] - 6(p_1)^4 \quad (3.17)$$

where $p_4(\tau_1, \tau_2, \tau_3)$ is the fourth order moment.

The second and third order cumulants are equal to the second and third order moments, respectively, if the signal $\{x(k)\}$ has a zero mean $p_1 = 0$. However, in order to create the fourth-order cumulants, we need to know the fourth-order and second-order moments in the equation provided below:

$$Q_4(\tau_1, \tau_2, \tau_3) = p_4(\tau_1, \tau_2, \tau_3) - p_2(\tau_1) \cdot p_2(\tau_3 - \tau_2) - p_2(\tau_2) \cdot p_2(\tau_3 - \tau_1) - p_2(\tau_2 - \tau_1) \cdot p_2(\tau_3) \quad (3.18)$$

In reality, dealing with cumulants rather than moments in the case of non-stationary signals is more usual and preferred due to the second characteristic function's distinctive linear quality. As a result, higher order spectra are commonly characterised as their (n-1) dimensional Fourier transformations in terms of nth-order cumulants.

If these cumulants are analysed in the frequency domain, the Fourier transform of these cumulants may be produced. The third order cumulant's Fourier transform is written as

Chapter 3: ECG Signal Analysis Using Higher Order Cumulants

$$\begin{aligned}\beta(\omega_1, \omega_2) &= X(\omega_1) X(\omega_2) X^*(\omega_1 + \omega_2) \\ &= \sum_{n_2=-\infty}^{\infty} \sum_{n_1=-\infty}^{\infty} (Q_3(\tau_1, \tau_2) \cdot \exp \exp(-j2\pi(\omega_1 n_1 + \omega_2 n_2)) \sum_{n_2=-\infty}^{\infty} \sum_{n_1=-\infty}^{\infty} (Q_3(\tau_1, \tau_2) \cdot \exp \exp(-j2\pi(\omega_1 n_1 + \omega_2 n_2))\end{aligned} \quad (3.19)$$

where $\beta(\omega_1, \omega_2)$ is the Bi-spectrum of $x(n)$, $Q_3(\tau_1, \tau_2)$ is the third order cumulant and $X(\omega)$ is the Fourier transform of $x(n)$. Similarly, the fourth order cumulant's Fourier transform is tri-spectrum, and it is written as

$$\begin{aligned}\Gamma(\omega_1, \omega_2, \omega_3) &= X(\omega_1) X(\omega_2) X(\omega_3) X^*(\omega_1 + \omega_2 + \omega_3) \\ &= \sum_{n_3=-\infty}^{\infty} \sum_{n_2=-\infty}^{\infty} \sum_{n_1=-\infty}^{\infty} (Q_4(\tau_1, \tau_2, \tau_3) * \\ &\quad \exp \exp(-j2\pi(\omega_1 n_1 + \omega_2 n_2 + \omega_3 n_3)) = \\ &\sum_{n_3=-\infty}^{\infty} \sum_{n_2=-\infty}^{\infty} \sum_{n_1=-\infty}^{\infty} (Q_4(\tau_1, \tau_2, \tau_3) * \exp \exp(-j2\pi(\omega_1 n_1 + \omega_2 n_2 + \omega_3 n_3))\end{aligned} \quad (3.20)$$

where $\Gamma(\omega_1, \omega_2, \omega_3)$ is the Tri-spectrum of $x(n)$, $Q_4(\tau_1, \tau_2, \tau_3)$ is the fourth order cumulant.

The cumulants are more preferable than moments because of having a number of additional advantages over moments such as:

- a) If $x_i, i=1, 2, \dots, N$ are random variables and $\alpha_i, i= 1, 2, \dots, N$ are constants, then $\text{cum}(\alpha_1 x_1, \alpha_2 x_2, \dots, \alpha_N x_N) = \prod_{i=1}^N \alpha_i \text{cum}(x_1, \dots, x_N)$.
- b) If a subset of N random variables $\{x_i\}$ is independent, then $\text{cum}(x_1, \dots, x_N) = 0$.
- c) Cumulants are additive in nature, i.e., $\text{cum}(x_0 + y_0, z_1, \dots, z_N) = \text{cum}(x_0, z_1, \dots, z_N) + \text{cum}(y_0, z_1, \dots, z_N)$.
- d) If the random variables $\{y_i\}$ are independent of the random variables $\{x_i\}, i= 1, 2, \dots, N$ then $\text{cum}(y_1 + x_1, \dots, y_N + x_N) = \text{cum}(y_1, \dots, y_N) + \text{cum}(x_1, \dots, x_N)$.
- e) If μ is a constant then $\text{cum}(\mu + x_1, x_2, \dots, x_N) = \text{cum}(x_1, x_2, \dots, x_N)$.

Because the third-order cumulant of a symmetric distribution equals zero, we must utilise fourth-order cumulants in such circumstances. Because certain processes have distributions with extremely small third-order cumulants and considerably larger fourth-order cumulants, we would employ the fourth-order cumulant or the tri-spectrum in these cases as well. In the

categorization of ECG signals, cumulants have never been employed. Third order cumulants were employed in [82] to obtain symmetry in the signal, which is then used for AR modelling, which aids in the enhancement of the ECG signal. This property of symmetry of every signal, may be utilised to classify it. The [83] uses this aspect of non-stationary signals to distinguish normal and abnormal non-stationary beats.

Results from various researches shows that the third and fourth order cumulants are insensitive towards noise and hence can be directly applied on the signals. There is no requirement of pre-processing when using the higher order cumulants. As a result, 3rd and 4th order cumulants have been employed in this suggested technique since 3rd order cumulant is concerned with skewness and 4th order cumulant is concerned with kurtosis. Skewness is a measure of any

Chapter 3: ECG Signal Analysis Using Higher Order Cumulants

distribution's asymmetry around its mean. Positive skew means the left side's tail is shorter or thicker than the right sides. Skewness does not follow the expected rule when one tail is short and the other is thick. A zero value, for example, indicates that the tails on both sides of the mean are balanced, as in a symmetric distribution.

Between the four types of ECG datasets utilised, there is some asymmetry in the waveforms. The peaked-ness of any ECG waveform is represented by the breadth of its peaks, and the kurtosis of a signal is a measure of the distribution's peaked-ness. Higher kurtosis indicates that more of the variance is due to rare severe deviations, and their Fourier transformations yield Bi-spectrum and Tri-spectrum for the signals, respectively, which can be employed as signal characteristics. As a result, these are used in the proposed method's multiple classifiers to improve accuracy and classification outcomes.

3.2.2 CLASSIFIERS

For classifying the various ECG signals, three classifiers are used which are as follows:

3.2.2.1. Support Vector Machine [SVM]

Because of its multi-classification capabilities in discriminating distinct classes, the SVM (Support Vector Machine) classifier is used for ECG signal categorization. The margin between the support vectors should be maximised in SVM, hence the hyperplane parameters f , f_0 should be minimised so that:

$$\text{Minimize } J(f, f_0) \equiv \frac{1}{2} \|f\|^2 \quad (3.21)$$

subject to

$$z_i \cdot (f^T x + f_0) \geq 1, i = 1, 2, \dots, N \quad (3.22)$$

The margin is obviously maximised when the norm is minimised. This is a quadratic (nonlinear)

optimization problem with a set of linear inequality constraints. Hence, the SVM decision function is expressed as equations

$$f = \sum_{i=1}^N c_i \cdot z_i \cdot x_i \quad (3.23)$$

$$\sum_{i=1}^N c_i \cdot z_i = 0 \quad (3.24)$$

To obtain high performance, [84] employed an SVM classifier with kernel filter. They refined the SVM classifier design by determining the optimal value of the parameters that alter the discriminant function and determining the best subset of features to feed the classifier. They'd utilised the identical method for multiclass categorization as well. SVM doesn't provide good results in classifying different ECG signals and hence, another classifier is used.

Chapter 3: ECG Signal Analysis Using Higher Order Cumulants

SVM and artificial neural networks are also used to categorise ECGs (ANN). In this situation, also train the network with some training data. A suitable training approach produces an ANN that can provide a non-linear mapping function capable of reflecting associations between given ECG features and heart illnesses. A well-designed ANN will exhibit good generalisation when an accurate input-output mapping is created, even when the test input is slightly different from the data used to train the network.

3.2.2.2. Fuzzy-2

SVM and ANN failed to generate the necessary results, as stated in the results section, thus the classification is done using the Fuzzy-2 classifier. It is a rule-based system that successfully employs several levels of uncertainty in a variety of engineering domains. Four components make up this classifier: a) a fuzzifier that creates fuzzy-2 sets from input and output by using a Membership Function (MF); b) 'IF... Then' rules to link input and output that have been fuzzified; c) an inference engine that combines the rules depending on the firing level; and d) two phases of defuzzification: After type-reduction to create a fuzzy-1 set from a fuzzy-2 set, defuzzification is used to provide output that is clear.

The Fuzzy-2 flowchart is shown in the fig.3.1

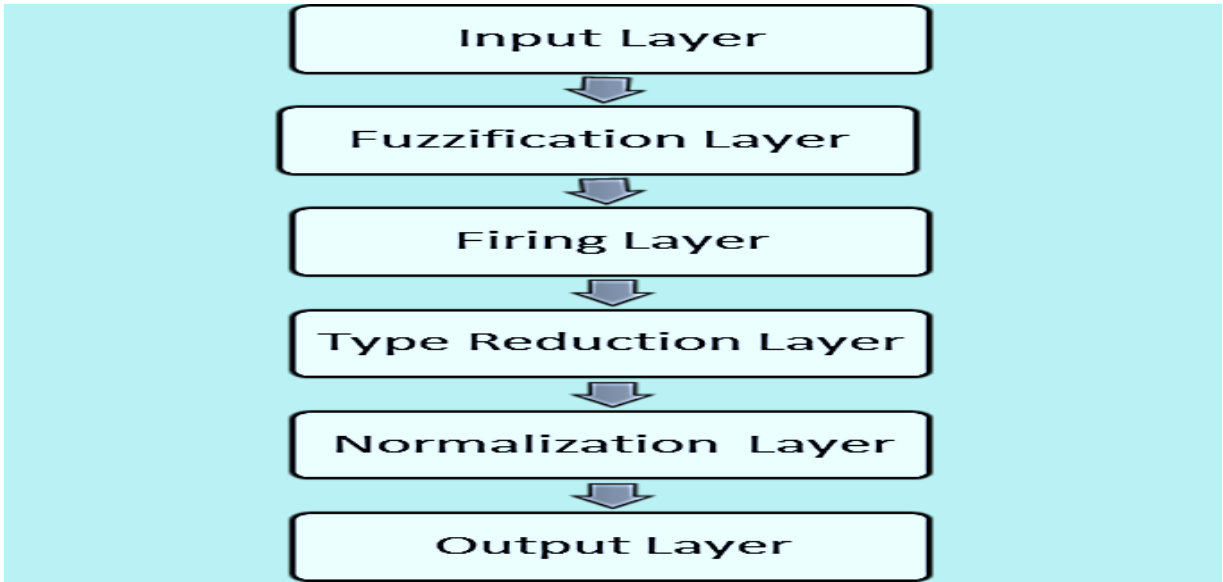


Fig.3.1 Fuzzy-2 flowchart

The definition of fuzzy-2 sets \tilde{A} is given by

$$\tilde{A} = \{(x, u), \mu_{\tilde{A}}(x, u) \mid \forall x \in X, \forall u \in J_x \subseteq [0,1]\} \quad (3.25)$$

$$\mu_{\tilde{A}}(x = x', u) \equiv \int_{u \in J_x} \frac{f_x(u)}{u} \quad (3.26)$$

Chapter 3: ECG Signal Analysis Using Higher Order Cumulants

where $0 \leq \mu_{\tilde{A}}(x, u) \leq 1$, $0 \leq f_x'(u) \leq 1$, J_x is a vertical slice of fuzzy-2 membership function $\mu_{\tilde{A}}(x,u)$ and $f_x'(u)$ is the amplitude of a secondary MF that model the uncertainty of exact Fuzzy-2 system in this case. By modifying the membership function settings, Fuzzy-2 is taught to decrease the error between the estimated output and the real output using ECG data of input and output variables. Later the system is used to predict outputs depending on the inputs. Fuzzy-2 is characterised by a concept known as Footprints of Uncertainty (FOU) as shown in fig.3.2

$$FOU(\tilde{A}) = \{(x, u): u \in J_x \subseteq [0,1]\} \quad (3.27)$$

Upper membership function is:

$$\bar{\mu}_{\tilde{A}(x)} = \overline{FOU(\tilde{A})} \forall x \in X \quad \overline{FOU(\tilde{A})} \forall x \in X \quad (3.28)$$

Lower membership function is:

$$\underline{\mu}_{\tilde{A}(x)} = \underline{FOU(\tilde{A})} \forall x \in X \quad \underline{FOU(\tilde{A})} \forall x \in X \quad (3.29)$$

We can cover the input/output domains with fewer fuzzy sets since FOU may express more uncertainty. This makes it easy to build the rule base using expert knowledge and improves the system's robustness. This classifier also is unable to provide efficient results in ECG signals

classification, results are even worse compared to ANN. So, in order to obtain better and efficient results, deep structured neural network is used.

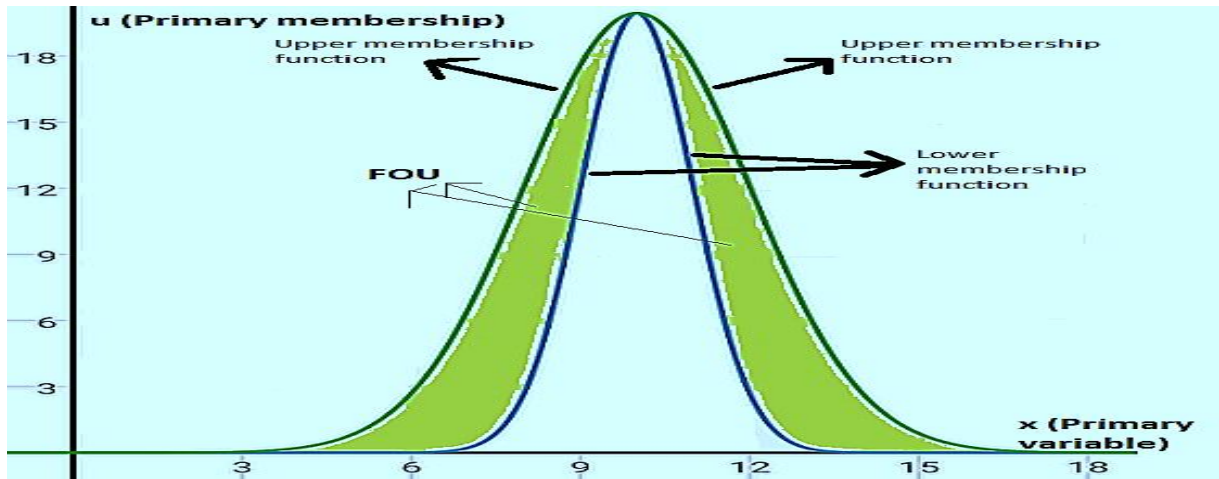


Fig.3.2 Fuzzy-2 membership function

3.2.2.3. Deep Structured Neural Network [DSNN]

The Deep Structured Neural Network, or DSNN, is built on the deep learning idea. In deep learning, a significant quantity of unlabelled data is used to learn features through unsupervised pre-training a multi-layer neural network and then supervised fine-tuning to slightly change learnt features for improved prediction using labelled data.

The suggested method's results are applicable to deep networks with more hidden layers. The

Chapter 3: ECG Signal Analysis Using Higher Order Cumulants

neuron values at the M-neuron input layer are denoted by the letter 'x.' The pth element of S^H is the vector of hidden neuron sigmoidal activations.

$$S_p^H = \frac{1}{1 + \exp(-\sum_{m=1}^M (r_{pm} \cdot x_m))} \quad (3.30)$$

where r_{pm} is the weight of the link that connects the mth visible and pth hidden neuron. S_n^d is the nth output neuron's value with activation.

$$S_n^d = \frac{\exp(\sum_{p=1}^P (v_{np} \cdot S_{ph}))}{\sum_{t=1}^N \exp(\sum_{p=1}^P (v_{n_1 p} \cdot S_{ph}))} \quad (3.31)$$

$$= p(g = n | x, \Theta)$$

where g denotes the N-valued target variable and t is its 1-in-N encoding, v_{np} is the weight of the link that connects the pth hidden and nth target neuron. S_n^t depends on input x and parameter matrices V and R.

After modelling a network, a loss function must be developed in order to evaluate and improve its outcomes, because the purpose of training is to decrease the error of this function, which is dependent on weights and bias. Backpropagation uses gradient ascent to update network

parameters Θ and maximise the log likelihood function $\log p(g|x, \Theta) (= \Gamma)$. The partial derivative of this log-likelihood function with respect to v_{nj} is

$$\frac{\partial \Gamma}{\partial v_{np}} = (d_n - S_n^d) \cdot S_p^h \quad (3.32)$$

and with respect to r_{pm} is

$$\frac{\partial \Gamma}{\partial r_{pm}} = S_p^h \cdot (1 - S_p^h) x_m * \sum_{n=1}^N (d_n - S_{nt}) \cdot v_{np} \quad (3.33)$$

As a result, the partial derivatives of the log-likelihood function that execute gradient ascent will be obtained. For regression, a linear signal function frequently replaces the Gibbs function at the output layer:

$$S_n^t = \sum_{p=1}^P (v_{np} \cdot S_{ph}) \quad (3.34)$$

As a result, the partial derivatives of the log-likelihood function that execute gradient ascent will be obtained. For regression, a linear signal function frequently replaces the Gibbs function at the output layer:

$$E = \frac{1}{2} \sum_{n=1}^N (d_n - S_n^d)^2 \quad (3.35)$$

3.3 PROPOSED METHODOLOGY

The proposed method is shown in the block diagram in fig.3.3. It is briefly described as follows:

a) First of all, third and fourth order cumulants were obtained for ECG datasets depicting various conditions of heart namely, Apnea, Normal, Arrhythmia and Tachyarrhythmia and then

Chapter 3: ECG Signal Analysis Using Higher Order Cumulants

Third and fourth order cumulants are subjected to a Fourier transform to produce bi-spectrum and tri-spectrum, respectively;

b) these cumulants are then used by various classifiers to categorize these ECG datasets; and
c) results from all classifiers were compared in order to achieve the best classification of ECG waveforms by comparing various classifiers.

3.3.1 BLOCK DIAGRAM

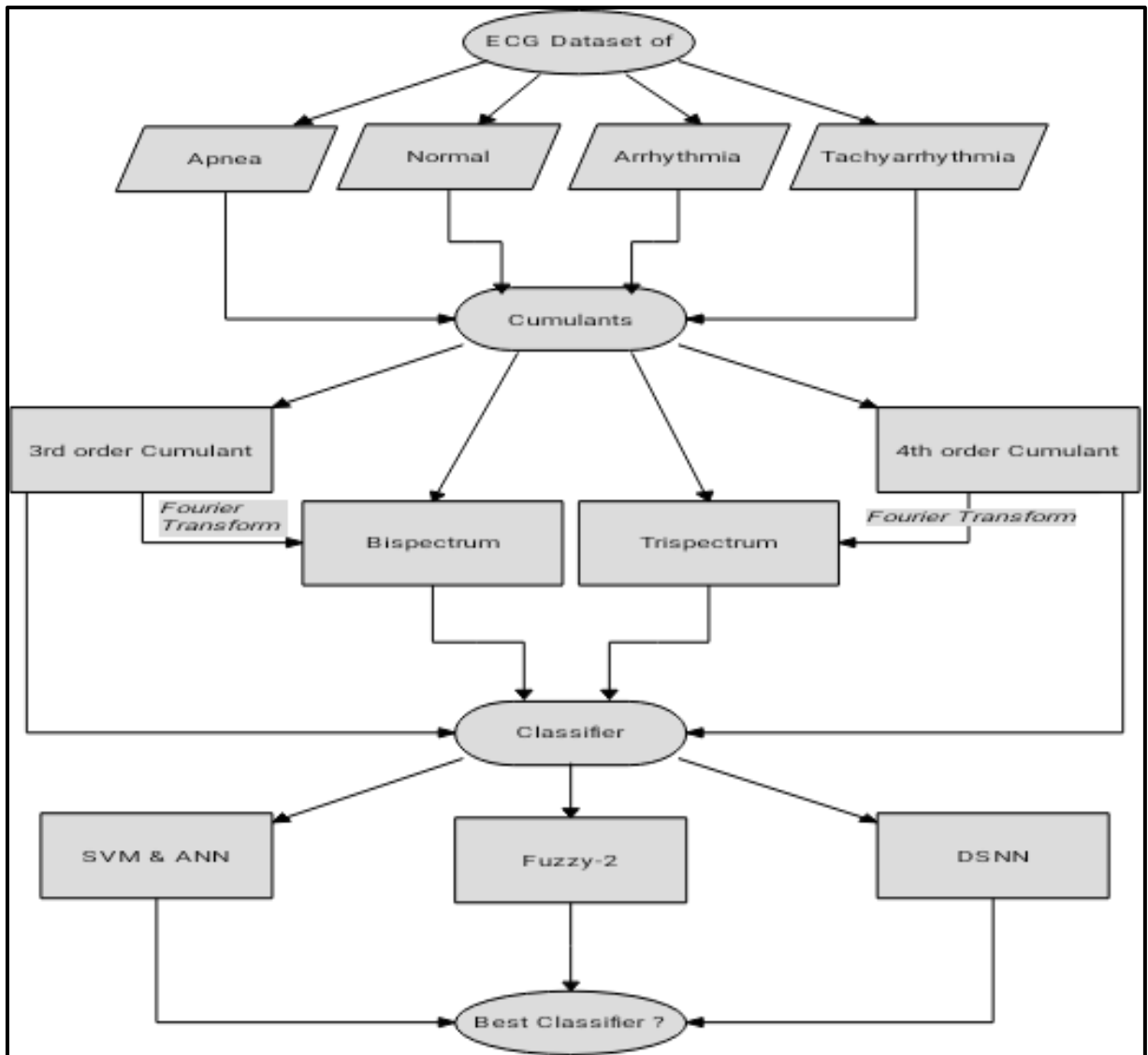


Fig.3.3 Block diagram of the proposed method

3.3.2 DATASET USED

Dataset used was downloaded from the MIT-BIH arrhythmia database of Physio bank ATM [85]. In this, Dataset of 20 subjects for each type of ECG depicting i.e., Apnea, Normal, Arrhythmia and Tachyarrhythmia was taken as per details shown in table 3.1:

Chapter 3: ECG Signal Analysis Using Higher Order Cumulants

Table 3.1: Used dataset description

ECG Signals	Total
Apnoea	20
Normal	20
Arrhythmia	20
Tachyarrhythmia	20

The general waveforms of these four different types of signals are shown in fig.3.4. These ECG waveforms differ from one another in several ways, as is readily shown in fig.3.4. These noticeable differences between them may be caused by the varying heart rates or cardiac states of various persons under various settings, like resting, exercising, effort, tension, being unconscious, or having a sluggish heartbeat, among others.

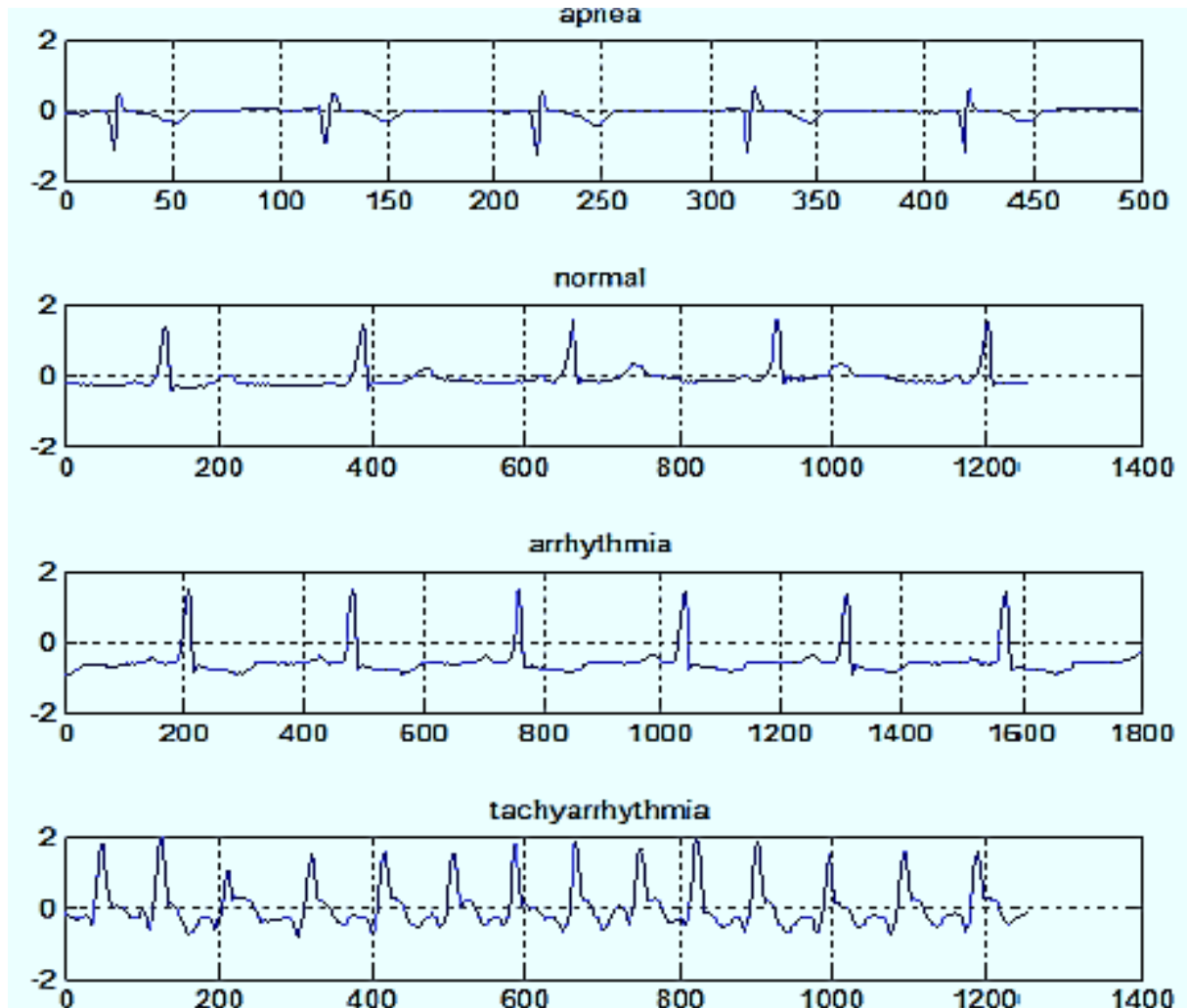


Fig.3.4 ECG signal waveforms

The various waveforms shown in the fig.3.4 depicts different cardiac conditions such as:

1] Apnea talks about the sleepy situation in the subject in which the subjects have an unconscious state of mind under resting situation;

Chapter 3: ECG Signal Analysis Using Higher Order Cumulants

2] A normal person typically has heartbeats between 60 and 100 beats per second and has a conventional ECG waveform with well-defined P-QRS-T peaks, which indicates a normal heart rate;

3] Arrhythmia ECG indicates slow heart rate less than 60 beats per second which is also known as bradycardia and whereas

4] Tachyarrhythmia also known as tachycardia shows the cases with fast heart rate of more than 100 beats per second.

3.3.3 TAKING THE ECG DATASETS

Dataset for ECG detection is loaded from the MIT-BIH arrhythmia database of Physio bank ATM to MATLAB workspace. The dataset used is further divided into training and testing data sets as as per details shown in table 3.2:

Table 3.2: Description of dataset used for classification

ECG Signals	Trainin g	Testin g	Total
Apnoea	12	8	20
Normal	12	8	20
Arrhythmia	12	8	20
Tachyarrhythmi a	12	8	20

3.3.4 CALCULATING THE CUMULANTS FOR THE ECG SIGNALS

Then, for each dataset, MATLAB calculates third and fourth order cumulants with their associated Fourier transformations. The skewness and kurtosis of the ECG signals are discussed in these computed cumulants. Their respective Fourier transformations result in bi- and tri-spectrums. As an input, these estimated cumulants will be used to develop and evaluate the classifiers.

3.3.5 CLASSIFICATION USING SVM, FUZZY-2 AND DSNN CLASSIFIERS

The classifier uses the higher order statistics of the ECG signals produced at the second step to identify the associated heart conditions. For reliable ECG identification and classification, this feature set comprises of higher order statistics that should effectively characterise the fluctuations in the input signals. To categorise the ECG signals in their appropriate class, the derived features will be fed into classifiers like SVM, Fuzzy-2, and DSNN classifiers as training and testing data.

3.4 RESULTS

Here, 12 datasets are selected randomly from each class, and there after total 48 datasets are used for training of classifiers. However, overall total number of datasets in the database was 80. Description of the dataset used is shown in the table 3.1 and table 3.2. Higher order

Chapter 3: ECG Signal Analysis Using Higher Order Cumulants

statistical parameters are used with this dataset to extract features. These characteristics include third- and fourth-order cumulants, which are analysed as bi- and tri-spectrums in the frequency domain, respectively. The third order cumulant discusses the distribution's asymmetry, and the fourth order cumulant provides information on how peaked that distribution is, as was

previously addressed in relation to these characteristics. The physiological signals, in this example the ECG, may be statistically and quantitatively analysed by combining these components.

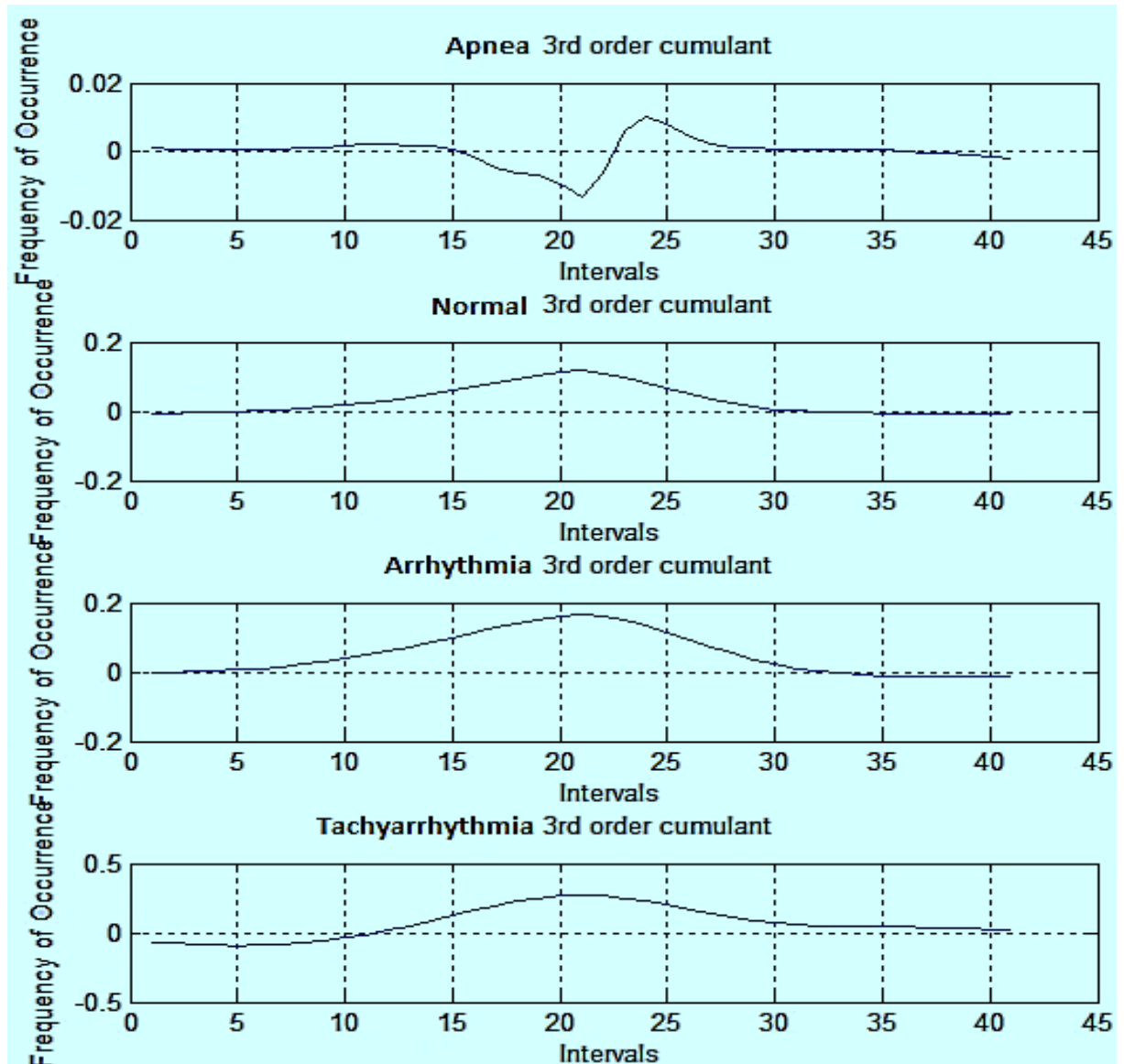


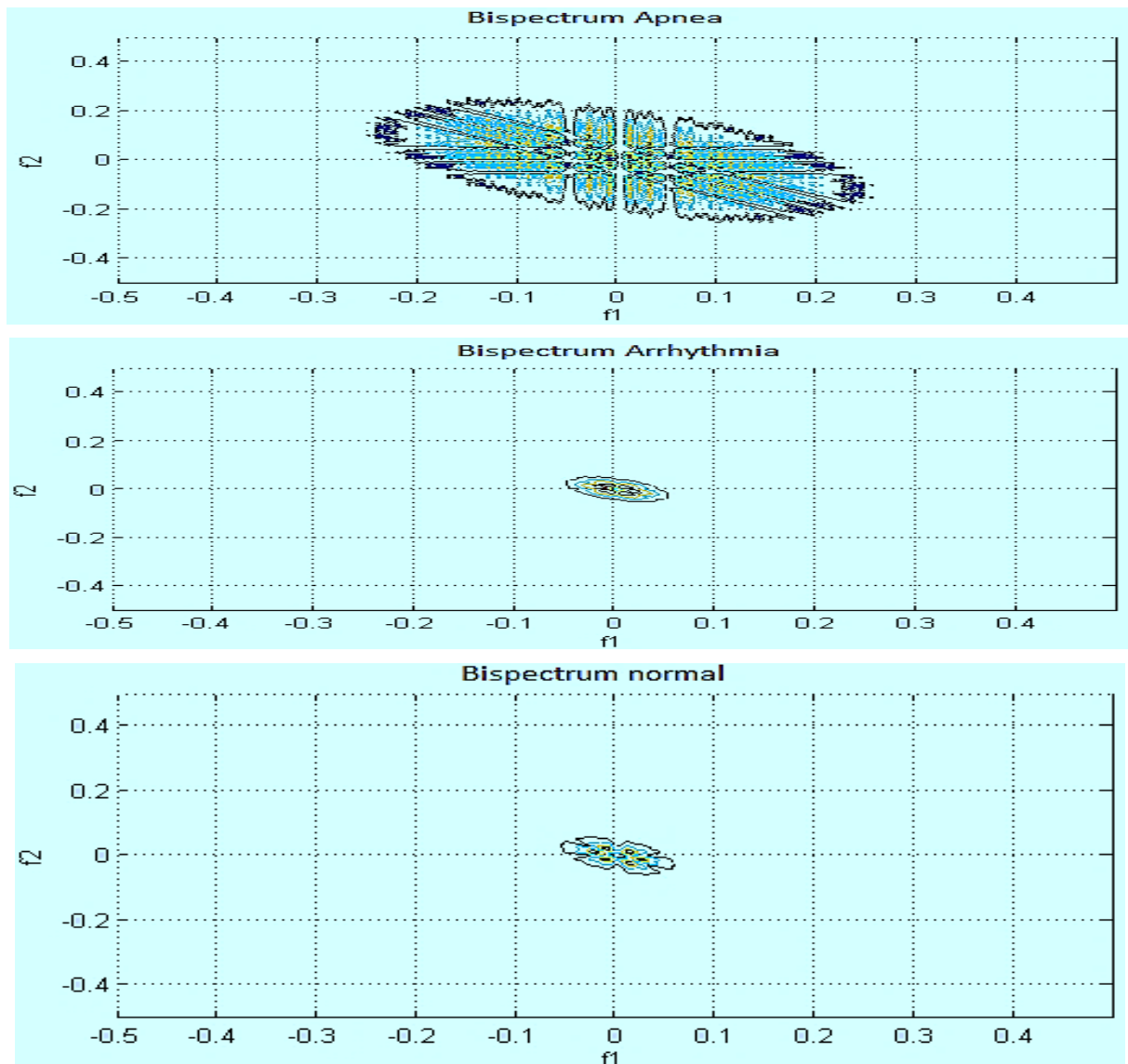
Fig.3.5 Third order cumulant obtained for dataset used

The datasets of the four selected signals are provided in fig.3.4 along with the third and fourth order cumulants, respectively. Additionally, each signal's plot of higher order statistics exhibits distinct fluctuation, as seen in figs. 3.5, 3.6, 3.7, and 3.8. The third order cumulant of the ECG signals is shown in Fig.3.5, and its bi-spectral Fourier transform is shown in Fig.3.6. The ECG signals employed in the proposed technique can be seen in the picture to have some variances

Chapter 3: ECG Signal Analysis Using Higher Order Cumulants

between them, which are clearly discernible by computing their third order cumulants in the time and frequency domain (i.e., bi-spectrum).

The average values of these cumulants, which are -0.3877 for apnea, 0.0032 for a healthy patient, 0.0007 for an arrhythmia, and 0.0159 for a tachyarrhythmia, may be used to compare them. These discrepancies in the third order cumulants of four different types of ECG signals are brought on by differences in the symmetry of those ECG signals. The third order cumulant waveform of apnea has one peak with a minimum value and one with a maximum value. This is because of the ECG waveform's asymmetry. The P-QRS-T waveform of a normal ECG is said to be the most symmetrical one since it has the fewest peaks achieved and offers a symmetric third order cumulant. The greatest peak of an arrhythmia wave provides the impression that it has the least amount of symmetry. Furthermore, tachyarrhythmia has the lowest amplitude of the third order cumulant since it has the greatest heart rate of all of them.



Chapter 3: ECG Signal Analysis Using Higher Order Cumulants

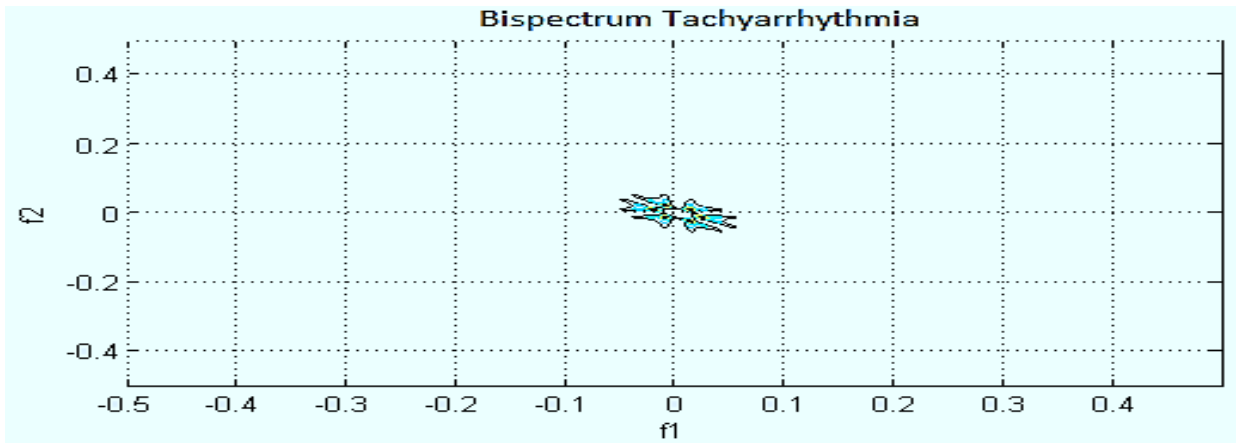


Fig.3.6 *Third order cumulant for dataset used in frequency domain (Bi-spectrum)*

These third order cumulants are depicted as their contour in the frequency domains of fig.3.6. We can see the varied ECG variations from the third order cumulant's asymmetry, which is also clearly evident in the frequency domain. This is because the four different types of ECG signals used to make these contours have different characteristics. A third order cumulant represents the frequency domain bi-spectrum of a signal. These values are averages, and signals whose cumulants with values similar to these values assist classifiers in categorising signals into the proper classes.

Figure 3.7 shows an ECG signal's fourth order cumulant, while Figure 3.8 shows its tri-spectrum Fourier transform. The figure demonstrates how the peaked-ness changes in the ECG signals used in the proposed approach cause fluctuations that can be seen in their fourth order cumulants in both the time and frequency domains (using Fourier transform of fourth order cumulant i.e., tri-spectrum). These may be compared using the average values, which are 11.9559 for apnoea, 2.3172 for a healthy patient, 3.1624 for an arrhythmia, and 2.9038 for a tachyarrhythmia. Like the third order cumulant, where symmetry in the signal was noticed, the kurtosis of these four various forms of ECGs is being compared in this instance. They estimated their fourth order cumulants, which are shown in Fig. 3.7, using the ECG signals shown in Fig.3.4. This graphic makes it obvious that each ECG has a different set of fourth-order cumulants. This variety is brought about by the fact that every topic has a distinctive peak.

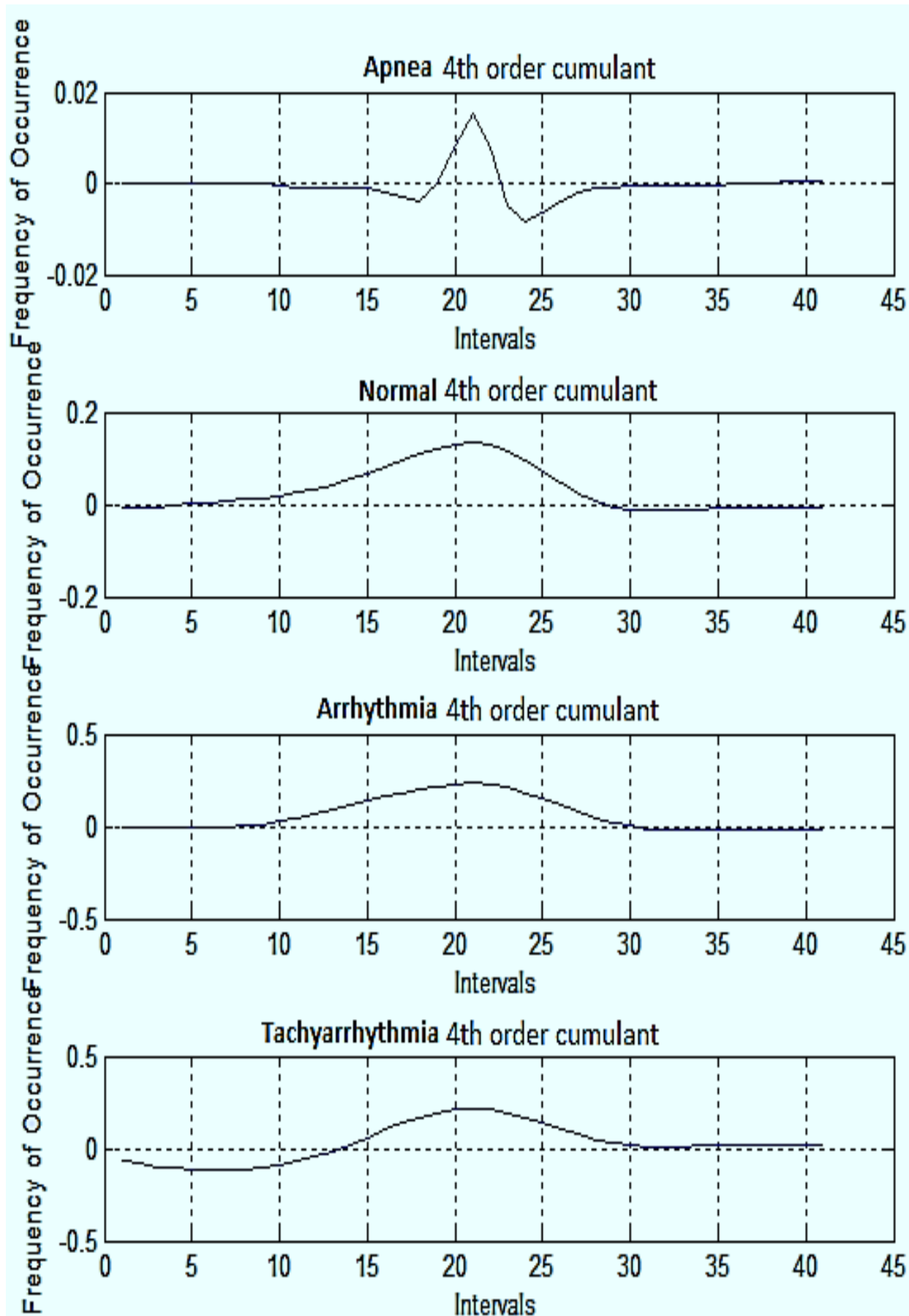


Fig.3.7 Fourth order cumulant obtained for dataset used

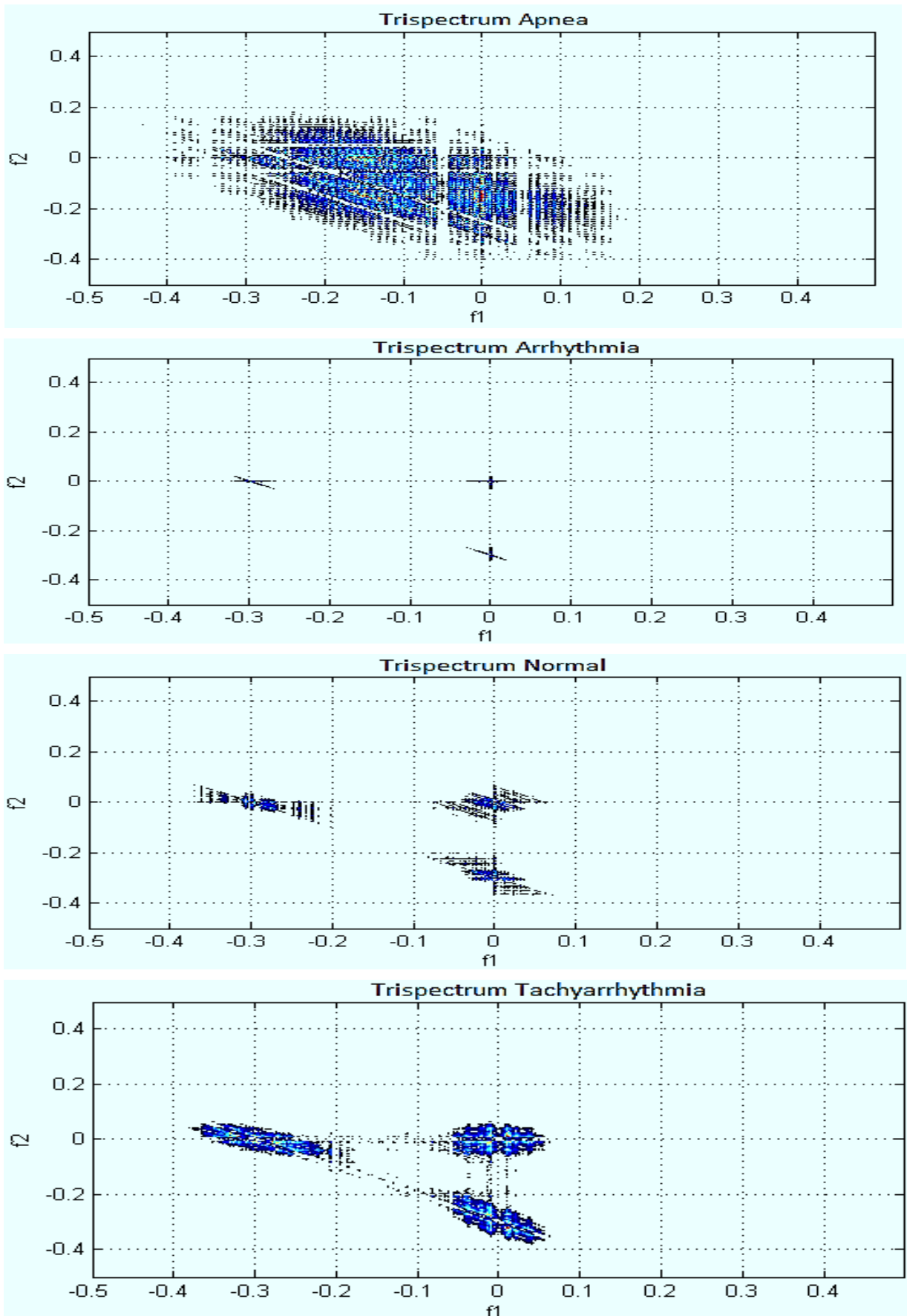


Fig.3.8 Fourth order cumulant for dataset used in frequency domain (Tri-spectrum)

Fourth order cumulants are now shown in Fig. 3.8 in the form of their corresponding contours, precisely as the bi-spectrum for the third order cumulant, in the frequency domains. The fourth order cumulant's peakedness, which is readily apparent in its frequency domain as well, provides us with a clearer understanding of the many ECGs employed in this study since the various contours are the result of the usage of four separate ECG signals. The signal's tri-spectrum, which is a fourth order cumulant in its frequency domain, is referred to. These values of the third and fourth order cumulants are employed in the classifiers used in this study, namely SVM, FUZZY-2, and DSNN, to categorise these ECGs into their respective classes. These values are also the average values.

The higher order statistical parameters collected are then employed in the classifiers to classify these ECG signals. First, SVM is utilized for classification. A total of 80 subjects' datasets are used in this classifier. The SVM is trained on 48 of these subjects, and the remaining are tested on the trained classifier. The SVM classifier's findings are provided in table 3.3, which also includes a confusion matrix for the dataset that was evaluated.

Table 3.3: SVM Confusion Matrix

Targets →					
Outputs ↓	AP	AR	NR	TC	Accuracy (%)
AP	7/8	0/8	0/8	0/8	87.5
AR	0/8	7/8	0/8	1/8	87.5
NR	1/8	0/8	8/8	1/8	100
TC	0/8	1/8	0/8	6/8	75

The initials AP, AR, NR, and TC, respectively, in this table stand in for apnoea, arrhythmia, normal, and tachyarrhythmia. Table 3.3 demonstrates that, with an average accuracy of just 87.5 percent, this classifier does not provide us a satisfactory result. In order to improve the results, the next classifier, ANN, is used. The neural network seen in fig. 3.9, which employs 48 subject cumulants for training and 32 for testing, is created by applying it to the dataset. The categorization of these ECG datasets by an Artificial Neural Network (ANN) is shown in Fig. 3.10.

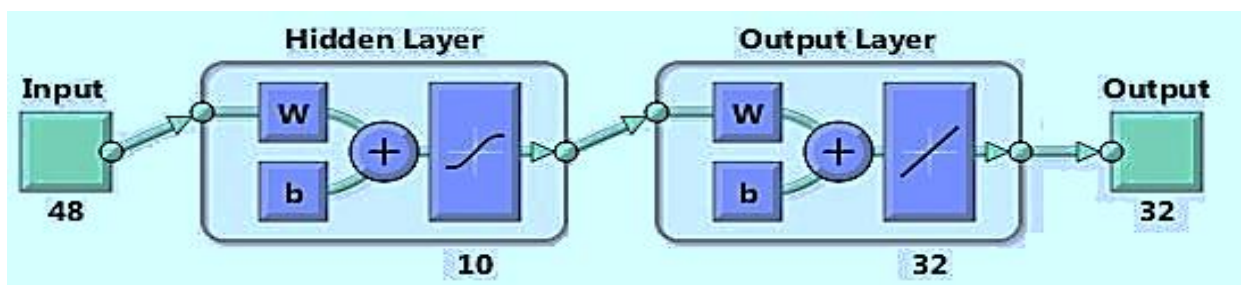


Fig.3.9 Neural Network Scheme for Proposed Method

The training, validation, and testing data for the ANN are shown in the charts. The dashed line in each figure represents the ideal outcome, when outputs equal aims. The solid line displays the outputs-to-objectives linear regression line that fits outputs and goals the best. The relationship between the outputs and the objectives is represented by the R value. If $R = 1$, then there is a perfect linear relationship between the outputs and the objectives. If R is close to 0, there is no linear relationship between the outputs and the objectives. In this instance, the training data show a respectable match. The results of the test and validation may also be observed to have R values over 0.9. The regression figure shows that throughout training, the value of R equals 0.989. When the testing dataset was applied to this, $R=0.966$ was obtained. A excellent validation value of 0.936 is also provided. Table 3.4 displays the confusion matrix for these ECG data that were classified using an ANN classifier. This table shows that the average accuracy is 96.6 percent, which is quite good and produces far better outcomes than SVM, which only achieves an accuracy of 87.5 percent. The cumulants obtained from these ECG datasets are then subjected to Fuzzy-2.

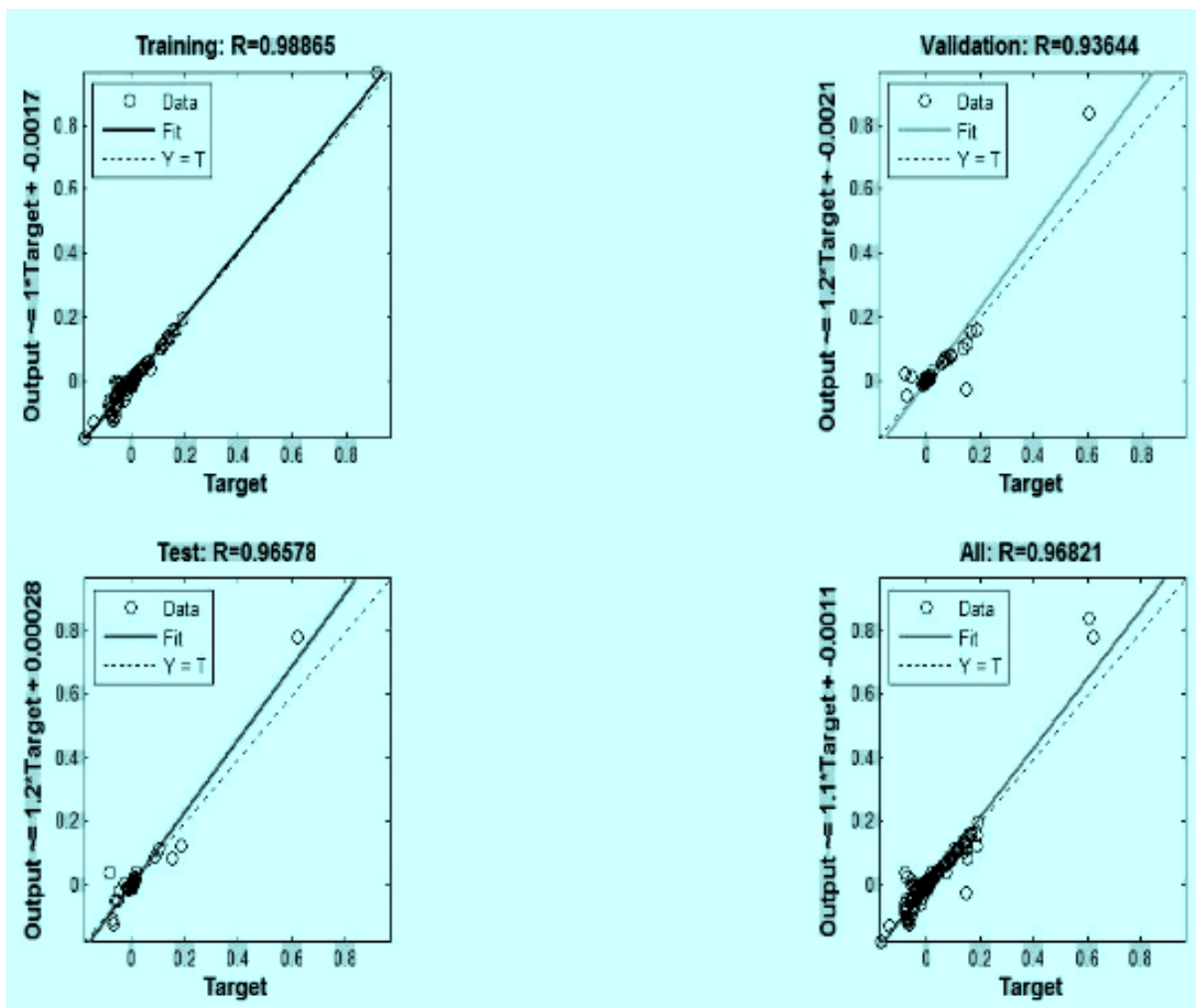


Fig.3.10 Regression plots for ANN

Table 3.4: ANN Confusion Matrix

Targets →					
Outputs ↓	AP	AR	NR	TC	Accuracy (%)
AP	8/8	0/8	0/8	0/8	100
AR	0/8	8/8	0/8	0/8	100
NR	0/8	0/8	8/8	1/8	100
TC	0/8	0/8	0/8	7/8	87.5

In the table 3.5 confusion matrix for the fuzzy-2 classifier is shown and it is clear from the matrix that results obtained are not satisfactory and even worse than the ANN and should be checked further using another classifier to have an improvement in the accuracy. Hence, for the same, Deep Structured Neural Network (DSNN) is used as the next classifier in which, when this same dataset is applied, results obtained are much better than the earlier methods used.

Table 3.5: FUZZY-2 Confusion Matrix

Targets →					
Outputs ↓	AP	AR	NR	TC	Accuracy (%)
AP	7/8	0/8	0/8	0/8	87.5
AR	0/8	7/8	0/8	0/8	87.5
NR	1/8	0/8	8/8	1/8	100
TC	0/8	1/8	0/8	7/8	87.5

Deep Structured Neural Network (DSNN) is used further for the results improvement. Its regression plot is shown in the fig.3.11. In this regression plot obtained, it can be seen from the plot that training value of R comes out as 0.999 and for the testing plot, it gives R=0.993. It also gives a good validation value of 0.999. Now it can be seen from the result that it has given better results compared to the SVM, ANN and Fuzzy-2. In this plot of DSNN, about 99.8% values of dataset gives accurate results and gives the best classifier among the classifiers used during this work. In its table of confusion matrix also i.e., shown in table 3.6, DSNN has given the best results. All the test datasets are accurately classified in their respective classes.

Table 3.6: DSNN Confusion Matrix

Targets →					
Outputs ↓	AP	AR	NR	TC	Accuracy (%)
AP	8/8	0/8	0/8	0/8	100
AR	0/8	8/8	0/8	0/8	100
NR	0/8	0/8	8/8	0/8	100
TC	0/8	0/8	0/8	8/8	100

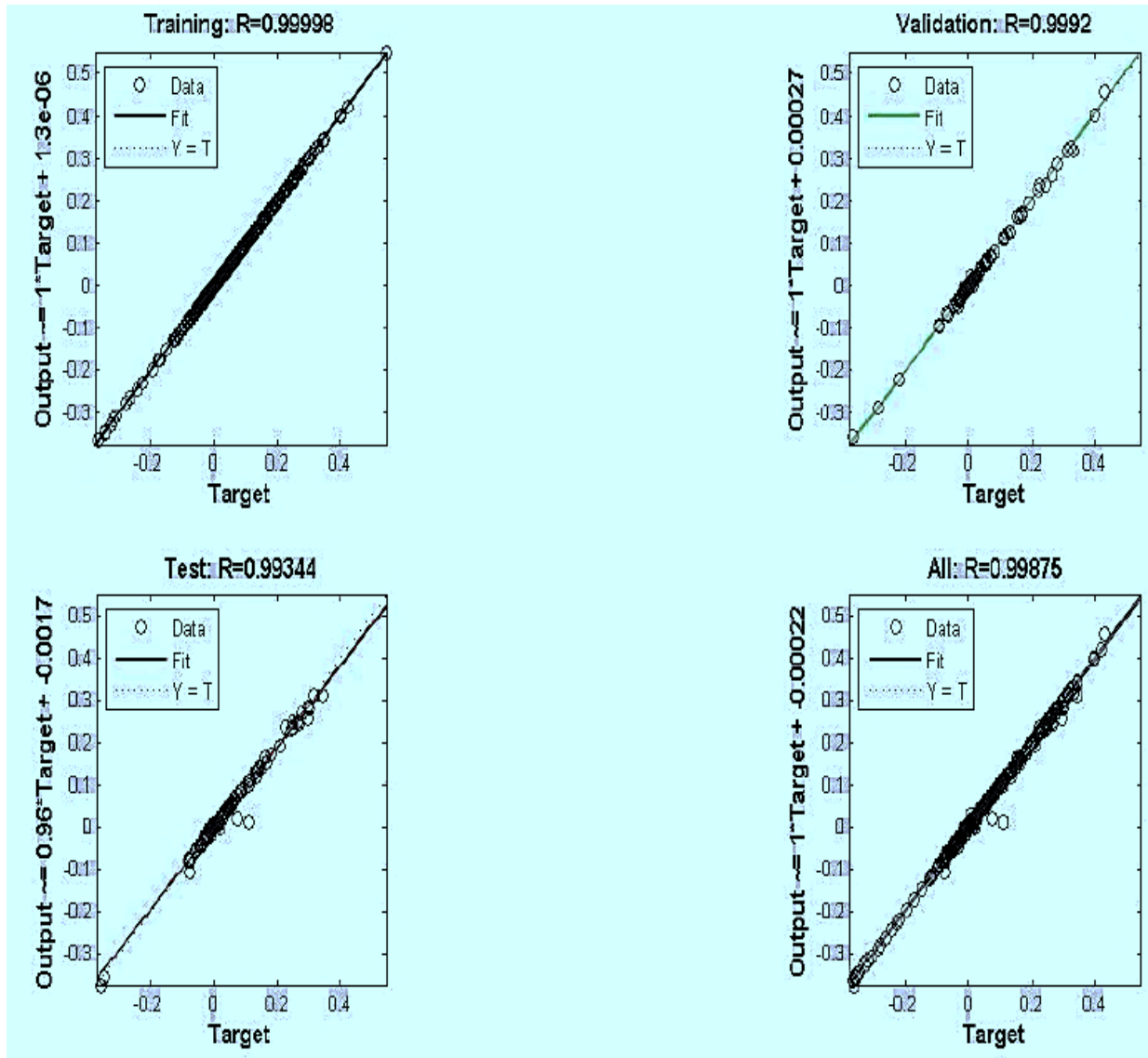


Fig.3.11 Regression plot for DSNN

The table 3.7 shows the comparison of all these classifiers used in this proposed method and it can be easily perceived from the table that Deep Structured Neural Network (DSNN) classifier gives the best results.

Table 3.7: Comparison of four classifiers

Classifier Name	Accuracy (%)
SVM	87.5
FUZZY-2	90.6
ANN	96.6
DSNN	99.8

The table 3.8 displays the comparison for the best method, here DSNN is clearly the best method which is used in this proposed method. This method provides the best results when it

is compared with the earlier methods using some other techniques i.e., other than cumulants that have already been used for the ECG classifications,

Table 3.8: Comparison of proposed method of ECG classification with other methods used

REFERENCES	METHODS USED	ACCURACY (%)
Proposed Method	DSNN	99.80
Palaniappan and Krishnan [21]	Neural Network	97.60
Proposed Method	ANN	96.60
Chiu et al. [22]	DWT	95.71
Yao and Wan [23]	PCA + Low Match Score (LMS)	91.50
Proposed Method	FUZZY-2	90.6
Proposed Method	SVM	87.5
Homer et al. [24]	kNN	85.20
Odinaka et al. [25]	Generative Model Classifier	76.90

3.5 SIGNIFICANT FINDINGS

In this classification of ECG, four classifiers as SVM & ANN, Fuzzy-2 and DSNN were used and DSNN is observed to be as the best classifier among these classifiers because of its repeated learning and analyzing ability. The results computed from DSNN classifier has the highest observed accuracy compared to the rest of the three classifiers and hence, DSNN is the best for using it for the ECG signals classification. In this proposed method, cumulants helps us to remove many divergences in the other type of ECG datasets. Therefore, the proposed method is used to detect this problem and addresses the issue very efficiently and accurately.

This chapter is based on the following work:

Rajesh Birok & Rajiv Kapoor “ECG Signal Analysis Using Higher-Order Cumulants” [To be communicated in SCIE/ESCI Journal]

CHAPTER 4

ECG DENOISING USING ANN AND CEEMD

4.1 INTRODUCTION

The electrocardiogram (ECG) is a quasi-periodic signal that measures the electrical activity of the heart. Thus, electrocardiogram (ECG) is simply a documentation of the electrical activities of the heart. It is used to assess whether a patient has any type of cardiac disorder and provides information content mainly in the 0.5-120 Hz range. The P wave, QRS complex, and ST segment make up the majority of its morphology; any extra structures in the ECG indicate noise or cardiac defects. In general, it is used to identify a number of cardiac faults such as arrhythmias, Atrial Fibrillation [AF] etc. The diagnosis of these disorders is generally made by experts who examines the ECG signal for specific morphologies. Due to this, an ECG signal's morphology is important, and it must be as noise-free as possible. Quite often the ECG gets corrupted by various kinds of artefacts, thus in order to gain correct information from them, they must first be denoised.

However, during acquisition process an ECG signal usually captures a vast range of different types of noise artefacts, rendering accurate diagnosis impossible. As a consequence, correct diagnosis necessitates a filtration procedure that removes the bulk of constituent noise while preserving details about the ECG signal's morphology. Any of the noises that can be present in any standard ECG are Power Line Interference (PLI), baseline wander, electrode touch noise, motion artefacts, and instrumentation noise etc., [86]. Baseline wander artefact occurs mainly as a result of the patient's breathing, making it omnipresent in almost all ECG signals. As it is one of the most common types of noise in an ECG, it is recommended for denoising in this chapter. This artefact is frequently seen during stress ECGs, especially as the patient's breathing rate rises. All of these morphological changes are normal and necessary for diagnosis, but most recent denoising procedures tend to filter them out, resulting in information loss [87]. Another reason we chose baseline wander for denoising in this study is that it hasn't got as much attention in the literature previously, so while there are fairly efficient methods are available for denoising PLI and other types of noises, the same cannot be said for baseline wander.

This chapter presents a novel approach for the filtering of low frequency artefacts of ECG signals by using Complete Ensemble Empirical Mode Decomposition (CEEMD) and Artificial Neural Networks [ANN], which removes most of the constituent noise while assuring no loss of information in terms of the morphology of the ECG signal. The contribution of the method lies in the fact that it combines the advantages of both CEEMD and ANN. The use of CEEMD ensures that the Neural Network does not get over fitted. It also significantly helps in building better predictors at individual frequency levels. The proposed method is compared with other state-of-the-art methods in terms of Mean Square Error (MSE), Signal to Noise Ratio (SNR) and Correlation Coefficient. The results show that the proposed method has better performance as compared to other state-of-the-art methods for low frequency artefacts removal from EEG.

4.2 THEORETICAL BACKGROUND

4.2.1 COMPLETE ENSEMBLE EMPIRICAL MODE DECOMPOSITION [CEEMD]

Any data set can be decomposed using CEEMD into a set of true Intrinsic Mode Functions (IMFs). The various IMFs obtained thus far are representations of the signal's various frequency components. The following is the procedure how CEEMD breaks down a signal into its constituent IMFs.

- Using EEMD, K realizations of the base signal with added White Gaussian noise ($x(n) + \varepsilon w^k(n)$) are achieved to obtain their first modes and thereby to create an ensemble of first IMFs by taking average to obtain first true IMF, using the following formula

$$\widetilde{IMF_1}[n] = \frac{1}{K} \sum_{k=1}^K IMF_1^k(n) \quad (4.1)$$

Where, $x(n)$ is the base signal (raw ECG signal for the first stage), $w^k(n)$ is White Gaussian noise for k^{th} realization, $IMF_1^k(n)$ is first IMF of k^{th} realization, ε is weight coefficient of added noise and $k = 1,2,3,4 \dots \dots \dots K$.

- At the first stage, residue is calculated by

$$r_1[n] = x[n] - \widetilde{IMF_1}[n] \quad (4.2)$$

- In the second stage of CEEMD, this residue signal is used as the base signal, and an ensemble of K residue realizations with white Gaussian noise is produced. The IMFs for each variable are first obtained, and then they are averaged to produce the second true IMF, which is provided as

$$\widetilde{IMF_2}[n] = \frac{1}{K} \sum_{k=1}^K E_1(r_1(n) + \varepsilon_1 E_1(w^k[n])) \quad (4.3)$$

- Similarly using equation (4.2) again, the second residue is calculated and used for third true IMF.
- The above-mentioned steps are continued until further decomposition is no longer possible and all the obtained true IMFs are subtracted from base signal to obtain the final residue, given as

$$r[n] = x[n] - (IMF_1[n] + \widetilde{IMF}_2[n] + \dots) \quad (4.4)$$

4.2.2 ARTIFICIAL NEURAL NETWORK [ANN]

Artificial Neural Networks (ANN) are a type of informative paradigm [88] that is based on how the human brain processes data. A neuron is the most basic component of such a system, and the processing power is determined by the number of these components and their interconnection. They necessitate initial training data, which must be carefully pre-processed to prevent overfitting. As a result, training must be done in such a way that the neural network's ability to respond to novel patterns is not harmed. The steps involved in setting up a network are

- Collection of data.
- Pre-processing of data.
- Initialization of weights of neural network and learning rate.
- Division of data set into training, testing and validation.
- Training of data: The network trains itself in such a way as to minimize a particular function such as MSE, the function to be minimized depends on the training rule to be used.
- Testing: A portion of the data set is reserved for testing of the network that has been developed. Here the output of the network is compared against a pre-determined output and its performance is checked.
- Cross Validation: This involves testing to ensure that training of the network is not leading to a loss in generalization.

4.3 PROPOSED METHODOLOGY

Flowchart of proposed method is given as Fig.4.1

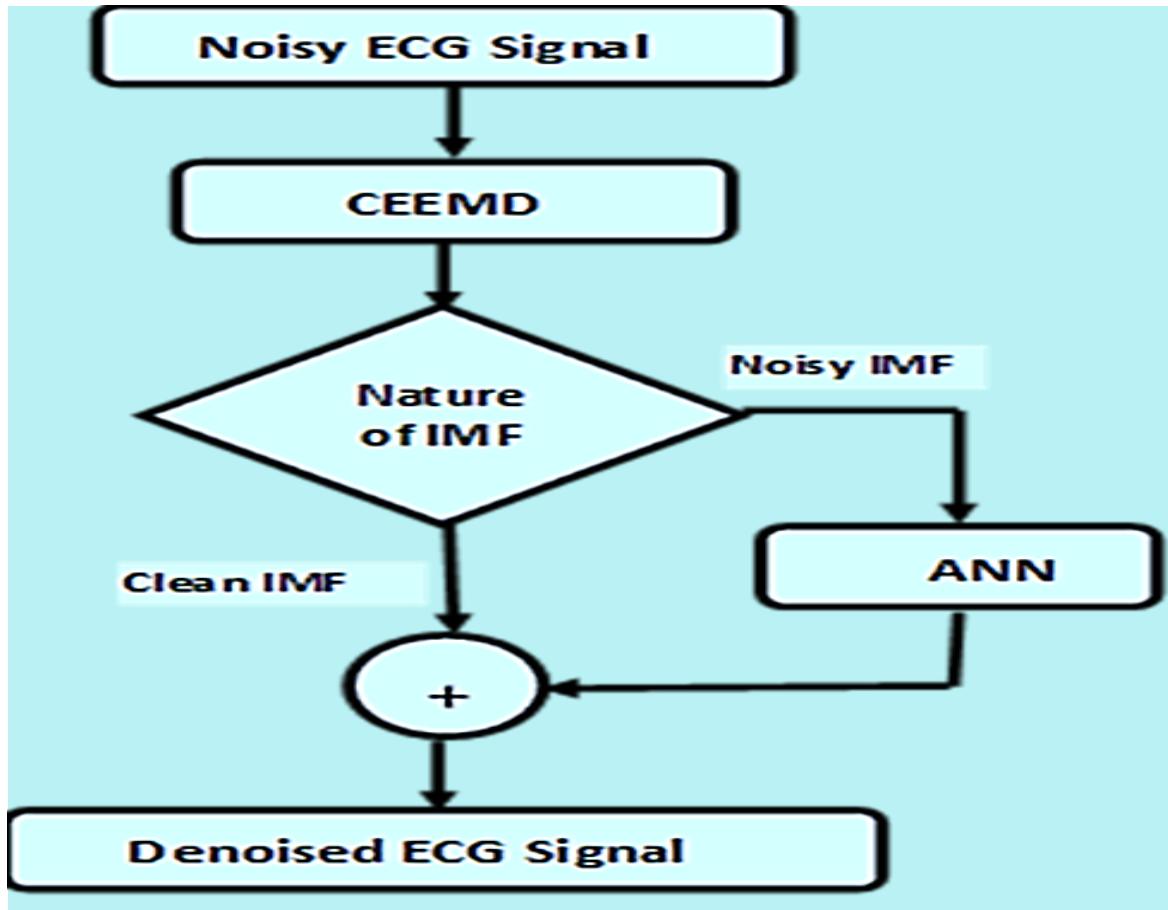


Fig.4.1 Flowchart of proposed method

The various steps of proposed method are

- Apply CEEMD to noisy ECG signal.
- IMFs are broken down into two groups, those affected by baseline wander and those relatively free of it.
- A neural network is created and trained to filter each baseline affected IMF.
- The entire network is tested and cross validated.
- Results are obtained based on three output parameters on different types of noises and test subjects

The CEEMD operation is used to decompose a noisy signal into N true IMFs. These IMFs have now been grouped into two categories: (i) noisy IMFs and (ii) clean IMFs. The Spectral Flatness (SF) of each individual IMF is used to calculate the number of noisy IMFs. The relationship between the Geometric mean (GM) and the Arithmetic mean (AM) is known as

Spectral Flatness (SF). It is defined as the ratio of the power spectrum's geometric mean to its arithmetic mean.

$$\text{Spectral Flatness (SF)} = GM / AM \quad (4.5)$$

Spectral Flatness measure is fuzzified to detect whether the IMFs are noisy or clean. Linguistic variable used are low, and high membership functions for Spectral Flatness.

The rules for spectral flatness are:

Rule 1: IF SF is in high range, THEN IMF is clean

Rule 2: IF SF is in low range, THEN IMF is noisy.

The noisy IMFs are each applied to a different Neural Network separately. The Neural Network is more effective at filtration because each of these IMFs performs filtering at the IMF level and has a greater periodic nature than the combined complete ECG signal. This also eliminates the possibility of overfitting. The Levenberg-Marquardt algorithm [89] is utilized in the suggested technique for Network with 10 hidden layers and 2 delays during the training phase. The number of layers is determined by a comparison study, and the layer with the lowest inaccuracy is selected. The Levenberg-Marquardt algorithm combines the Gauss-Newton technique and the steepest descent method. The basic idea behind the algorithm is as follows: It uses a combined training method and the steepest descent algorithm when the curve is complicated. When the curve can be confidently approximated to be quadratic, it switches to the faster Gauss-Newton technique. The Levenberg-Marquardt algorithm is trained in the manner described below: With the randomly generated initial weights and evaluate the total error (SSE).

1) Do an update as directed by the following equation to adjust weights

$$w_{k+1} = w_k - (J_k^T J_k + \mu I)^{-1} J_k e_k \quad (4.6)$$

- 2) With the updated weights, evaluate the total error.
- 3) If the current total error is increased as a result of the update, then retract the step (reset the weight vector to the previous value), increase combination coefficient μ by a factor of 10 or by some other factor and then go to step 2 and try another update.
- 4) If the current total error is decreased as a result of the update, then accept the step (keep the weight vector as the current one), decrease the combination coefficient μ by a factor of 10 or by the same factor as step 4.
- 5) Go to step 2 with the new weights until the current total error is smaller than the required value.

4.4 RESULTS

The MIT-BIH ST change database [90] is used to receive ECG signals for training and testing. This database contains 28 ECG recordings of varying lengths, sampled at 360 Hz, the majority of which were captured during exercise stress tests and show transient ST depression. The last five records (323 through 327) are ST elevation extracts from long-term ECG recordings. The pure ECG signal is augmented with a baseline wander noise estimation derived from the MIT BIH noise stress test database [91].

The above-mentioned data sets are then fed into a Levenberg–Marquardt algorithm with 10 hidden layers and 2 delays, which is used to train a neural network. For training, 70% of the total available data set is used. Input data from varying noisy ECG records is used to train the networks. When network generalization stops improving, cross validation is used to measure it and to stop training. Cross validation is carried out on 15% of the data set.

In order to test proposed method, Mean Square Error (MSE), Signal to Noise Ratio (SNR) and Correlation Coefficient ($R_{X_{original} X_{denoised}}$) are used as testing parameters. These parameters are defined as

$$\text{Output Mean Square Error [MSE]} = \frac{\sum (X_{original} - X_{denoised})^2}{N} \quad (4.7)$$

$$\text{Output Signal to Noise Ratio [SNR in dB]} = 10 * \log \frac{\sum (X_{original})^2}{\sum (X_{original} - X_{denoised})^2} \quad (4.8)$$

$$\text{Correlation Coefficient [} R_{X_{original} X_{denoised}} \text{]} = \frac{cov(X_{original}, X_{denoised})}{\sigma_{X_{original}} \sigma_{X_{denoised}}} \quad (4.9)$$

where,

$X_{original}$ is pure ECG signal,

$X_{denoised}$ is denoised ECG signal,

cov is convolution function, and

σ is variance.

For the better denoising performance the smaller value of output MSE and larger value of output SNR is desired. The Correlation Coefficient between original ECG signal and denoised ECG signal provides the effectiveness of any method to preserve morphological information present in the ECG signal. Here in this case, large values of Correlation Coefficient indicates that proposed method better preserves morphological information present in the ECG signal.

Fig. 4.2 – 4.4 shows the plots of denoised signals using combinations of Neural Network with EMD, EEMD and CEEMD for three different ECG signals recordings. The tables 4.1-4.3 shows the results of denoising methods using combinations of Neural Network with EMD, EEMD and CEEMD for the same three different ECG signals recordings.

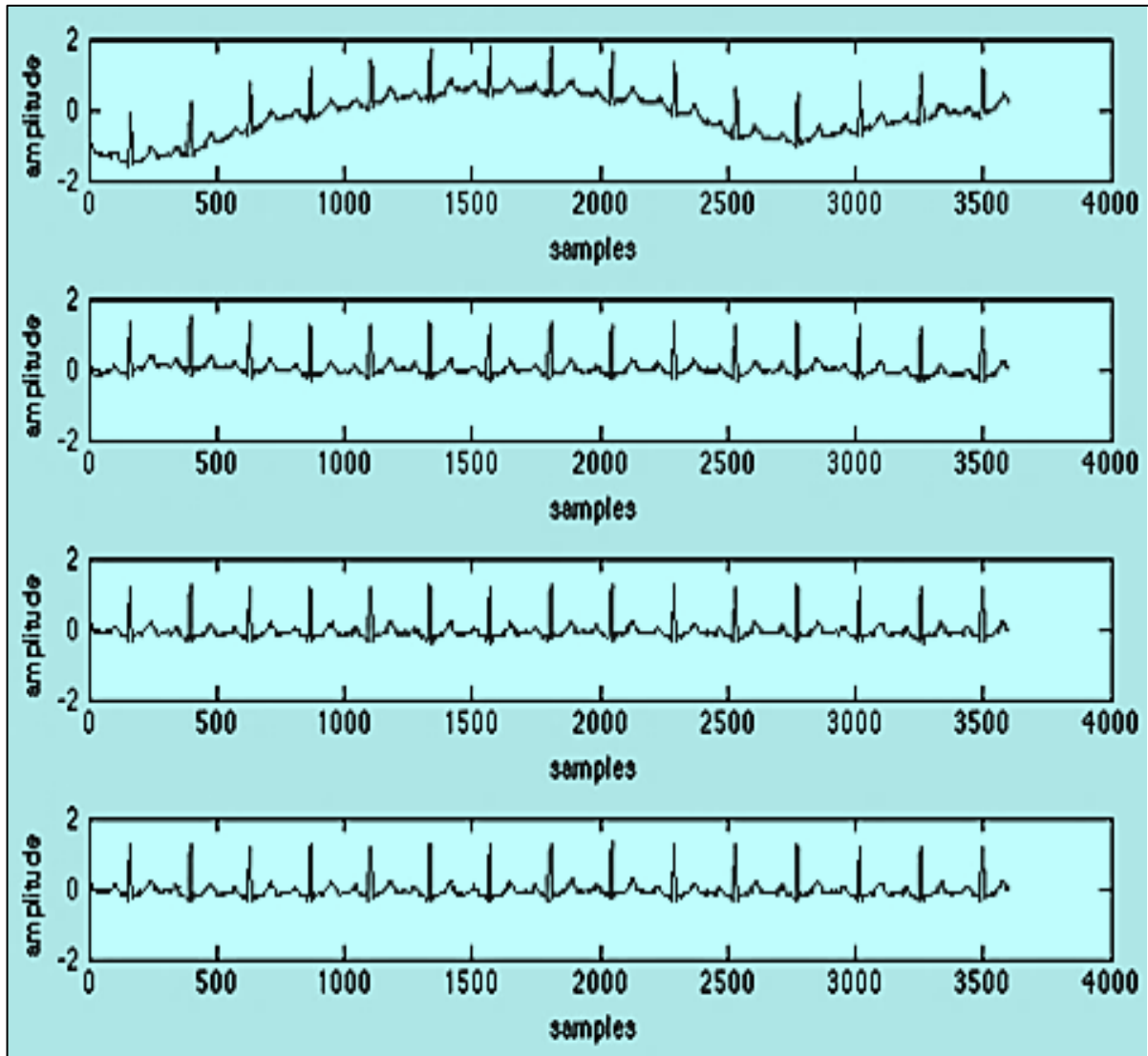


Fig.4.2 (a) Noisy signal (Recording-1) (b) Denoised signal using EMD and Neural Network (c) Denoised signal using EEMD and Neural Network (d) Denoised signal using CEEMD and Neural Network.

Table 4.1: Recording-1

Parameter	(Input SNR = -19.0489, Input MSE = 0.3699)		
	<i>EMD and ANN</i>	<i>EEMD and ANN</i>	<i>CEEMD and ANN</i>
<i>MSE</i>	0.0122	0.0030	0.0016
<i>SNR</i>	14.8793	29.0949	35.3016
<i>Correlation Coefficient</i>	0.9655	0.9671	0.9898

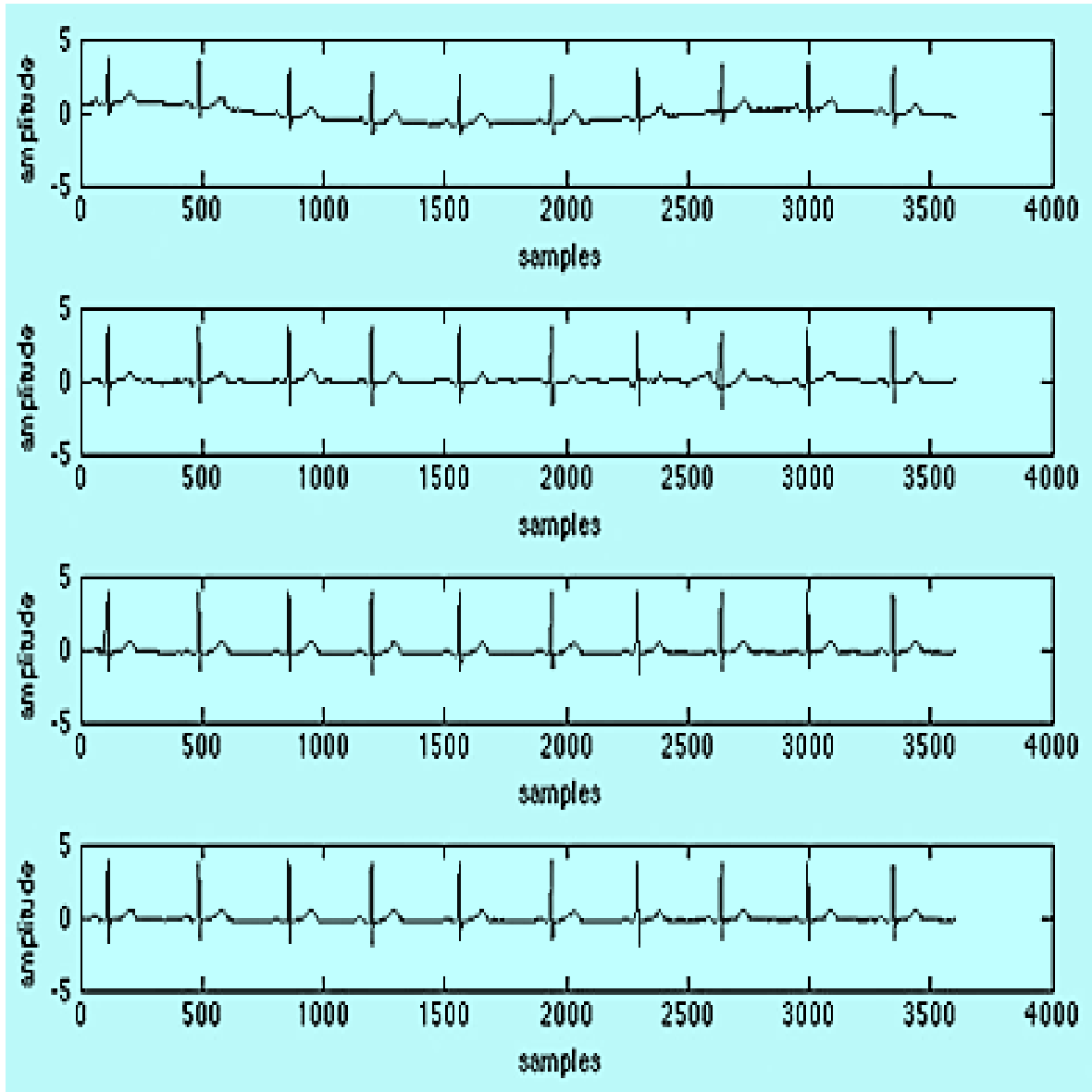


Fig.4.3 (a) Noisy signal (Recording-2) (b) Denoised signal using EMD and Neural Network (c) Denoised signal using EEMD and Neural Network (d) Denoised signal using CEEMD and Neural Network.

Table 4.2: Recording-2

Parameter	(Input SNR = -2.0869, Input MSE = 0.2115)		
	<i>EMD and ANN</i>	<i>EEMD and ANN</i>	<i>CEEMD and ANN</i>
<i>MSE</i>	0.0453	0.0076	0.0073
<i>SNR</i>	13.3992	31.2956	31.5658
<i>Correlation Coefficient</i>	0.9509	0.9881	0.9887

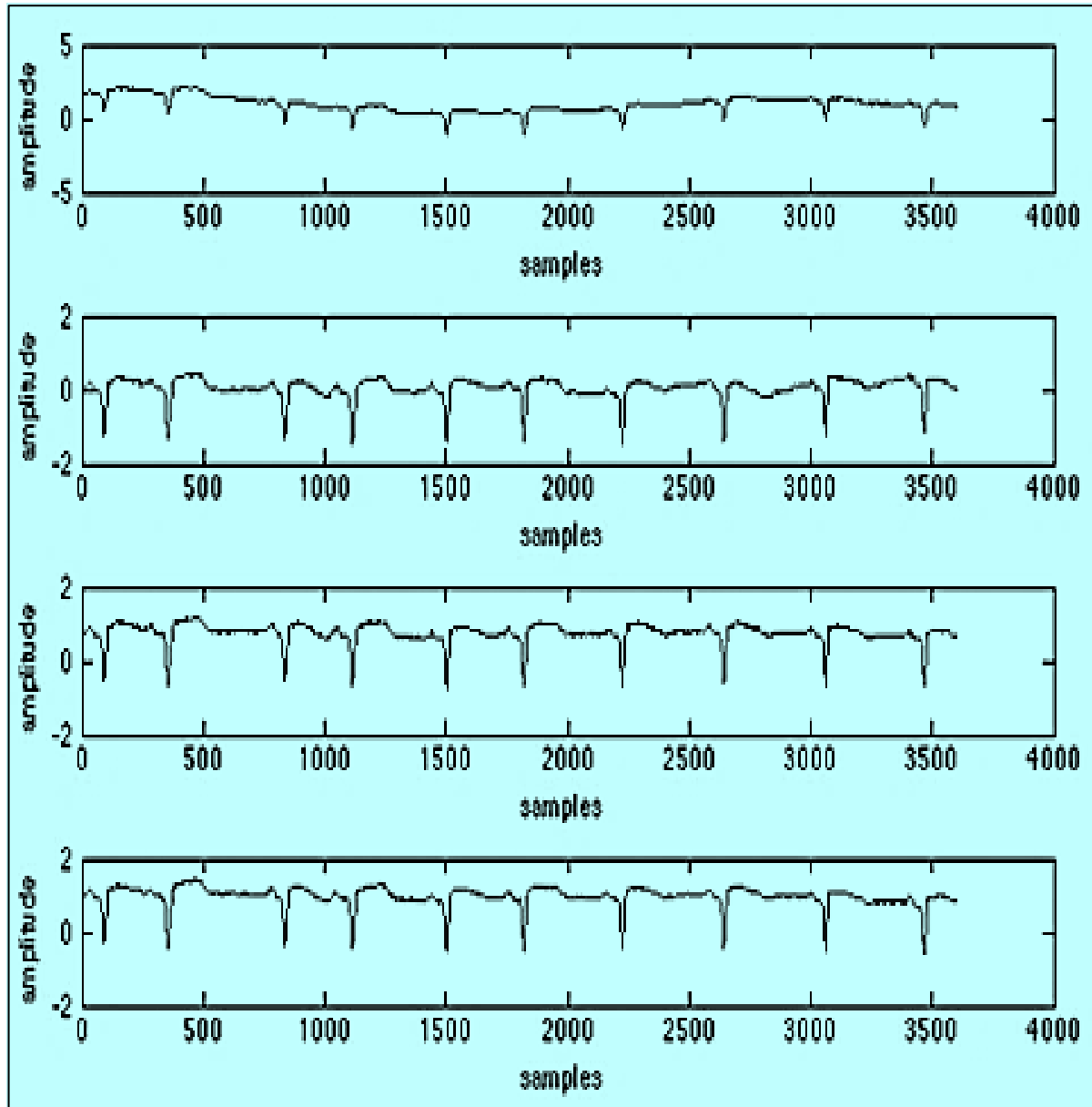


Fig.4.4 (a) Noisy signal (Recording-3) (b) Denoised signal using EMD and Neural network (c) Denoised signal using EEMD and Neural Network (d) Denoised signal using CEEMD and Neural Network.

Table 4.3: Recording-3

Parameter	(Input SNR = -15.0319, Input MSE = 0.2114)		
	<i>EMD and ANN</i>	<i>EEMD and ANN</i>	<i>CEEMD and ANN</i>
<i>MSE</i>	0.08182	0.0250	0.0033
<i>SNR</i>	1.5102	12.9336	56.6881
<i>Correlation Coefficient</i>	0.9066	0.9352	0.9966

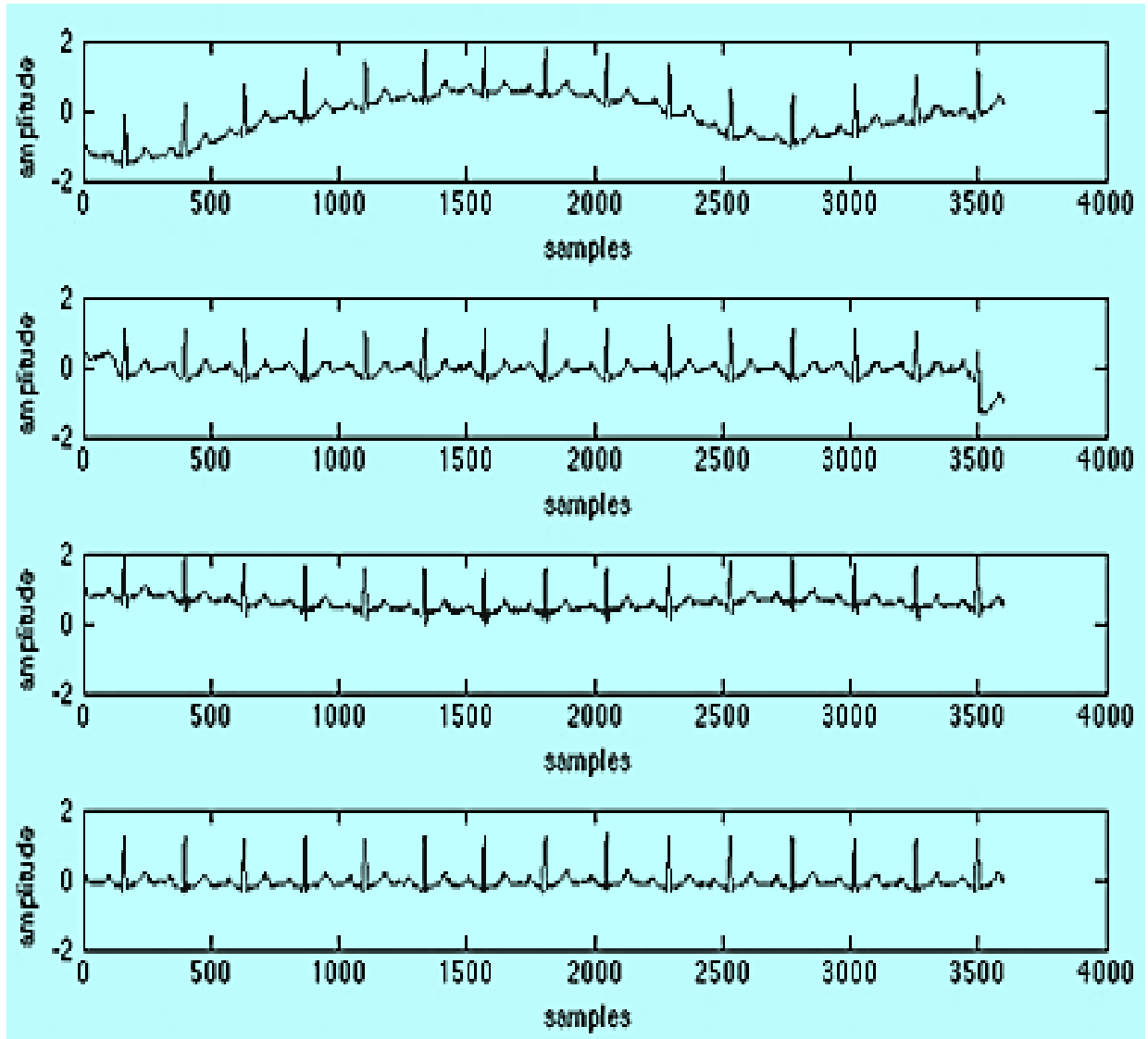


Fig.4.5 (a) Noisy signal (Recording-1) (b) Denoised signal using EMD and Morphological Operator (c) Denoised signal using Neural Network (d) Denoised signal using CEEMD and Neural Network.

Table 4.4: RECORDING-1

Parameter	(Input SNR = -19.0489, Input MSE = 0.3699)		
	<i>CEEMD and Morphological Operator</i>	<i>ANN</i>	<i>CEEMD and ANN</i>
<i>MSE</i>	0.0118	0.0095	0.0016
<i>SNR</i>	21.7005	23.7690	35.3016
<i>Correlation Coefficient</i>	0.9363	0.9457	0.9898

The CEEMD-based approach outperforms both EMD and EEMD in terms of results. For ECG signal recording-1, fig.4.5 presents plots of denoising techniques using CEEMD and Morphological Operator, Neural Network, and a proposed combination of CEEMD and Neural Network. The table 4.4 shows the results of the denoising technique for ECG signal recording-1 using CEEMD and Morphological Operator, Neural Network, and a proposed combination of CEEMD and Neural Network.

In terms of all three parameters, the proposed technique outperforms the combination of CEEMD with Morphological Operator and Neural Network. Other ECG signal recordings yielded the same results.

4.5 SIGNIFICANT FINDINGS

When examining the results, it is clear that simple Neural Networks can produce excellent results at times, but their performance is inconsistent. The addition of CEEMD ensures that the system runs smoothly. The results show that the proposed method is clearly superior to other methods in the literature. The use of CEEMD has increased the filtration properties of Neural Networks while also preventing overfitting. Furthermore, since the filtration will be conducted mainly at lower frequencies, any high frequency cardiac defects will not be filtered, which is an important consideration.

This chapter is based on the following work:

Rajesh Birok, Rajiv Kapoor & Mahipal Singh Choudhry “ECG Denoising Using Artificial Neural Networks and Complete Ensemble Empirical Mode Decomposition” Turkish Journal of Computer and Mathematics Education [TURCOMAT], ISSN: 2382-2389 in Volume 12, No. 2 (2021). [SJR-0.218] [Published in SCOPUS Indexed Journal]

CHAPTER 5

GENETIC PARTICLE-FILTER IMPROVED FUZZY-AEEMD FOR ECG SIGNAL DE-NOISING

5.1 INTRODUCTION

The electrical conduction activity of the heart is recorded by the electrocardiogram (ECG). These are extremely weak signals having a restricted bandwidth of 0.05-120 Hz. These signals are used by doctors, particularly cardiologists, to diagnose cardiac conditions and disorders. During acquisition, the ECG signal is polluted with different artefacts such as PLI, Patient–electrode motion artefacts, Electrode-pop or contact noise, Baseline Wandering, and Electromyogram (EMG) noise. In the presence of such undesirable signals, analyzing ECG data to evaluate heart function becomes challenging. As a result, de-noising the ECG signal is critical to avoid misunderstanding of the patient's heart activity.

This study proposes de-noising of the electrocardiogram signal based on the Genetic Particle filter and Fuzzy Thresholding using Adaptive Ensemble Empirical Mode Decomposition (AEEMD), which efficiently reduces noise from the ECG data. A two-phase approach for reducing noise from ECG signals is proposed in this research. With the aid of Adaptive Ensemble Empirical Mode Decomposition, the noisy signal is decomposed into real Intrinsic Mode Functions (IMFs) in the first phase. Because it eliminates the mode-mixing effect, therefore, AEEMD is superior to EMD or EEMD or CEEMD. Spectral Flatness of each IMF and Fuzzy Thresholding are used in the second step to get IMFs that have been contaminated by noise. To reduce noise from corrupted IMFs, a Genetic Particle filter is used.

5.2 THEORETICAL BACKGROUND

The Electrocardiogram is frequently contaminated through noise and artefacts.

Various artefacts are:

- 1. Power-Line Interference (PLI):** PLI artefact is defined as 50-60 Hz power line frequencies with less than 1 Hz bandwidth. Power line interference can have an amplitude of up to 50% of the FSD level.

2. **Baseline Wander:** The major cause of baseline wander artefact is breathing at drifting frequencies of 0.15 Hz to 0.3 Hz. Baseline shift or drift is another name for baseline wander artefact.
3. **Muscle Noise/ Electromyographic Artefact:** The ECG data is tainted by electrical bio-potential caused by EMG or muscle contraction. With a frequency of 10kHz, the amplitude of muscle noise swings up to 10% of the FSD level.
4. **Motion Artefact:** When the motion of an electrode or a change in impedance between electrodes is overlaid on the electrocardiogram activity, it is referred to as motion artefact.
5. **Electrode Contact Noise:** This touch noise is caused by the electrodes losing contact with the subject's skin.
6. **Data Collection Device and Electrosurgical Noises:** It is produced at frequencies ranging from 100 kHz to 1 MHz by medical equipment and signal processing gear.

5.2.1 ENSEMBLE EMD [EEMD]

Ensemble EMD (EEMD) [92] is used to eliminate the mode-mixing consequence. It primarily solves the original EMD's mode mixing problem by regularly injecting white noise into the intended signal. It is also known as a Noise-Assisted Data Analysis system (NADA). EEMD consists of EMD and taking corresponding IMFs ensemble average of 'n' number of trials. These ensemble averages output treats as final result of EEMD. The ECG signal is decomposed into real Intrinsic Mode Functions using Ensemble EMD techniques (IMFs).

The process of decomposition using EEMD can be done in following steps [51]:

- (i) To the established original signal, a random white noise signal is introduced.

$$x_j(t) = x(t) + A \cdot n_j(t) \quad j=1,2,\dots,M,$$

The amplitude of additional white noise is denoted by A, and the number of trials is denoted by M.

- (ii) Obtained signal ($x_j(t)$) is decomposed into IMFs using EEMD:

$$x_j(t) = \sum_{i=1}^{N_j} c_{ij} + r_{N_j}, \quad (5.1)$$

Here, c_{ij} denotes the i^{th} IMF of the j^{th} trial, r is the residue and N_j represents IMF number of the j^{th} trial.

- (iii) Repeat these processes until the predetermined ensemble trial number is reached, and every time, add a different random noise signal.

- (iv) For evaluating ensemble mean of the resultant IMFs of the decompositions is denoted as (c_i):

$$c_i(t) = \frac{\sum_{j=1}^M c_{ij}}{M} \quad i=1, 2, \dots, K, \quad (5.2)$$

Where K denotes the minimum number of IMFs in the trial.

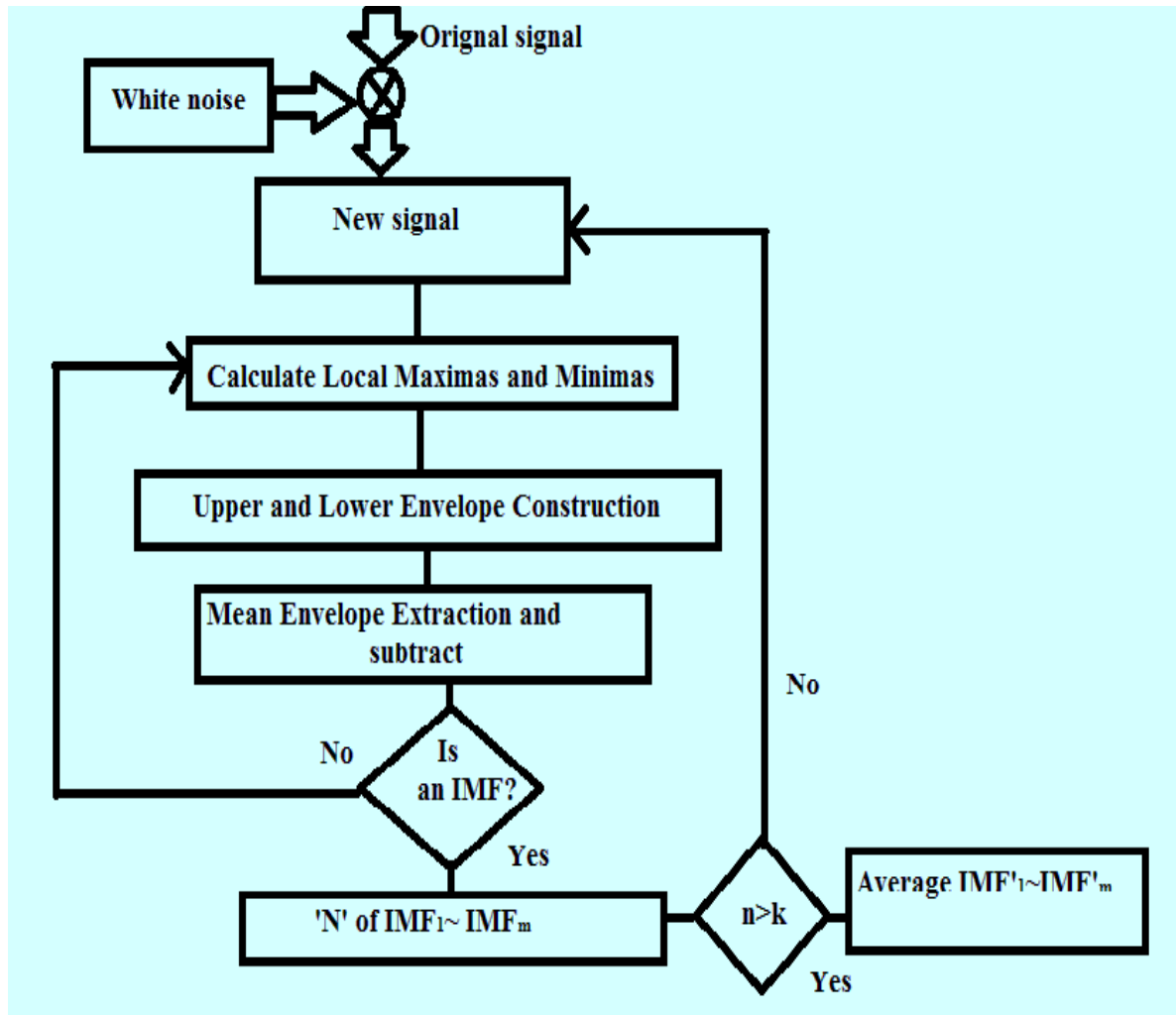


Fig.5.1 Flow chart of EEMD method

The mode mixing problem is one of the major flaws of original EMD's, implying that many decomposition components appear in the same frequency waveform or that certain decomposition components contain a variety of frequency waveforms. Wu and Huang [51] proposed the EEMD noise-assisted data analysis system. In certain circumstances, EEMD overcomes the problem of mode mixing by introducing white noise to the starting input. The EEMD approach is a great step forward in EMD development, considerably increasing the algorithm's dependability. The Genetic Algorithm was used to improve the EEMD method's self-adaptiveness.

EMD also suffers from an end effect problem, in which the signal envelopes dictated by the extreme points might reflect its appearance, filtering out the higher frequency component and only representing the signal's lower frequency component throughout the EMD process. However, all the data between them should cover the upper and lower envelopes. The end points can't generally be both maximum and minimum that results in difficult to recognize the extrema exactly. To resolve this problem *Leitao Zhang et al.* [93] proposed an end shifting method to resolve the end effect issue from EMD.

5.2.2 ADAPTIVE EEMD [AEEMD]

To lessen or decrease the irregularity as much as feasible, the extra white noise must impact the original signal's extrema. A random noise with a specified fixed amplitude value, on the other hand, affects the extrema (and hence lowers the present mode of mixing) but has no impact on the extrema.

Instead, an adaptive approach (AEEMD) is proposed and many signals are used to test its efficiency and applicability.

$$SNR_j(t) = 20 \log \left(\frac{x(t)}{Amp_j n_j(t)} \right) \tag{5.3}$$

$$Amp_j(t) = 10^{-\left(\frac{SNR}{20}\right)} \left(\frac{x(t)}{n_j(t)} \right) \tag{5.4}$$

where $j=1,2,3,\dots,M$.

The amplitude rate for each data point in a sample is obtained by adding random white noise and applying the Signal-to-Noise Ratio (SNR) as in equation (5.3) & (5.4). Given the appropriate SNR, there will be confidence that the initial signal's extrema will be suitably influenced. A noisy ECG signal polluted with numerous artefacts is seen in fig.5.2.

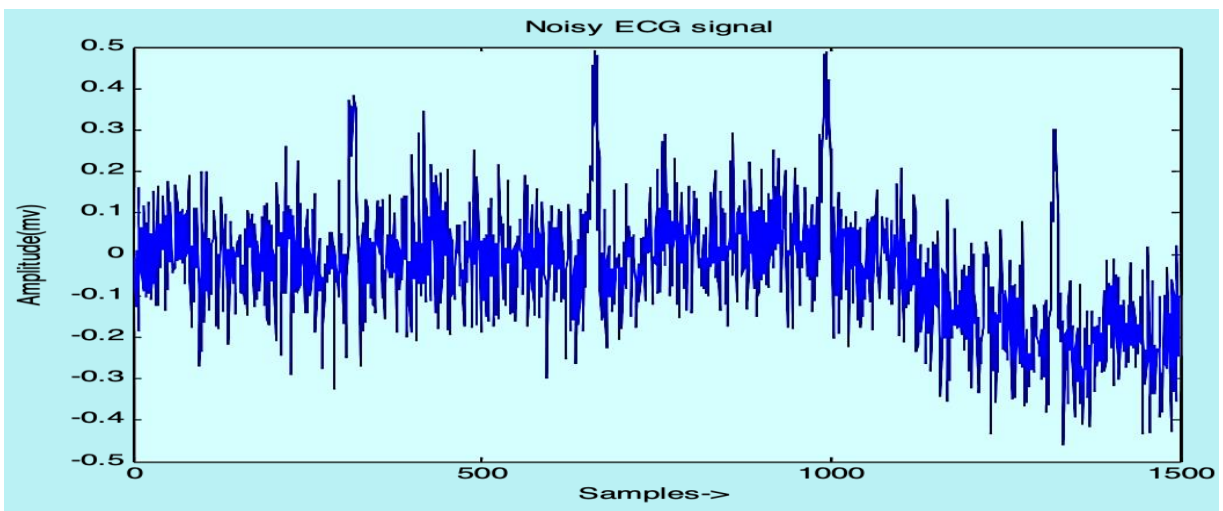


Fig.5.2 Noisy ECG signal

Chapter 5: GP-F Improved fuzzy-AEEMD for ECG Signal De-noising

A predetermined constant value is created by multiplying a specified fixed value (0.3) by the standard deviation of the original signal. As a result, impacting the extrema is dependent on the value of random noise at the extrema's location. An adaptive value is derived using the suggested approach in order to retain the SNR ratio. It indicates that the amplitude of any randomly generated noise will be high enough to effect the extrema. Figures 5.14, 5.15, and 5.16 demonstrate how the suggested amplitude functions more efficiently on the extrema when noise is added to the original signal.

5.2.3 FUZZY THRESHOLDING [FT]

Fuzzy rules are well-defined in terms of statistical properties which determine the required range of thresholds is known as Fuzzy Thresholding [94].

5.2.4 GENETIC PARTICLE FILTER [GP-F]

A Genetic Algorithm (GA) is embedded into the Standard Particle Filter (S-PF) is known as GA-PF [95], [96] which is used to overcome the degeneracy problem. It improves the self-evolution and self-adaptation. The block diagram of the proposed GA-PF method is shown in fig.5.3.

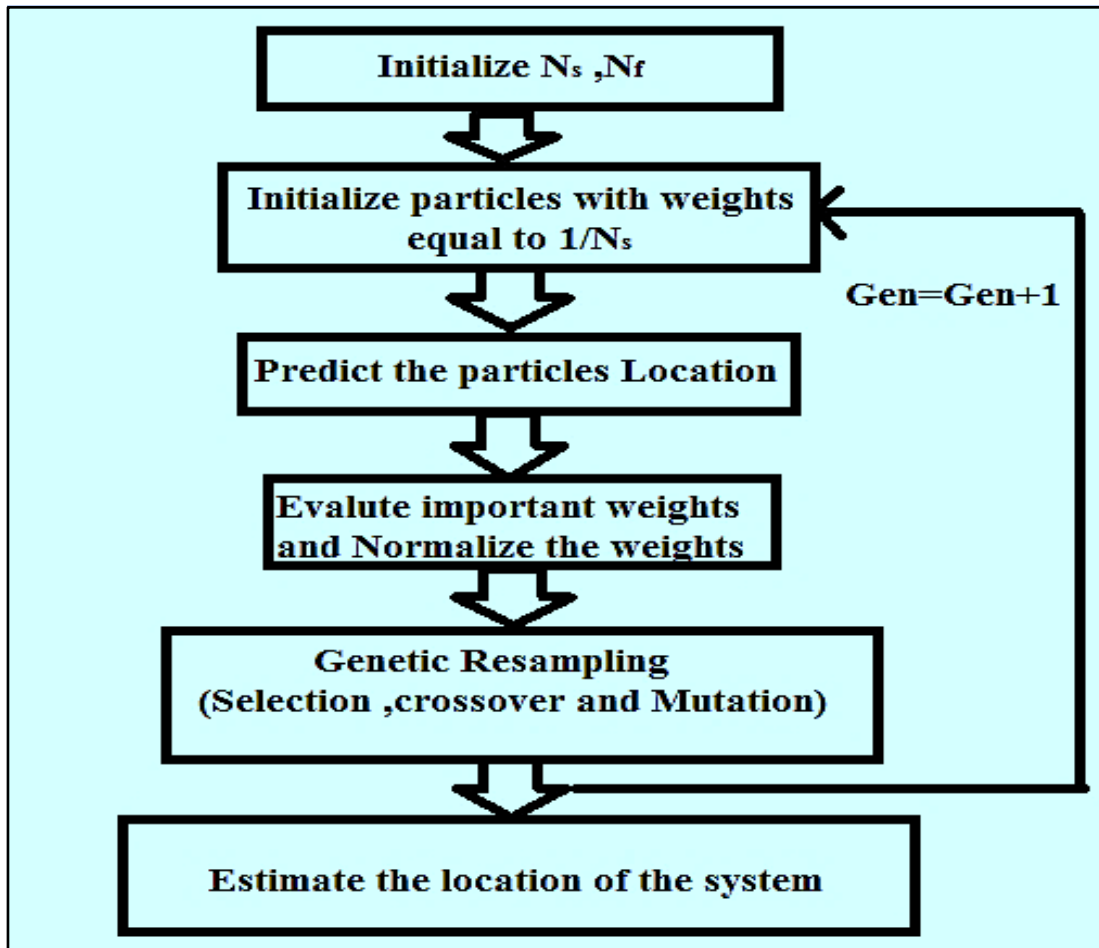


Fig.5.3 Block diagram of the Proposed GA-PF method

Chapter 5: GP-F Improved fuzzy-AEEMD for ECG Signal De-noising

Electrocardiogram signals were obtained from the hospital's database, then $n(t) = y(t) + m(t)$, where $y(t)$ is the original ECG and $m(t)$ is the added noise signal & is used to obtain the noisy signal $n(t)$. The AEEMD technique is used to breakdown the $n(t)$ signal into Intrinsic Mode Functions. To get IMFs, a noisy signal is routed via the EMD technique. Ensemble means of correlating IMFs are used to produce true IMFs as a targeted signal. The Spectral Flatness (SF) of each individual IMF is used to calculate the amount of noisy intrinsic mode functions. The link between the Geometric mean (GM) and the Arithmetic mean (AM) is known as spectral flatness (AM). It is defined as the ratio of the power spectrum's geometric mean to its arithmetic mean.

$$\text{Spectral Flatness (SF)} = \text{GM} / \text{AM} \quad (5.5)$$

To determine if the IMFs are noisy or not, the Spectral Flatness metric is fuzzified. For Spectral Flatness, low, medium, and high membership functions were utilised, as illustrated in fig.5.4. The rules for spectral flatness are:

Rule 1: IF SF is in high range, THEN IMF is clean

Rule 2: IF SF is in medium range, THEN IMF is noisy

Rule 3: IF SF is in low range, THEN IMF is very noisy.

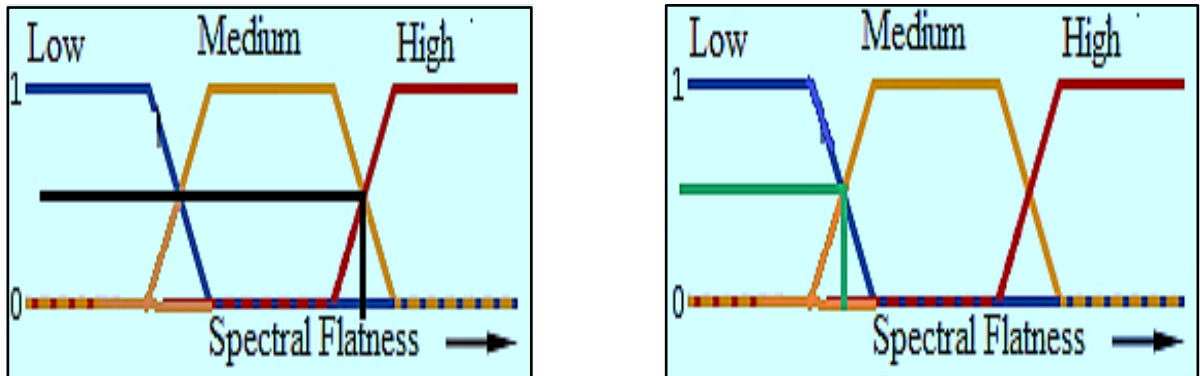


Fig.5.4 Membership function for Fuzzy-2

Now applying Rule 1,

Take minimum of membership of Spectral Flatness

Noisy = min (0.09, 0.08) = 0.08

Now applying Rule 2,

Take minimum of membership of Spectral Flatness

Noisy= min (0.03, 0.05) = 0.03

Chapter 5: GP-F Improved fuzzy-AEEMD for ECG Signal De-noising

According to the fuzzy max-min implication, 'min' membership is noisy when combining the criteria. Spectral flatness is used to automatically determine noisy intrinsic mode functions. To eliminate the noise from the noisy IMFs, the Genetic Particle Filter is used.

5.3 PROPOSED METHODOLOGY

The purpose of this research is to assess the performance of the proposed algorithm (AEEMD) under various ECG signal situations.

The ECG signal de-noising method is given as:

- (a) To collect ECG signals and add random white noise.
- (b) To breakdown the signals into some IMFs using the EEMD with varied amplitudes of additional white noise. To extract the feature, the first IMFs with the most dominating information are picked.
- (c) To calculate the total energy E_i of the first m IMFs:

$$E_i = \int_{-\infty}^{\infty} |c_i(t)|^2 dt \tag{5.6}$$

(d) To create a feature vector with the energies of the m selected IMFs:

$$FV = [E_1, E_2, \dots, E_m] \quad (5.7)$$

(e) To normalize the feature:

$$FV = \left[\frac{E_1}{E}, \frac{E_2}{E}, \dots, \frac{E_m}{E} \right] \quad (5.8)$$

where, $E = \left(\sum_{i=1}^m |E_i|^2 \right)^{1/2}$

In Programming of MATLAB software was used to construct an algorithm for de-noising the ECG signal in the block diagram of the suggested technique for the ECG de-noising method shown in fig.5.5. The ECG signal is decomposed into Intrinsic Mode Functions using AEEMD techniques (IMFs). Then, utilizing Fuzzy Thresholding, IMFs that are dominated by noise are automatically identified and filtered using Genetic Particle algorithms to eliminate the noise and increase the adaptive processing's computing efficiency.

Chapter 5: GP-F Improved fuzzy-AEEMD for ECG Signal De-noising

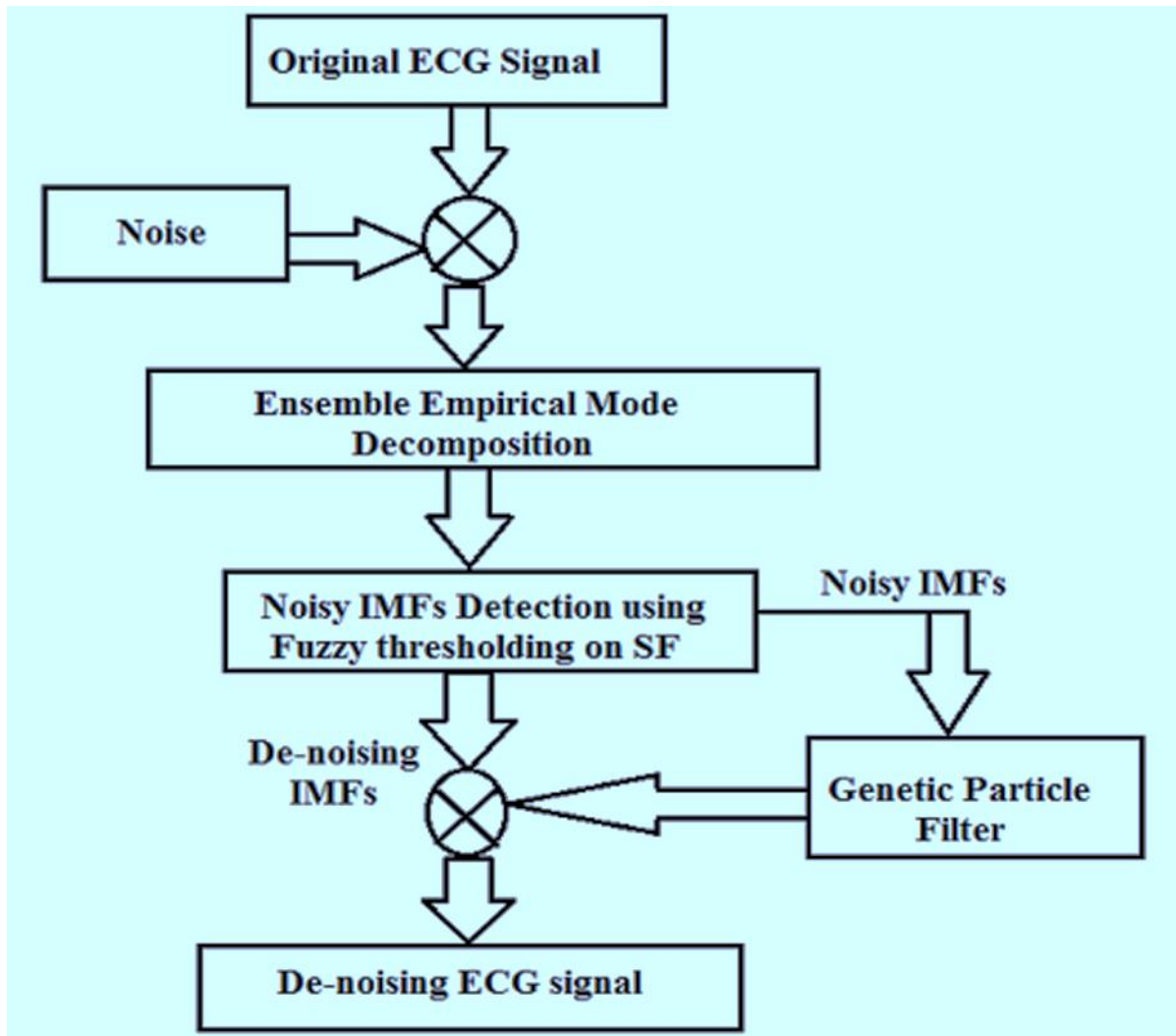


Fig.5.5 Block diagram of the proposed ECG de-noising method

5.4 RESULTS

The suggested algorithm's performance is evaluated using five distinct local hospital databases. The de-noising of the ECG signal is done in such a way that impulsive sounds are suppressed at multiple levels while the desirable ECG signal is preserved. It is impossible to totally eradicate noise, but it is feasible to reduce it to a minimum. SNR and RMSE measurements are used to evaluate the performance of our suggested approach.

Parameters of Proposed algorithm listed as follows: -

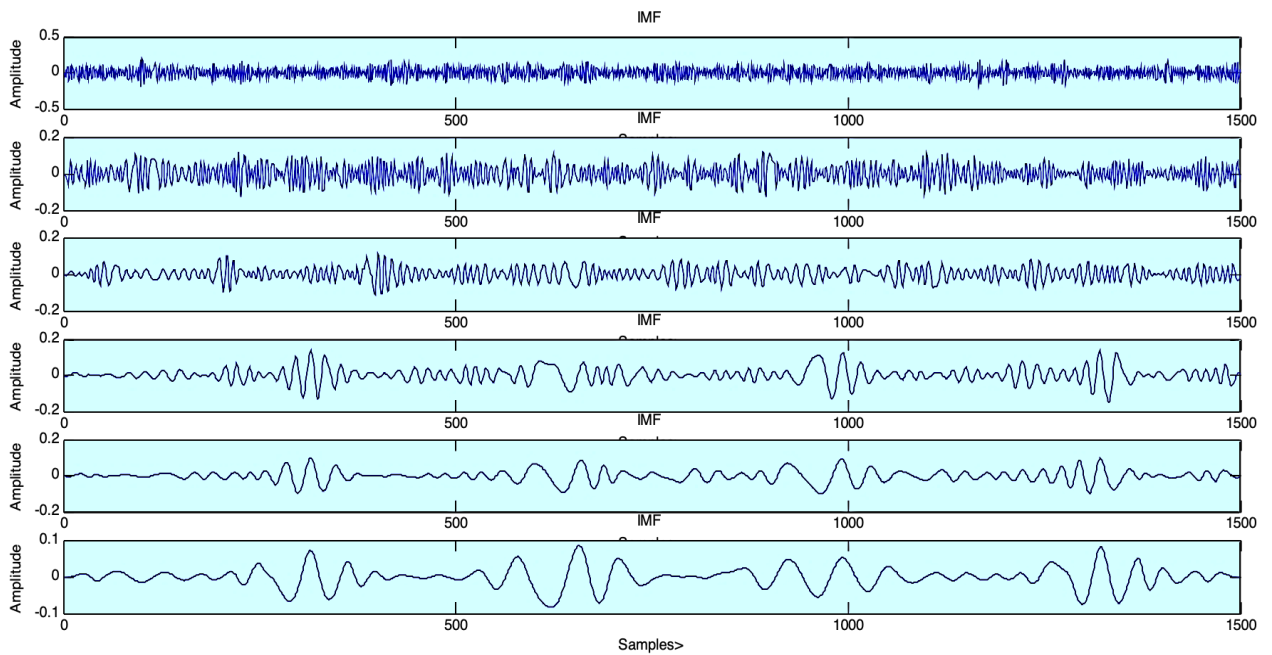
Number of particles =100

Crossover probability =0.8

Mutation probability =0.1

Maximal Acceptable generation T=20

Fig.5.6 shows the decomposition of this noisy ECG signals into IMFs components which are



obtained by AEEMD method.

Chapter 5: GP-F Improved fuzzy-AEEMD for ECG Signal De-noising

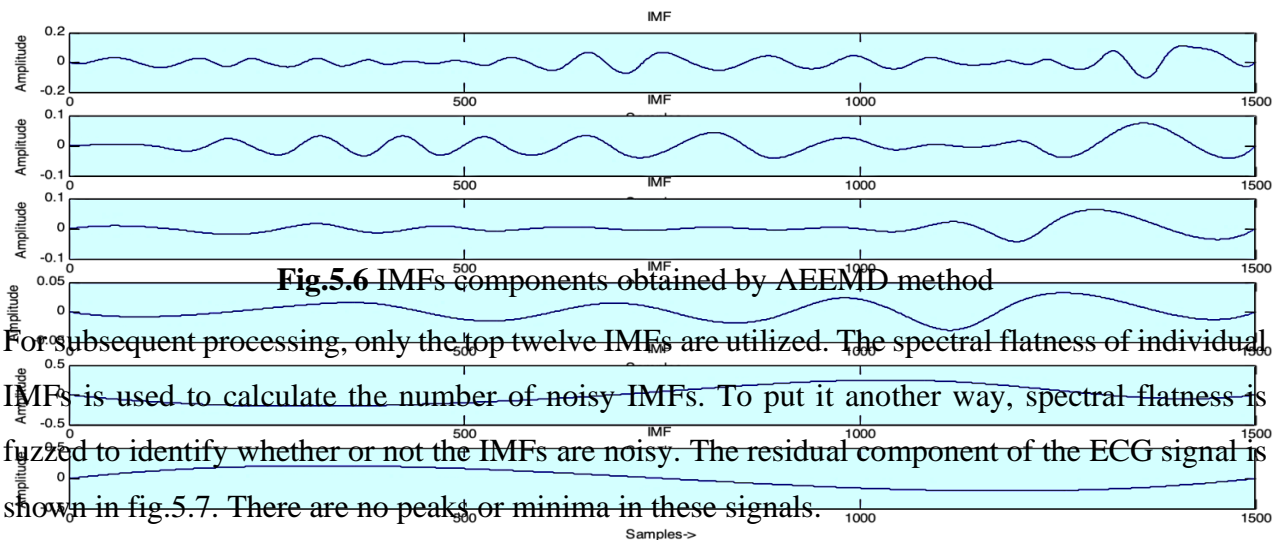


Fig.5.6 IMFs components obtained by AEEMD method

For subsequent processing, only the top twelve IMFs are utilized. The spectral flatness of individual IMFs is used to calculate the number of noisy IMFs. To put it another way, spectral flatness is fuzzed to identify whether or not the IMFs are noisy. The residual component of the ECG signal is shown in fig.5.7. There are no peaks or minima in these signals.

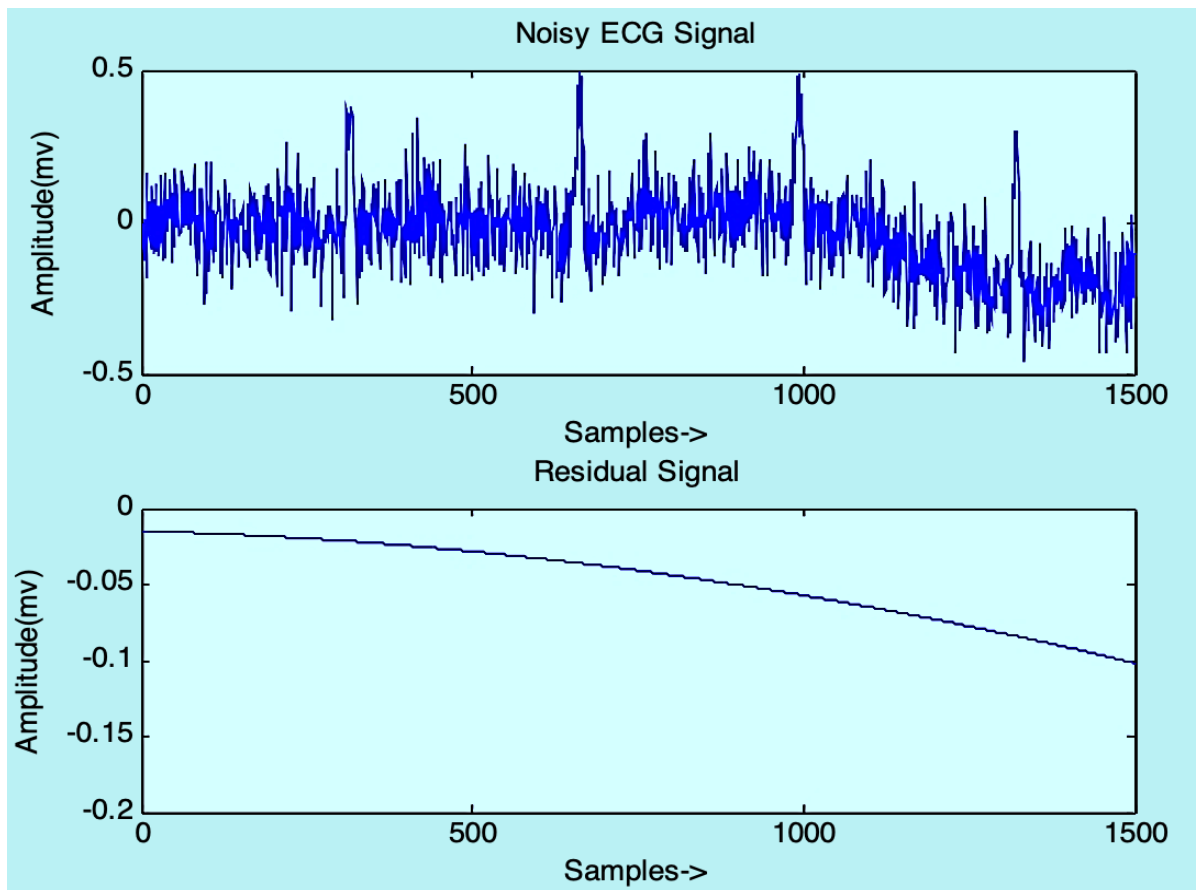


Fig.5.7 Noisy ECG signal and residual signal

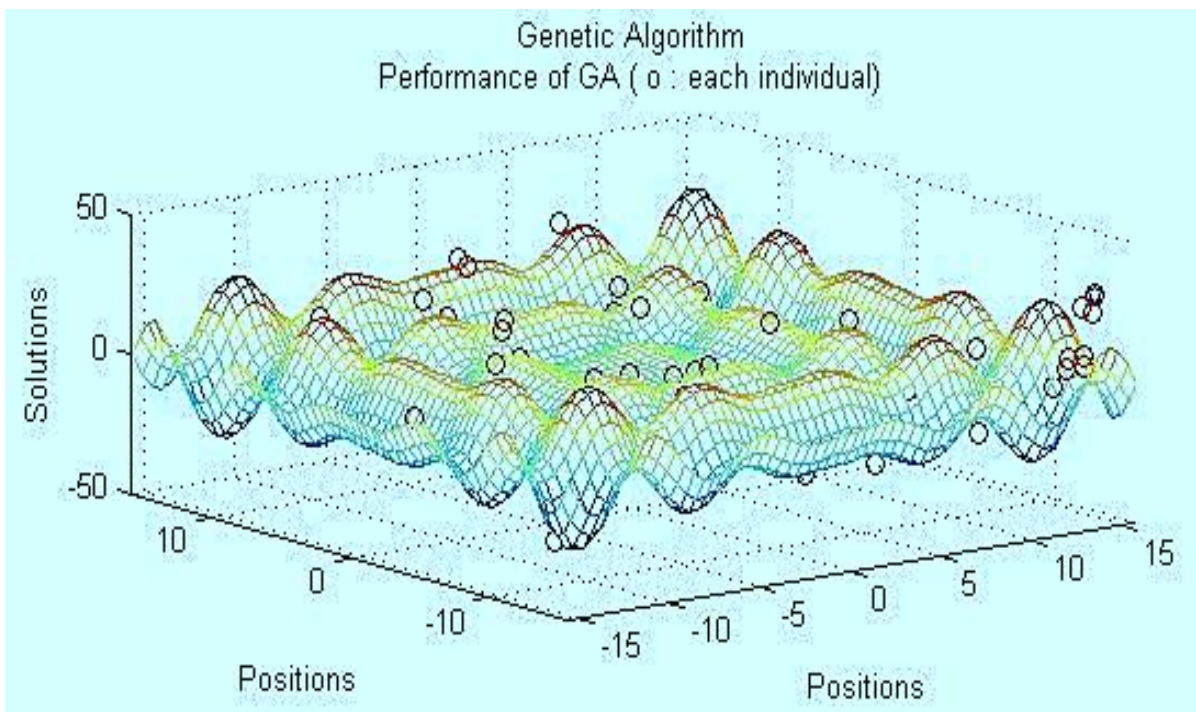


Fig.5.8 Performance of Genetic Algorithm (o: each individual)

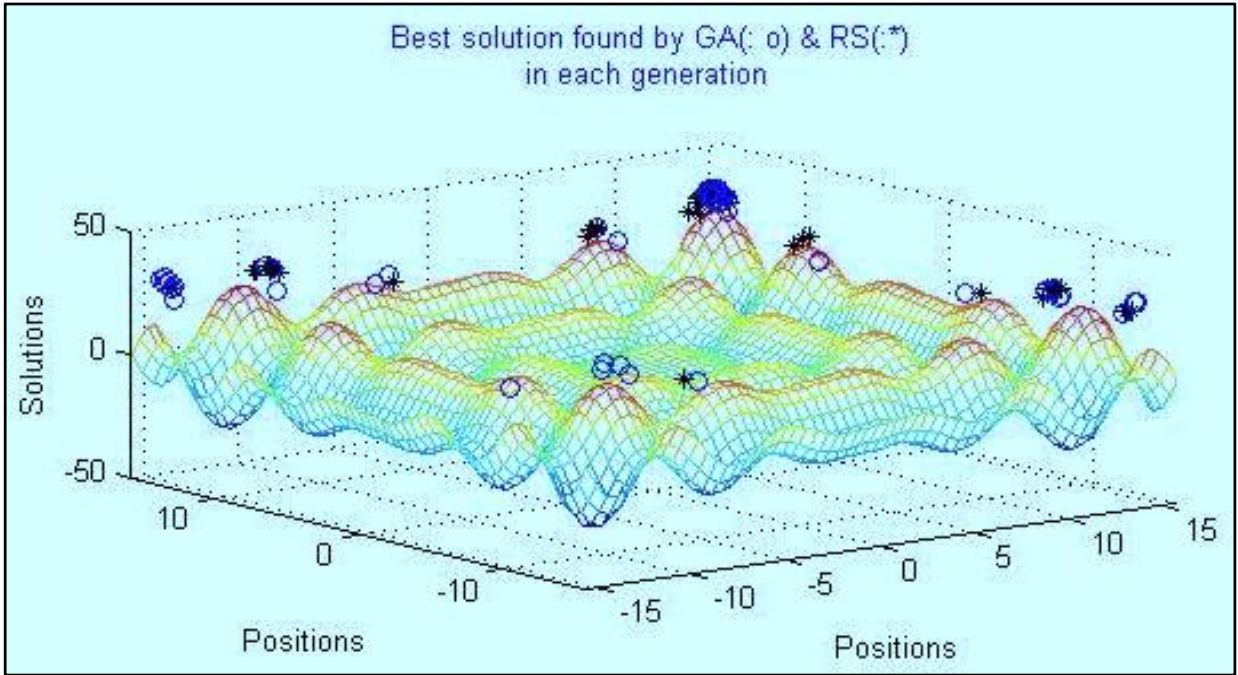


Fig.5.9 Best solution by Genetic Algorithm (: o) and RS (: *) in each generation

The performance of the genetic algorithm is seen in fig.5.8, which depicts the individual's weights as the particle's fitness function. In each generation, fig.5.9 depicts the greatest fitness function achieved using the Roulette wheel selection (RS) approach. Individually, the maximum level of fitness is immediately reserved for the next generation.

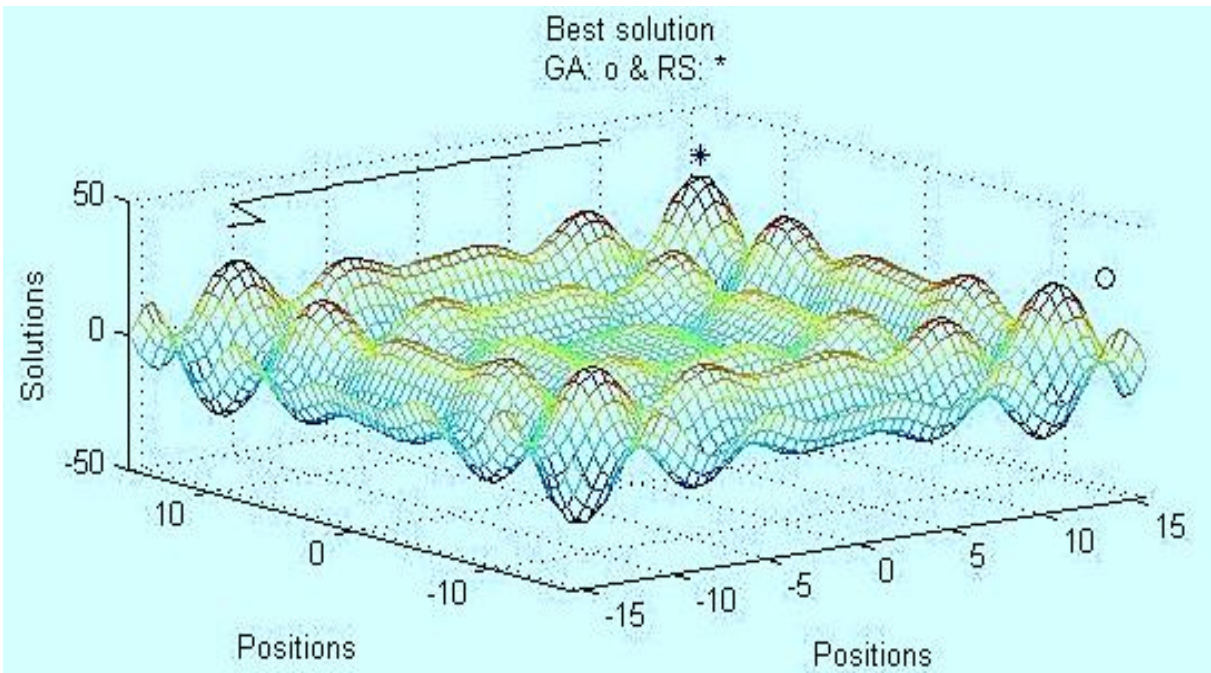


Fig.5.10 Best solution by Genetic Algorithm (: o) and RS (: *) for overall

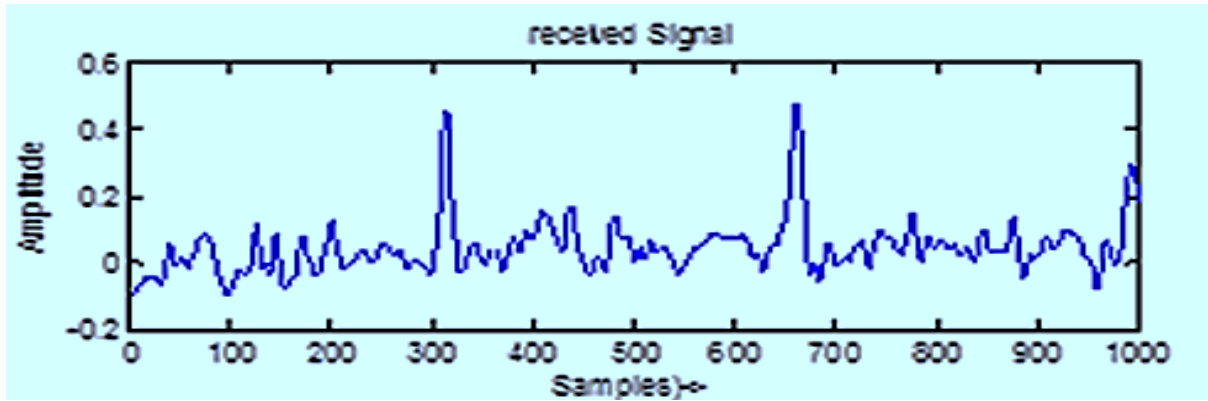


Fig.5.11 De-noised ECG signal

The greatest fitness function across all generations is shown in fig.5.10. The genetic particle filter is used to filter the noisy IMFs. The ECG signal is then rebuilt by combining the filtered IMFs with the remaining signal IMFs. The result is a de-noised ECG signal, as seen in fig.5.11. The SNR and RMSE are used to estimate the performance of our method. Signal to Noise Ratio (SNR) and Root Mean Square Error (RMSE) are acronyms for Signal to Noise Ratio and Root Mean Square Error, respectively. These variables are used to compare the proposed approach against the existing method. The SNR can be calculated as the follow:

$$SNR = 10 * \log_{10} \left(\frac{output^2}{(input - output)^2} \right) \quad (5.9)$$

The RMSE can be calculated as the follow:

$$RMSE = \sqrt{\sum_{t=0}^{L-1} [(original\ signal - reconstructed\ signal)^2] / L} \quad (5.10)$$

The values of the SNR measure for the outcomes of several current techniques with the suggested method are shown in table 5.1. Existing approaches are EMD based technique, Genetic Particle Filtering etc., with five different databases.

Table 5.1: SNR values comparison of proposed approach with other known techniques

Database	Wavelet Based Techniques (SNR in dB)	EMD Based Techniques (SNR in dB)	Particle Filter Method (SNR in dB)	Proposed Method (SNR in dB)	% Age improvement with Particle Filter Method
Database1	10.9142	12.9997	14.0853	17.7205	25.80%
Database2	11.1984	13.8093	15.2512	18.8058	23.30%
Database3	10.1845	13.8138	15.9588	19.9987	25.31%
Database4	10.4252	14.0839	16.0254	18.5141	15.52%
Database5	11.9732	14.3374	14.8569	17.3418	16.72%
Average	10.9391	13.8088	15.2355	18.4761	21.33%

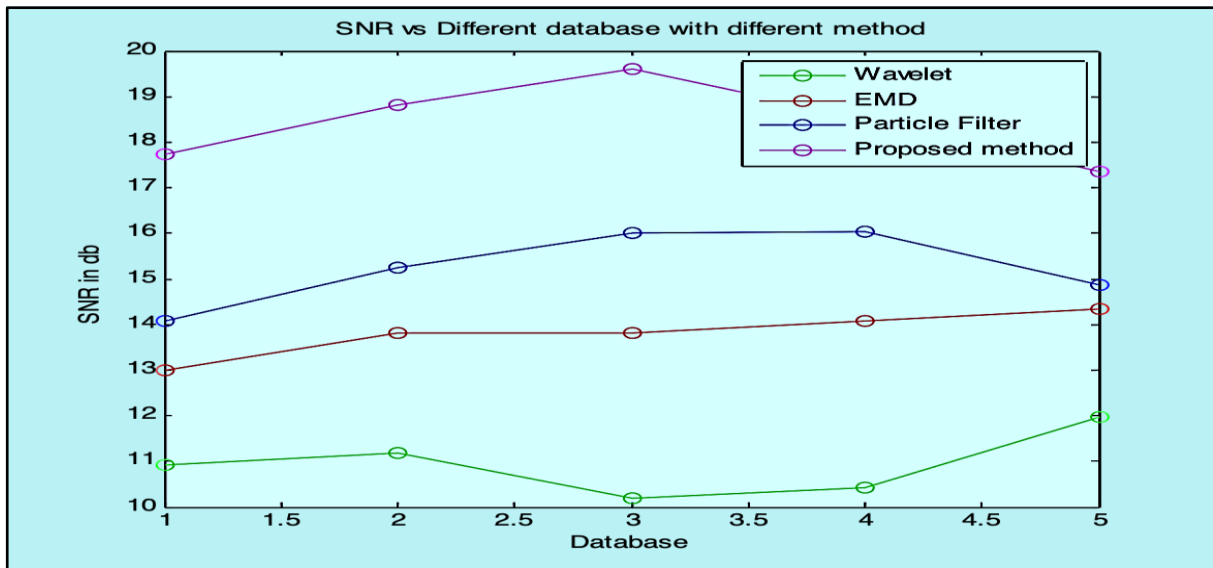


Fig.5.12 SNR vs different database with different method and proposed method

The table 5.2 represents the values of RMSE measure for the results of various existing approaches with proposed method.

Table 5.2: Comparison of RMSE values for different database of existing methods with proposed method

Database	Wavelet Based Techniques (RMSE in dB)	EMD Based Techniques (RMSE in dB)	Particle Filter Method (RMSE in dB)	Proposed Method (RMSE in dB)	% Age improvement with Particle Filter Method
Database1	0.299	0.224	0.198	0.131	-33.83%
Database2	0.271	0.215	0.179	0.112	-37.43%
Database3	0.310	0.212	0.162	0.105	-35.18%
Database4	0.302	0.199	0.152	0.119	-21.71%
Database5	0.255	0.191	0.187	0.137	-26.73%
Average	0.287	0.208	0.175	0.120	-30.97%

Wavelet approaches have shown to be popular and superior than older methods [71]. The best de-noising approach so far across all wavelet families is the Daubechies-4 (dB4) wavelet combined with soft thresholding. Wavelet algorithms are used to describe both time and frequency information at the same time. When thresholding approaches are utilized, they can improve ECG signals. The popularity of wavelet-based ECG de-noising algorithms can be attributed to this. However, the wavelet transform approach has certain drawbacks: (i) Due to the use of hard thresholding, the reconstructed ECG signal showed oscillations. (ii) Using soft

thresholding can lower the ECG signal amplitude, particularly the R waves amplitude, which is a big worry because the R-wave is vital for diagnosing cardiac illness.

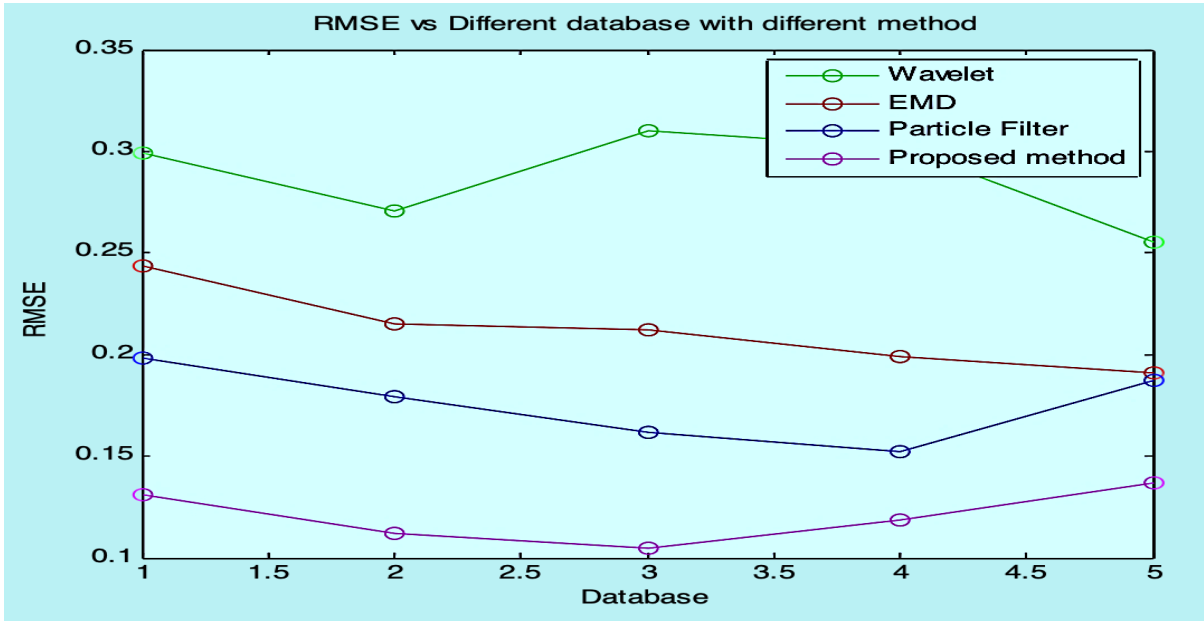


Fig.5.13 *RMSE vs different database with different method and proposed method*

Because of these constraints, researchers have turned to Empirical Mode Decomposition (EMD) to de-noise ECG signals. Intrinsic Mode Functions are a set of oscillatory functions that are decomposed from a signal (IMFs). The ECG signal is partially recreated by reducing noisy IMFs in one EMD-based technique. The removal of signal information as well as noise is one of this method's drawbacks. A metric called as Spectral Flatness (SF) is employed in another technique to detect noisy IMFs. The ECG signal is subsequently de-noised by filtering away the noisy IMFs. However, the EMD methodology has some drawbacks as a de-noising method for ECG signals, including (i) the mode mixing effect (ii) EMD also has the issue of end effect and instability [66].

All of the restrictions mentioned above have been addressed in this suggested solution. The performance of the proposed method is clearly superior to that of current algorithms with various forms of artefacts, as shown in tables 5.1 and 5.2 and figures 12, 13 and 17. When compared to EMD, Wavelet, and Particle Filter based approaches that are often used as an ECG signal de-noising method with five various types of Databases, the suggested algorithm's SNR findings show better outcomes and reduced Root Mean square Error (RMSE). The suggested technique increased the average SNR and RMSE of the de-noised data by 21.33 percent and -30.97 percent, respectively, over the second best Particle Filter method.

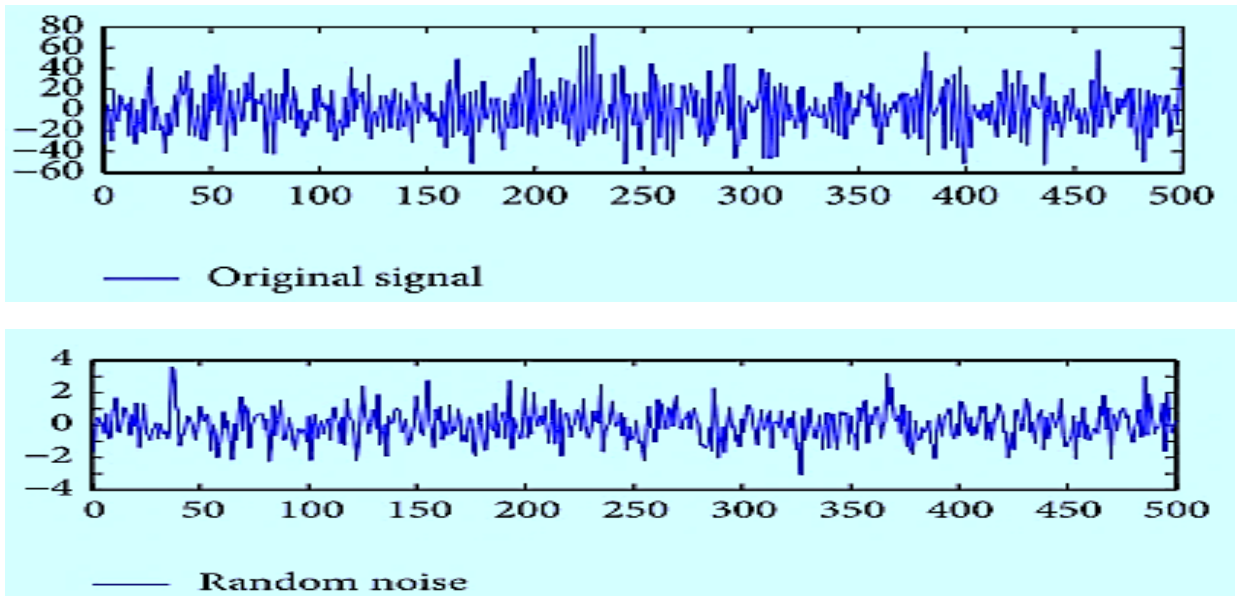


Fig.5.14 Original signal and added random noise

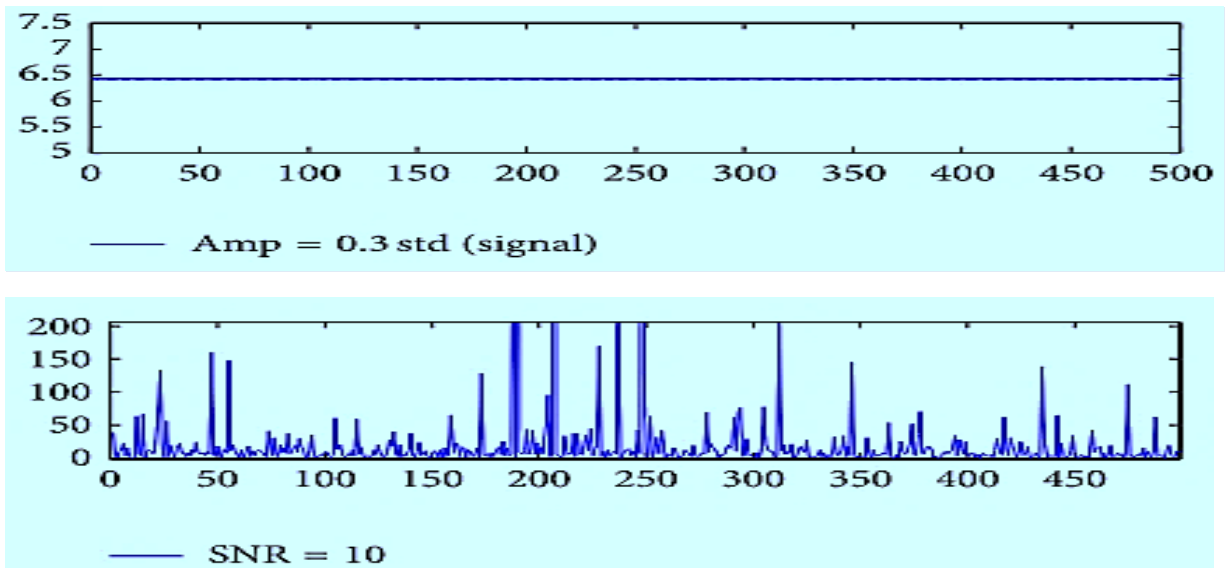


Fig.5.15 Original signal multiplied by std (0.3), AEEMD with SNR 10

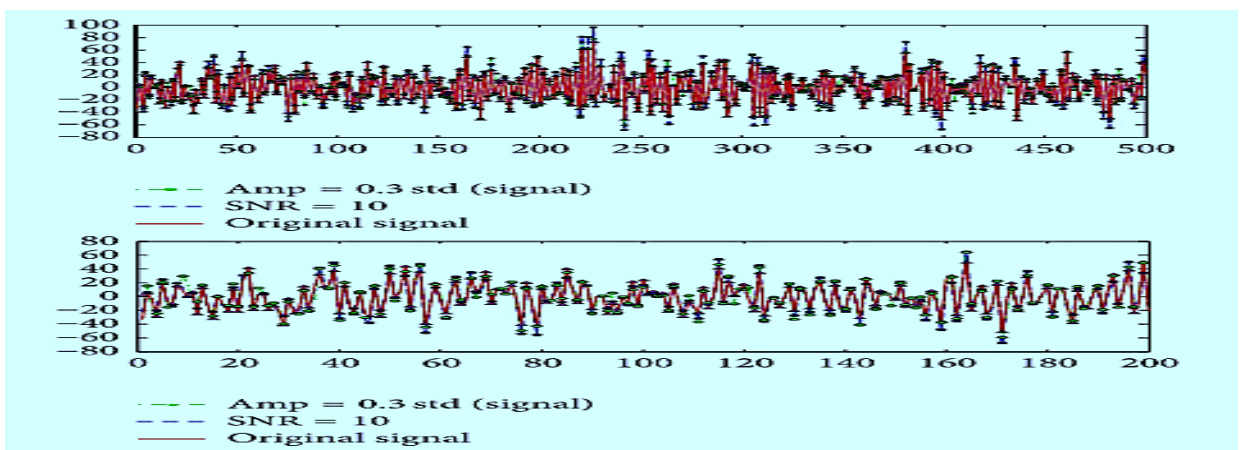
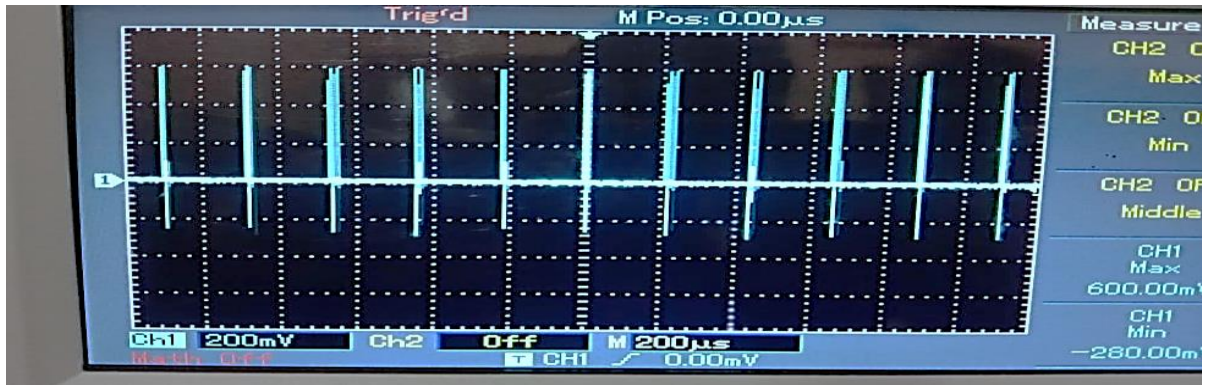


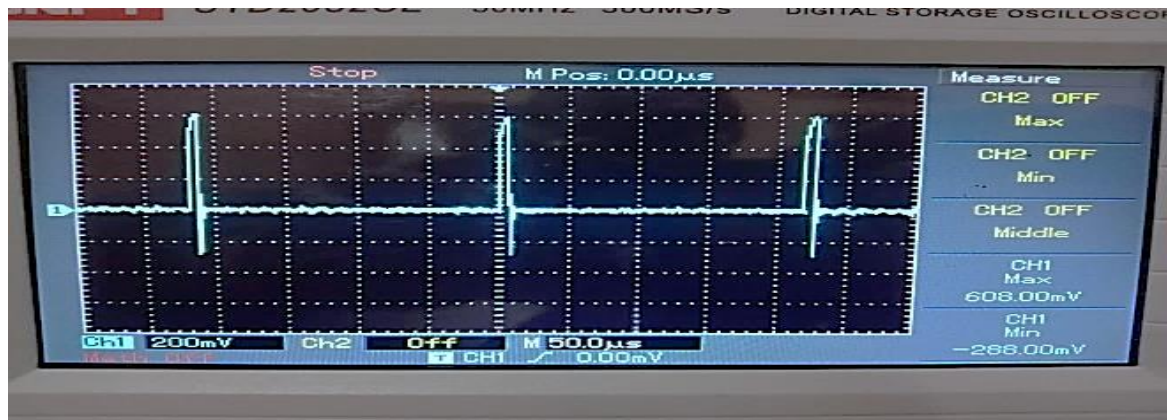
Fig.5.16 The effect of using constant amplitude 0.3 std and the AEEMD process



(a) Original Signal



(b) Noisy Signal



(c) De-noised Signal

Fig.5.17 DSO output acquired through proposed algorithm (AEEMD)

5.5 SIGNIFICANT FINDINGS

In this work, de-noising of an ECG signal using a Genetic Particle Filter and Fuzzy Thresholding with the aid of AEEMD outperforms EMD-based techniques and other current noise removal methods in terms of SNR & RMSE. The ECG signal is separated into IMFs using the AEEMD procedures. The Adaptive Ensemble EMD (AEEMD) represents a significant

advancement in noisy ECG signal filtering approach adaptability, flexibility, versatility, and robustness. The AEEMD is superior than the EMD because it eliminates the signal's mode-mixing effect. Spectral Flatness is utilized to automatically discover Intrinsic Mode Functions (noisy) using Fuzzy Thresholding.

To achieve a clean ECG signal, the remaining noisy intrinsic mode functions are filtered using the Genetic Particle Filter. The Genetic Algorithm Particle Filter enhances the process of self-evolution and adaption. De-noising performance has been increased by combining the benefits of the AEEMD over EMD technology and the Genetic Particle Filter over the particle filter. The testing findings revealed that our suggested signal de-noising approach is superior in both qualitative and quantitative measurements. When compared to the best current approach, the suggested method outperforms previous techniques with excellent quality output ECG signal in terms of average SNR (21.33 percent) and RMSE (-30.97 percent). Overall, the proposed method provides the better accuracy compared to other methods.

This chapter is based on the following work:

Rajiv Kapoor & **Rajesh Birok** “Genetic particle filter improved fuzzy-AEEMD For ECG signal de-noising.” *Computer Methods in Biomechanics and Biomedical Engineering*, ISSN: 14768259, 10255842 DOI: 10.1080/10255842.2021.1892659 [SJR-0.354]. [Published in SCIE]

CHAPTER 6

DESIGN OF LOW COST BIOIMPEDANCE MEASURING INSTRUMENT

6.1 INTRODUCTION

Biomedical signal measurement is one of the most important aspects of biomedical signal analysis and interpretation to support scientific hypotheses and medical diagnosis. Biomedical signal measurement aims at appropriately acquiring and measuring biomedical signals for accurate improved diagnosis and proper medicine management. Extensive research is going on in the field of Bio-Medical Measurements and Instrumentation. Researchers and investigators in this field are striving hard to find out new ways and methods for diagnosis and measurement of health parameters for the welfare of the mankind.

Broadly, there are two types of techniques for measuring biomedical signals namely non-invasive and invasive techniques. Here, invasive refers to medical devices that enters the human body, whereas non-invasive techniques do not involve any physically entry, cutting or puncturing of the human body by any means. Recently, minimally invasive devices and techniques have revolutionized the medical field. Overall, minimally invasive technology has substantially improved ease of patient care, outcomes and recovery. However, minimally invasive devices are still invasive in some sense.

6.2 THE HUMAN-INSTRUMENT SYSTEM

The following are the components of a human-instrument system:

- Subject or Patient**
- Stimulus or Activity Procedure**
- Transducers**
- Signal-Conditioning Equipment**
- Display Equipment**
- Recording, Data Processing, and Transmission Equipment**
- Control Devices**

6.3 IMPORTANT FACTORS FOR THE DESIGN OF BIOMEDICAL INSTRUMENTS

Biometrics is the study of measuring physiological characteristics and factors. The following are some of the factors to consider while designing, specifying, or using biomedical instruments:

- ❑ **Isolation** of the subject or patient is critical to ensure that the person is not electrocuted.
- ❑ **Range of Operation:** It is the signal or parameter being monitored for minimum and maximum values.
- ❑ **Sensitivity** is the lowest discernible signal fluctuation. This determines the system's resolution.
- ❑ **Linearity** is required, over at least a portion of the working range. Any nonlinearities discovered during signal processing may need to be incorrect values afterwards.
- ❑ **Hysteresis:** It is basically the lag caused by the direction of change in the parameter being measured. Hysteresis can introduce bias into a measurement and should be taken into account.
- ❑ **Frequency Response:** It is the fluctuation in sensitivity with frequency. The sensitivity of most systems encountered in practise exhibits a lowpass behaviour, which means that as the frequency of the input signal increases, the sensitivity of the system diminishes. To compensate for the loss of high-frequency sensitivity, signal restoration techniques may be necessary.
- ❑ **Stability** - an unstable system may prevent measurement reproducibility and uniformity.
- ❑ **Signal-to-Noise Ratio (SNR):** Simply, it is the ratio of signal strength to noise level.
- ❑ **Accuracy** entails the effects of component tolerance, movement, or mechanical faults, as well as drift.

6.4 GENERAL CONSTRAINTS IN THE DESIGN OF MEDICAL INSTRUMENTATION SYSTEMS, BIOMEDICAL SIGNAL ACQUISITION AND ANALYSIS

Medical equipment is generally used to assess physiological characteristics of the human body, however, in certain cases, it is also utilised to provide a stimulus or some sort of energy to the human body for diagnosis and therapy. Despite the fact that biomedical equipment has a long history and is widely used in health care and research, biomedical signal gathering, processing,

and analysis face several practical challenges. Each form of signal has its own set of challenges and, as a result, its own set of potential solutions. The following concerns should be given special attention:

- Inter-relationships and Interactions among Physiological Systems
- Effect of the Instrumentation or Procedure on the System
- Physiological artefacts and Interference
- Inaccessibility of the Signal Source
- Variability of Physiological Parameters
- Interference among Physiological Systems
- Transducer Interface Problems
- High Possibility of Artefacts
- Safe Levels of Applied Energy
- Patient Safety Considerations
- Human Factor Considerations
- Reliability Aspects
- Government Regulations

The following are some of the other main aspects that influence the design of a medical measuring instrument:

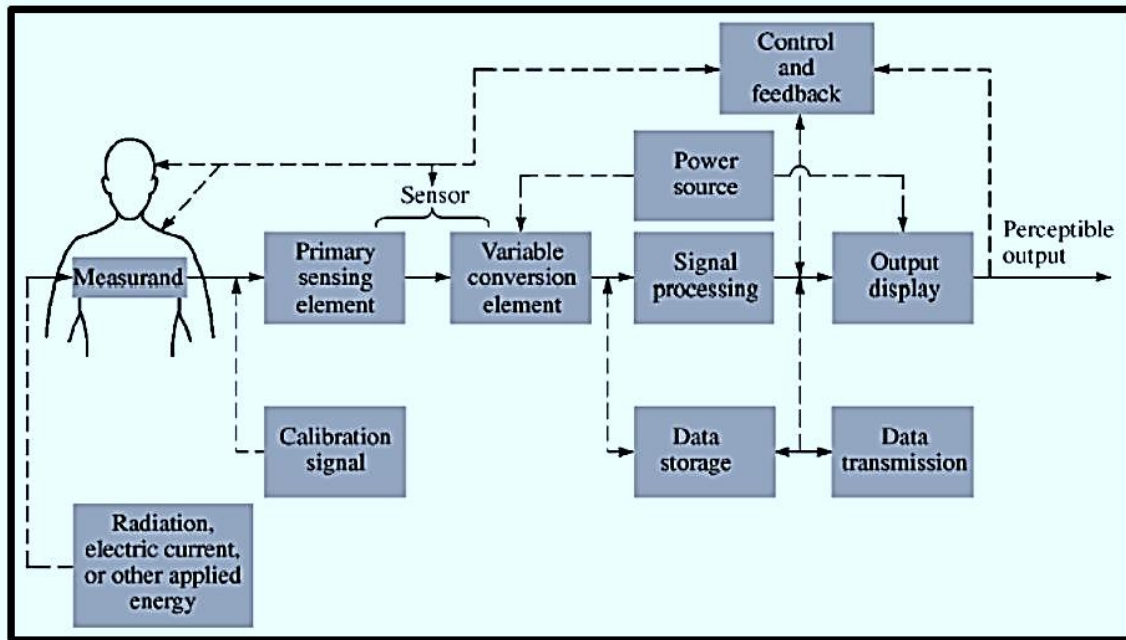
- **Measurement Range:** When compared to non-medical parameters, measurement ranges are generally fairly small. Microvolt signal range make up the vast bulk of signals.
- **Frequency Range:** The bulk of biological signals are in the audio frequency range or below, with many of them include dc and ultra-low frequency components.

As a result, it should come as no surprise that the design of medical devices is constrained by a variety of considerations. There are other general issues that must be taken into account during the original design and development of a medical device such as:

- Signal Considerations**
- Environmental Considerations**
- Medical Considerations**
- Economic Considerations**

6.5 BASIC MEDICAL INSTRUMENTATION SYSTEM

Generalized Medical Instrumentation System



* Elements and connections shown by dashed lines are optional for some applications.

Fig.6.1 *Generalized Medical Instrumentation System*

The primary purpose of biomedical equipment is to measure or determine the presence of a physical quantity that can aid medical practitioners in better diagnostics and treating patients. As a result, hospitals and other medical institutions now utilise a variety of instrumentation systems. The biomedical instrumentation systems have certain similar characteristics with other instrumentation systems. The four basic functioning components of any medical device (Fig.6.1) are as follows:

- Measurand**
- Transducer/Sensor**
- Signal Conditioner**
- Display System**

In addition to the aforementioned, the signal that has been processed after signal conditioning might be sent to:

- Alarm System
- Data Storage
- Data Transmission

Chapter 6: Design of Low Cost Bioimpedance Measuring Instrument

Most medical equipment systems require calibration at regular periods in order to perform properly. The sensor input is frequently subjected to the calibration signal. The patient is given some form of stimulation or energy, and the impact it has on the patient is measured in many medical tests. A visual stimulus, such as a flash of light or an auditory tone, or direct electrical stimulation of a neuron, might be used. Control and feedback might be manual or automated.

Microprocessors & microcontrollers currently handle almost all measuring and recording equipment, making it feasible to build equipment with little human interaction, calibration, and setup procedures. On the functional systems and sub-systems of the human body, measurements may be taken at numerous levels. In the medical science, there are two sorts of measurements: in vivo as well as in vitro. In vivo measures, such as pressure measurements in the heart chambers, are taken on or within the living thing. In vitro measurement, on the other hand, involves taking measurements outside of the body, such as collecting ECG, EEG signals.

6.6 PERFORMANCE REQUIREMENTS OF MEDICAL INSTRUMENTATION SYSTEMS

In contrast to a standard, sensor/transducer data is usually represented in terms of current intensity, voltage level, frequency, or signal phase. Most transducers, on the other hand, produce current signals, which may be easily converted to voltage using operational amplifiers with suitable feedback. The frequency response of the system should, in general, be compatible with the signal being measured. Erroneous signal components that can occur at any frequency within the system's band pass are referred to as noise. The instruments are built in such a way that noise is kept to a minimum, allowing for precise and sensitive measurement. It is critical to improve the signal-to-noise ratio in order to extract information from noisy data. The main performance requirements of biomedical instrumentation systems are:

- It should be capable enough to implement the most complex algorithms.
- Its performance should be unaffected by uncontrollable factors like component age and temperature.
- Its design parameters can be modified more readily since they are software-based rather than hardware-based.

In medical tools, the results of measurements are frequently shown on analog metres or digital screens. Digital displays are favoured for display over analog metres because of their superior resolution, accuracy, and robustness. Now a days computers are increasingly being utilised to manage equipment and to implement the man-machine interface. Moreover, high-resolution colour graphic panels are being employed for display reasons. A keyboard is the most common

Chapter 6: Design of Low Cost Bioimpedance Measuring Instrument

peripheral instrument connected to virtually all forms of data collection, processing, and controlling operations in medical equipment.

6.7 NON-INVASIVE BIOMEDICAL TECHNIQUES

Non-invasive techniques are more suitable than the invasive ones if sufficient accuracy can be achieved using them. Examples of non-invasive medical devices and techniques includes:

- External Bandages, Splints and Casts.
- Stethoscopes & Blood Pressure Monitors,
- Bio-Impedance based diagnostics such as BIA (Bio-Impedance Analysis), EIT (Electrical Impedance Tomography), IPG (Impedance Plethysmography), ICG (Impedance Cardiography)
- X-Rays & Computed Tomography [CT] Scan.
- Magnetic Resonance Imaging [MRI] Scan.
- Positron Emission Tomography [PET] Scan, Dual-energy X-ray Absorptiometry [DXA or DEXA] Scan etc.
- Hearing Aids and Holter monitoring
- ECG, EEG, EOG, EMG, EGG etc.

Among the above mentioned non-invasive available medical devices and techniques, perhaps bio-Impedance based diagnostics is still highly unexplored and underrated owing to insufficient research efforts. Later or sooner bio-impedance based diagnostics will become most prominent non-invasive diagnostic techniques as there is not only thrust on pure non-invasive diagnostic techniques, in fact it's the need of the hour.

6.8 THEORETICAL BACKGROUND: BIOIMPEDANCE

It is a well-established fact that the electrical bio-impedance of a part of the human body can provide valuable information regarding physiological parameters of the human body, if the signal is correctly detected and interpreted. Therefore bio-impedance based signal measurement

is going to be one of the most important Non-Invasive techniques to measure various physiological parameters of human body such as: -

- Intra-Cellular Fluid (ICF) & Extra-Cellular fluid (ECF),
- Total Body Water (TBW) & Electrical Cardiometry,
- Skin Water Content & Skin Conductance,
- Impedance Imaging (Tomography) & Transthoracic Impedance Pneumography,

Chapter 6: Design of Low Cost Bioimpedance Measuring Instrument

- Ablation Monitoring and measurement of Respiration Rate,
- Body Composition Assessment,
- Electrical Impedance Tomography (EIT) etc,

Keeping above scenario in mind accordingly, an efficient low-cost bioelectrical impedance measuring instrument was developed, implemented, and tested in this study. Primarily, it is based upon the low-cost component-level approach so that it can be easily used by researchers and investigators in the specific domain. The measurement setup of instrument was tested on adult human subjects to obtain the impedance signal of the forearm which is under investigation in this case. However, depending on the illness or activity under examination, the instrument can be used on any other part of the body. The current injected by the instrument is within the safe limits and the gain of the biomedical instrumentation amplifier is highly reasonable. The technique is easy and user-friendly, and it does not necessitate any special training, therefore it can be effectively used to collect bioimpedance data and interpret the findings for medical diagnostics. Moreover, in this paper, several existing methods and associated approaches have been extensively explored, with in-depth coverage of their working principles, implementations, merits, and disadvantages, as well as focused on other technical aspects. Lastly, the paper also deliberates upon the present status, future challenges and scope of various other possible bioimpedance methods and techniques.

6.8.1 FREQUENCY RESPONSE OF BIOIMPEDANCE

The anatomical, physiological, and pathological state of biological cells and tissues determine the bioimpedance frequency response. Therefore, the bioimpedance study can provide much more information related to the anatomy and physiology of a cell or tissue. Since the bioimpedance response is a variable of signal frequency, therefore bioimpedance analysis with multifrequency inputs can give detailed information of cell or tissue properties, which can help in better cell or tissue characterization. It also fluctuates depending on the frequency of the applied ac signal [5, 6]. As a result, the frequency response of biological cells and tissues is

influenced not only by their physiological and physiochemical composition and structure, but also by the frequency of the applied signal.

The few bioimpedance analysis techniques which makes use of lumped estimation of the bioimpedance values of the cell or tissue samples are BIA, IPG, and ICG etc. Bio-Electrochemical Impedance Spectroscopy (EIS) measures and analyses bioimpedance at different frequencies. Thus, EIS provides not only a lumped approximation of the cell or tissue

Chapter 6: Design of Low Cost Bioimpedance Measuring Instrument

sample's bioimpedance values at relatively higher frequency (generally 50 kHz), but also the details required to have better understanding of the many complex bioelectrical phenomena such as dielectric dispersions and relaxation.

The bioimpedance measurement can be broadly divided into two categories namely "single-tone" signals and "multi-tone" signals measurements. The analysis of "single-tone" signals is very straightforward, but measurements take longer, whereas use of a multi-tone signal allows for simultaneous coverage of the entire frequency spectrum. However, use of a multi-tone signal may result in an algorithm which can be more complex for analysis purpose [97]. Moreover, the dielectric properties of the object determine the required frequency range for bioimpedance measurements, which typically spans 3 to 4 decades in the kHz to MHz range. In general, wider range of frequencies improves fitting accuracy but at the cost of complicating measurements. Furthermore, (SNR) of measured signals also effects the fitting accuracy [98].

6.8.2 TYPES OF ELECTRODE CONFIGURATIONS

When an alternating current is used in bioimpedance testing, the electrode displays a frequency-dependent impedance at its interface with the tissue/solution known as Electrode Polarisation Impedance (EPI). Any change in the type of material which is in contact with the electrode also affects the magnitude and as well as the phase of the electrode impedance of tissue/solution. As a result, the total calculated impedance of the system is equal to the sum of the EPI and impedance of the tissue/solution [4]. Finally, the impedance will be determined by the magnitude of the applied AC signal, type of electrode used and electrode material used as well as its dimensions and geometrical structure [99]. To perform bioimpedance measurements, we need at least two electrodes to make a closed circuit for the electrical current to pass through it [4]. Therefore, bioimpedance measurements are performed with two or four electrodes. In both methods, the current or driving electrodes (as illustrated by the red coloured electrodes in fig.6.2 are known as input or excitation electrodes, whereas the electrodes upon which the frequency dependent ac potential ($V(f)$) is determined are known as voltage or sensing or output electrodes (as depicted by blue coloured electrodes in fig.6.2. It should be observed that bioimpedance

measurements can be inaccurate due to factors such as movement and improper electrode placement [99]. Bioimpedance measurements are typically done with gel electrodes to minimise electrode-skin impedance. The usability of dry electrodes is studied in [100] because this type of electrode is not suitable in many measurement environments. For bioimpedance measurement, there are two kinds of electrode configurations. As the name suggests, the

Chapter 6: Design of Low Cost Bioimpedance Measuring Instrument

two-electrode system or setup in fig.6.2(a) uses only two electrodes for impedance measurement, and thus the current signal injection or current-carrying as well as voltage measurement or voltage pickup are done with the same electrodes. For unipolar measurements, electrode configuration with one very small and one very large electrode can also be used for measurements [101].

The two-electrode technique suffers from contact impedance due to polarisation impedance at the electrode's surfaces [4], and the measured data covers the voltage drop due to contact impedance. While, analysing the measured signal polarisation impedance in the output signal should be extracted and considered [102, 103]. Overall, the results obtained using this method are interesting, however they do not provide an accurate signal on the electrode's surface [104]. In four electrode configurations or setups, two independent electrode pairs are used for current injection and detecting changes in voltage or voltage measurements [101, 105]. A constant amplitude current signal is injected through the outer electrodes, known as current electrodes or driving electrodes in fig.6.2(b) with red colour, while the frequency dependent output voltage signal produced is measured at two points within the current electrode, known as voltage electrodes or sensing electrodes in fig.6.2(b) with blue colour.

In this configuration, as the distance between electrode pairs was increased, the magnitude of the measured impedance decreased [4, 106]. A number of factors influence the effect of electrode polarisation impedance which includes electrode content, size, measuring frequency, sample impedance, and so on. The main advantage of four electrode configuration over its counterpart two electrode configuration is that the voltage electrodes are non-current carrying, due to this it eliminates polarisation impedance and thus reduces the effect of contact impedance at the electrode and tissue or electrolyte interface. Therefore, using a four-electrode system, is a well-known and popular method of lowering the effect of electrode polarisation impedance [107]. Furthermore, four electrode configuration measurements are more sensitive and accurate.

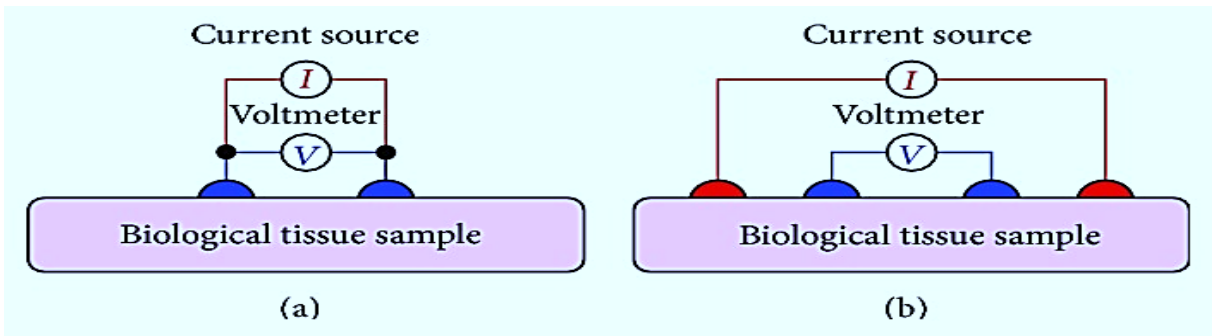


Fig.6.2 Bioimpedance measurement using: (a) two-electrode method, (b) four-electrode method.

Chapter 6: Design of Low Cost Bioimpedance Measuring Instrument

6.9 PROPOSED METHODOLOGY

The instrument designed consists of power supply, current source, voltage sensing unit and data acquisition system. Fig.6.3 depicts the general block diagram of the measuring instrument. The current source circuit is used to generate a sinusoidal current of amplitude in the range of $600\ \mu\text{A}$ - $800\ \mu\text{A}$ and a frequency of $50\ \text{kHz}$ [4]. The voltage sensing unit is used to amplify and remove the high frequency components from the signal sensed by voltage sensing electrodes. The signal is then given to the data acquisition system. The contact surface dimensions of all test electrodes are the same, and the carrier is a circular printed circuit board. To compare the electrode's characteristics, the electrode-skin impedances are measured under a variety of signal frequencies, contact durations, contact pressures, positioning positions, and subjects. All measurements are often done with silver/silver chloride (Ag/AgCl) dry gel electrodes for contrast [100]. The instrument has four Ag/AgCl electrodes, two on the outside and two on the inside, which are used as current electrodes and voltage electrodes, respectively. This type of arrangement is known as a tetra polar arrangement. Such an arrangement has been implemented by J. J. Wang et.al. [108] to use forearm impedance plethysmography for monitoring cardiac pumping function.

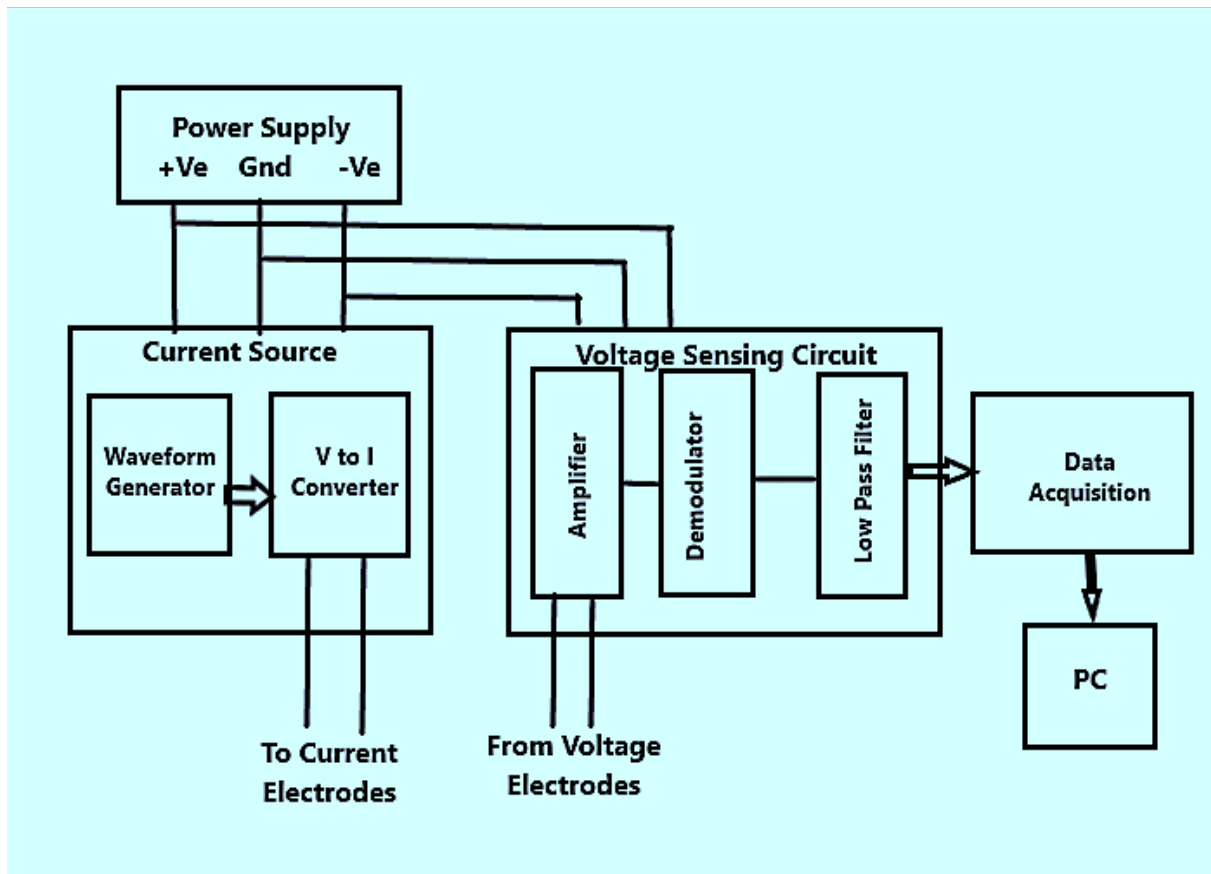


Fig.6.3 General block diagram of Measuring Instrument

6.9.1 WAVEFORM GENERATION

This is the first stage of the instrument and also the most critical one. All the parameters for this stage are very important as far as subject's safety and the output of the device is concerned. As this is the first stage any noise added at this stage will get amplified in the subsequent stages. A good waveform generator should have a single frequency output with very low value of total harmonic distortion and should have a very low frequency drift. A Wein bridge oscillator can be used to generate a sinusoidal waveform [109]. The oscillator is designed for a frequency of 50 kHz as this frequency is widely accepted in clinical use as a standard [110]. Among all types of voltage source generators, an oscillator produces the output with the most stable frequency as compared to other sources. Wein bridge oscillator is implemented using an op-amp, which gives a stable output with a single frequency for a particular combination of resistors and capacitors. Proper limiter circuit is also used in the circuit to keep the poles of the oscillator on the imaginary axis. One major problem with using Wein bridge oscillator is that the instrument designed cannot be used for bioimpedance spectroscopy.

A comparator, integrator and wave shaping circuit can be used to generate square, triangular and sinusoidal waveform of variable frequency [111]. The comparator and integrator circuit

used together generate square and triangular waveforms. Triangular waveform is shaped using a shaping circuit to generate sinusoidal waveform. The maximum frequency achieved by this circuit using 741 op-amp is 26 kHz. This method can be used for excitation in lower frequency range but lower frequencies are not used in bioimpedance spectroscopy as electrodes get polarized at lower frequencies. It has also been observed during our laboratory experiments that there was no biomodulation obtained in the output signal when a current of frequency less than 20 kHz was injected into human body.

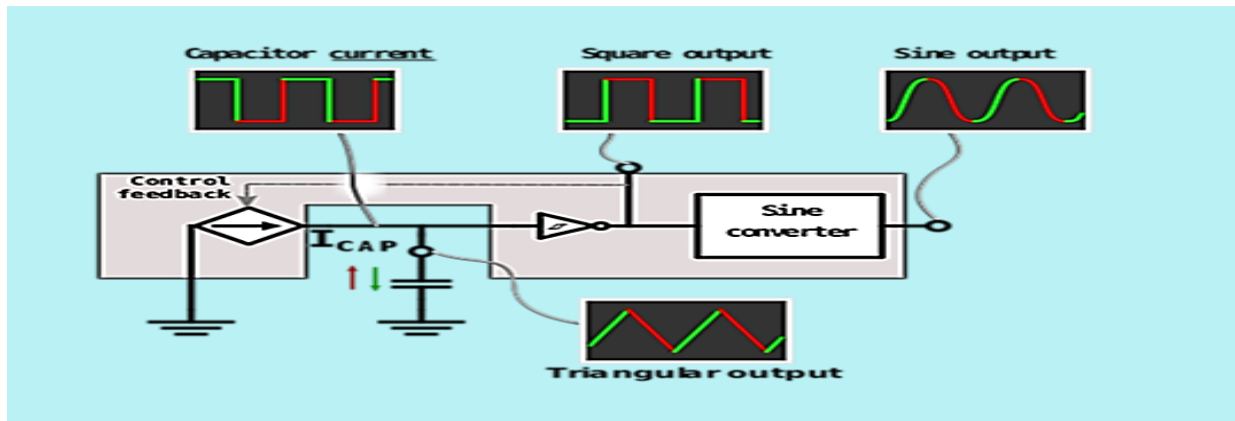


Fig.6.4 Schematic diagram of ICL8038

Chapter 6: Design of Low Cost Bioimpedance Measuring Instrument

The instrument designed uses a monolithic integrated circuit ICL8038 (Fig.6.4.) to produce high accuracy sine, square and triangular waveforms [112]. The frequency can be selected externally from 10 kHz to 100 kHz using a potentiometer. The output of ICL8038 is stable over a wide range of temperature and supply variations. The total harmonic distortion for ICL8038 varies from 1% to 2% depending on the model selected.

6.9.2 V TO I CONVERTOR

One of the most important sub circuits in bioimpedance measurements is the current driver as it is capable of working over a wide range of frequency and impedance. The main requirements of a current driver are high output impedance, short phase delay and minimal harmonic distortion. Depending on whether they are open loop or closed loop, analogue current drivers are grouped into two groups. The features of each design are described [113].

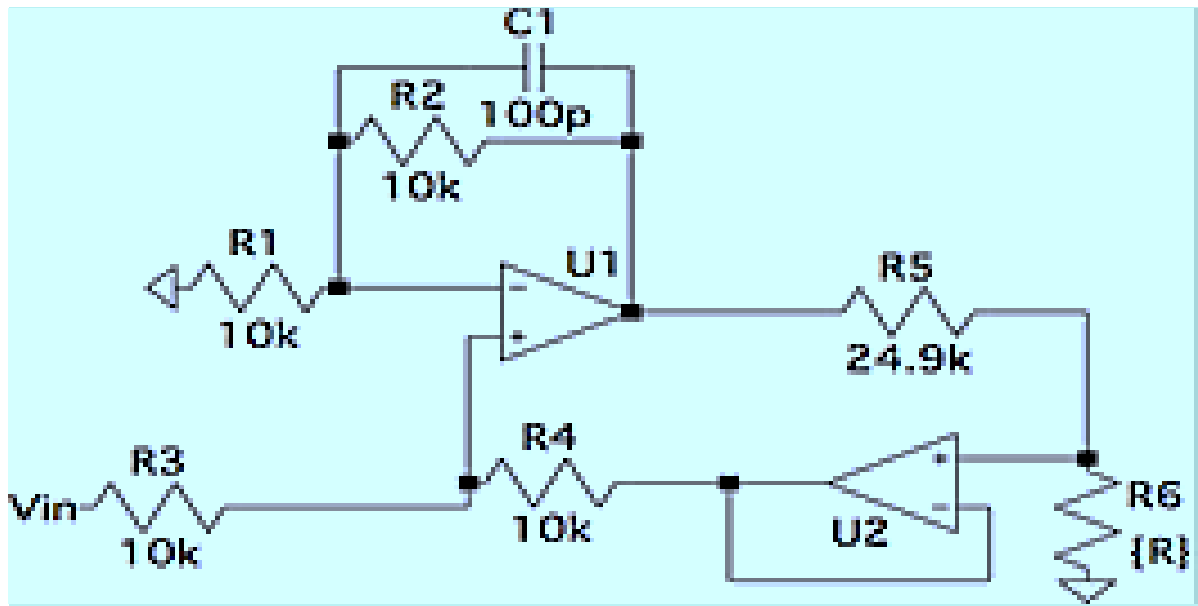


Fig.6.5 Circuit diagram for Voltage to Current converter

The voltage waveform generated using 8038 is converted into current, which is injected into human body. The current generated is within the safe limits (600 μ A- 800 μ A). The V to I converter is intended to run in the 10 kHz to 100 kHz frequency range.

The main requirement for a current source is that it should supply a constant amount of current irrespective of the impedance of the load connected to it. When the output impedance of the current source is much greater than the load impedance then the current through the load is maintained constant regardless of the load value. F. Seoane et.al have analyzed Howland circuit as V to I converter [114]. In this instrument Howland circuit with buffer is used for voltage to current conversion. Fig.6.5 is the circuit diagram for voltage to current converter. The buffer stage increases the output impedance of the V to I converter. The input impedance

Chapter 6: Design of Low Cost Bioimpedance Measuring Instrument

of the circuit is around 20 k Ω . Fig.6.6 depicts the simulation results for circuit of Fig.6.5. The resistance {R} in the fig.6.5 represents the load to which current would be injected. The impedance of the human body is in the range 1 k Ω - 3 k Ω . In simulation the resistance {R} is varied from 0.1k to 5k in steps of 500 Ω . It is verified using the simulation results that the current through the load is almost constant (10 μ A variation) irrespective of the load resistance.

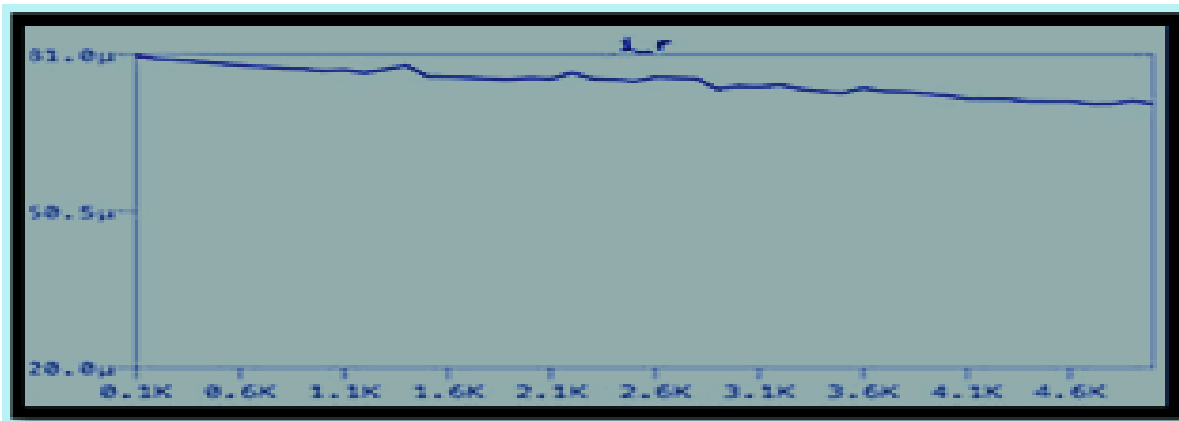


Fig.6.6 Variation of current through $\{R\}$ with respect to change in value of load resistance, y-axis is the current through the load and x-axis is the impedance of the load connected to the V to I converter.

6.9.3. INSTRUMENTATION AMPLIFIER

The voltage sensed from the section of human body is in range of millivolts. The input signal is amplified using a difference amplifier. A single op-amp can also be used as a difference amplifier but due to its low input impedance it cannot be used. The input impedance of the single op-amp difference amplifier can be increased by introducing a buffer at each of the inputs of the amplifier and instead of using a unity gain follower one can also have some gain from the first stage.

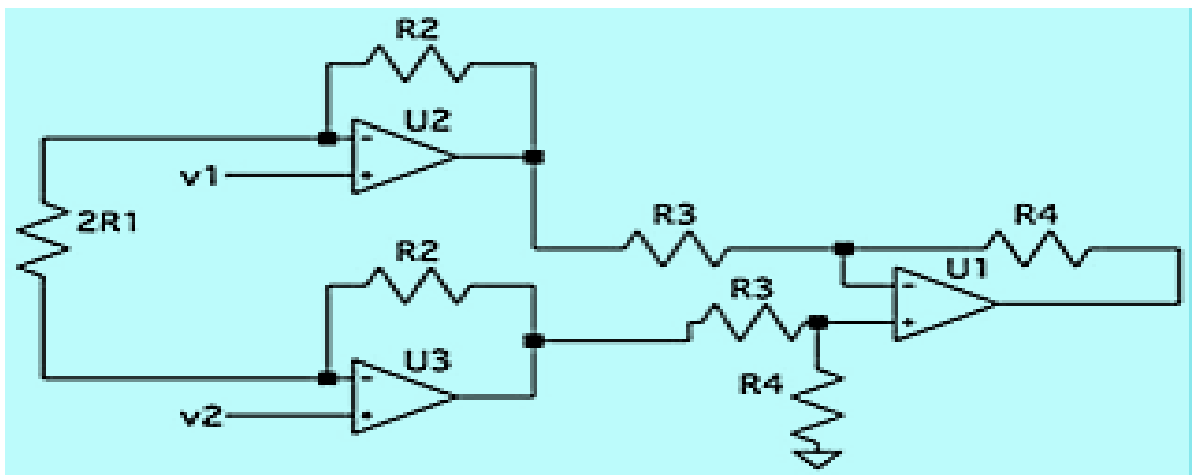


Fig.6.7 Circuit Diagram for Instrumentation Amplifier

Chapter 6: Design of Low Cost Bioimpedance Measuring Instrument

This leads to the circuit of instrumentation amplifier as shown in fig.6.7. The instrumentation amplifier has high CMRR and high input impedance and has been very effectively used in biomedical applications such as EEG and ECG. The analysis for instrumentation amplifier has been given by Adel S. Sedra and Kenneth C. Smith [109] and its use as a biopotential amplifier has been analyzed by Nagel J.H [115]. The gain for the instrumentation amplifier is given below.

$$gain = \frac{R_4}{R_3} \left(1 + \frac{R_2}{R_1} \right) \quad (6.1)$$

The signal from the electrodes is given as input to the two terminals of the instrumentation amplifier. The gain of the amplifier is 26.44 dB. The first two op-amps are used for gain and the third operational amplifier is used for common mode rejection. In the circuit designed $R_4=R_3$ and R_2/R_1 is equal to 20. The input impedance of the amplifier is equal to the input impedance of the operational amplifier. Frequency response analysis of the instrumentation amplifier depicts that the phase and gain are constant in the frequency range of interest. Fig.6.8 depicts the frequency response of the instrumentation amplifier in which the continuous plot is the magnitude plot and dotted plot is the phase plot.

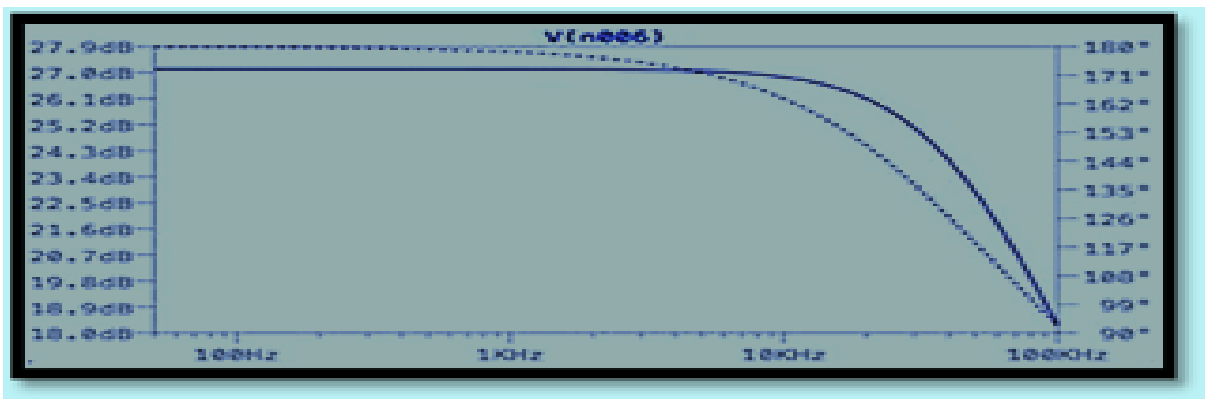


Fig.6.8 Frequency response analysis of the Instrumentation Amplifier

6.9.4 DEMODULATOR

The signal obtained from the human body is an amplitude modulated signal, where the carrier is the current waveform that we have introduced into the human body. In this case the high frequency carrier is a sinusoidal waveform with a frequency of 50 kHz and the modulating bioimpedance signal is low frequency signal with frequency components less than 50 Hz. Webster and Tompkins [116] have suggested use of full wave rectifier for demodulation. The modulating signal can be extracted using a simple envelope detector circuit as shown in fig.6.9. Asynchronous demodulation has been used so that square and triangular waveform excitation

Chapter 6: Design of Low Cost Bioimpedance Measuring Instrument

can also be used in addition to the sinusoidal waveform.

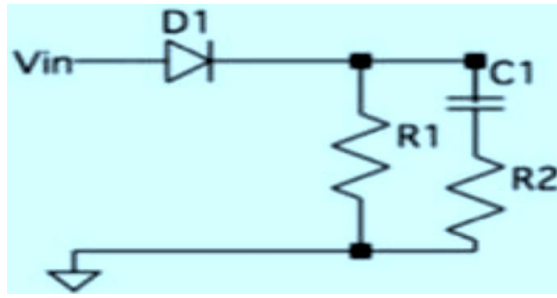


Fig.6.9 Circuit Diagram of simple envelope detector

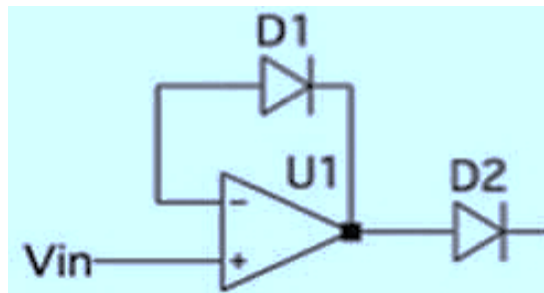


Fig.6.10 Precision Detector

For the first cycle diode is forward biased and it charges the capacitor to the first peak value. The charging time constant should be such that the capacitor voltage follows the input signal.

$$\tau_{charging} \ll \frac{1}{f_c} \quad (6.2)$$

Where f_c is the frequency of the carrier. The charging times constant depends on source resistance R_s , forward bias diode resistance r_d and capacitance C_1 .

$$\tau_{charging} = ((R_s + r_d + R_2) || R_1) C_1 \quad (6.3)$$

$$R_s + r_d + R_2 \ll R_1 \quad (6.4)$$

\therefore

$$\tau_{charging} = (R_s + r_d + R_2) C_1$$

When the input signal drops, diode becomes reverse bias (as capacitor is charged to a higher voltage) and the capacitor voltage remains at the initial level. During this time (when diode is reverse bias) the capacitor discharges through the resistor R_1 .

Chapter 6: Design of Low Cost Bioimpedance Measuring Instrument

$$\tau_{discharging} = R_1 C_1 \quad (6.5)$$

The discharging time constant should be large so that the capacitor discharges slowly but it

should not be so large that it is unable to trace the low frequency modulating signal. The discharging time constant should follow the following relation

$$\frac{1}{B} \gg \tau_{discharging} \gg \frac{1}{f_c} \quad (6.6)$$

Where B is the bandwidth of the low frequency bioimpedance signals. For the calculation of the values of resistances and capacitance, value of B is taken equal to 50 Hz. The diode used in the circuit is forward biased when the incoming voltage is greater than 0.7V, therefore the low voltage signals cannot be detected. Taking into account this problem related to cut off voltage of diode, a precision diode [109] is used in this circuit in place of normal diode. A precision diode is an operational amplifier with a diode in the negative feedback followed by a diode whose anode is connected at the output pin of the op-amp. The cutoff voltage for a precision diode is approximately equal to zero volts. Fig.6.10 is the circuit for precision diode. The output of the demodulator is given to the low pass filter stage through a buffer. Improved output buffering and peak detector gain greater than unity is achieved with an output voltage follower. This leads to circuit of precision envelope detector in fig.6.11. The precision envelope detector is much more accurate than the simple envelope detector as the voltages below 0.7V are also detected by this circuit. Droop due to detector diode leakage can be removed through the use of bootstrapping feedback that holds detector diode bias at zero when the diode is not conducting.

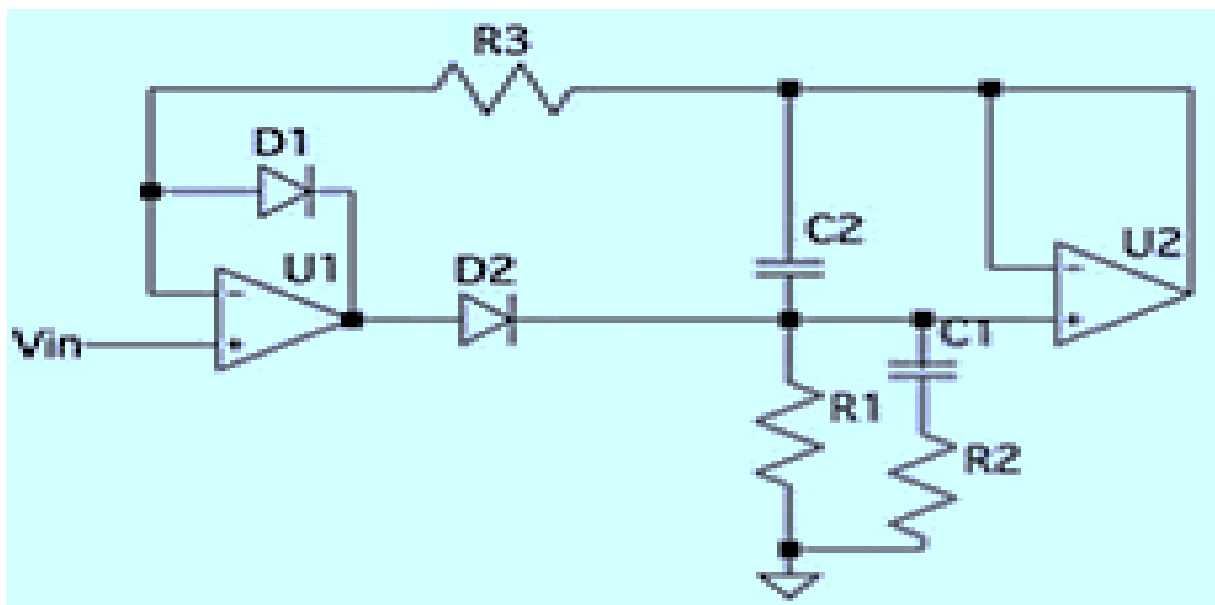


Fig.6.11 Precision Envelope Detector

Chapter 6: Design of Low Cost Bioimpedance Measuring Instrument

6.9.5 LOW PASS FILTER

The signal from the demodulator contains high frequency components, which needs to be

filtered out before the signal is given as input to the analog to digital converter of data acquisition. The low pass filter is used as an antialiasing filter. A second order Chebyshev low pass filter with a cutoff frequency of 40 Hz is used. Chebyshev filters differ from Butterworth filters in that they have a steeper roll-off and more passband (type I) or stopband (type II) ripple. Chebyshev filters have the property of minimizing the difference between the idealized and real filter characteristics over the filter's range, but with passband ripples. The output of the low pass filter is given to data acquisition system implemented using Arduino UNO board.

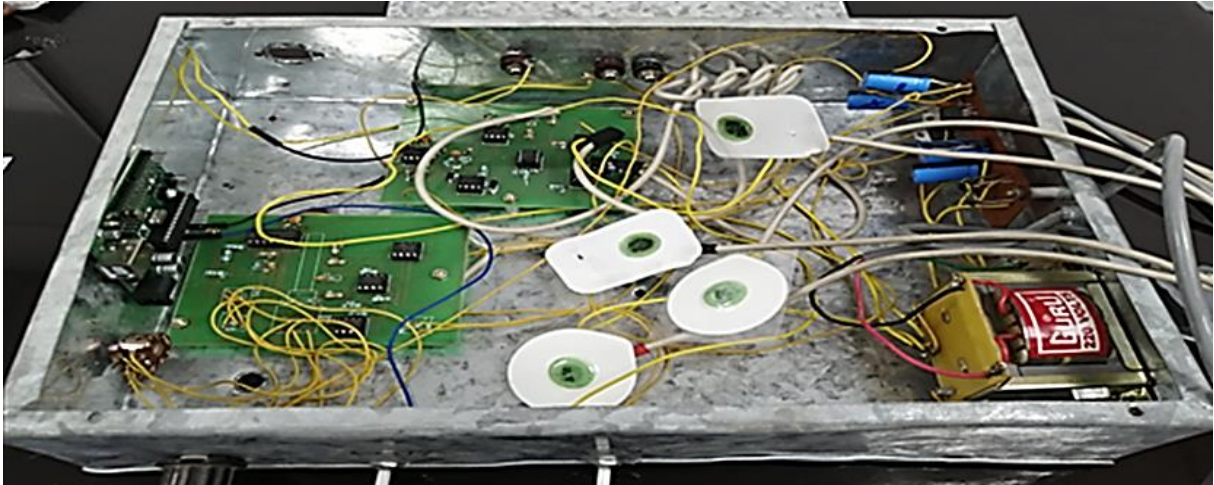


Fig.6.12 *Final version of designed Bioimpedance Measuring Instrument*

6.9.6 ASSUMPTIONS, MEASUREMENT PROTOCOL AND DATA ACQUISITION

According to the BIA assumptions, the human body can be considered as a homogenous conductor having cylindrical dimensions, in which impedance is directly proportional to length of the cylinder and inversely proportional to the cross-sectional area of the cylinder base (Fig.6.13).

BIA formulation processes typically make the following assumptions for ease of calculation, though in practise the human body varies from these assumptions:

- The human body is assumed to be a cylinder;
- The cylindrical shape is defined by its height and weight;
- Homogeneous and evenly distributed body composition is considered;
- The body compositions have no individual differences or variations;
- The environment parameters like temperature, other physiological parameters such as body heat or stress are assumed to be constant.

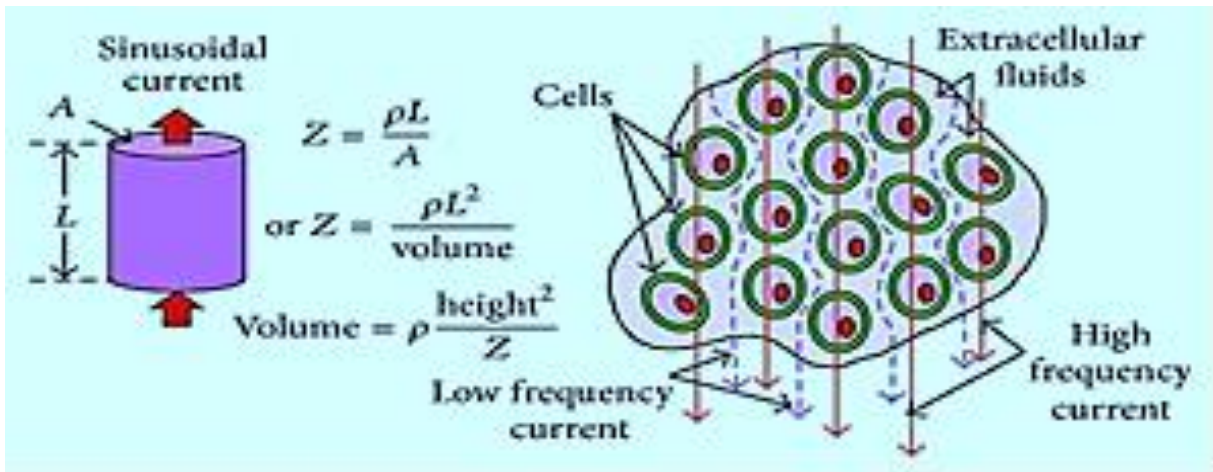


Fig.6.13 The human body's impedance when modelled as a homogeneous cylindrical volume conductor

The capacitive reactance which is due to the capacitive nature of cell membranes and caused by a selectively applied AC signal allows current to pass through these cell membranes using current paths largely depends upon the signal frequency (Fig.6.13). The high frequency current flows through ECF and cells, including membranes and intracellular fluids, and penetrates cell membranes. The low frequency current passes through ECF only as the cell membrane reactance prevents its flow through it. The BIA technique can be used to determine the (TBW) which is nothing but combination of ECW and ICW. However, it should be done at a particular frequency of the applied AC signal.

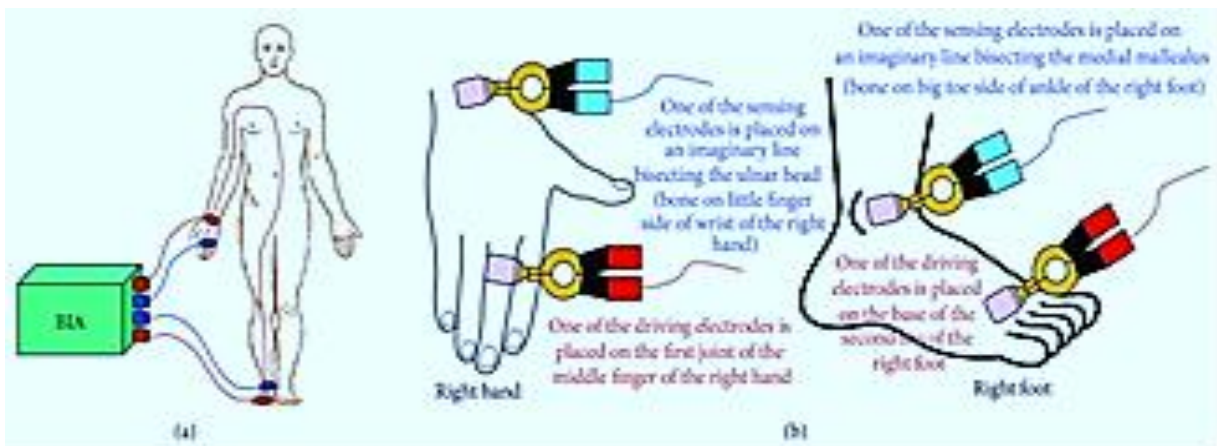


Fig.6.14 General test setup for BIA

The instrument designed was tested on patients at St. Joseph hospital, Ghaziabad, India. Prior approval for the study was taken from the concerned authorities. Twenty-five adult human subjects (aged 25-60 years) participated in this study. The general test setup for BIA is shown

Chapter 6: Design of Low Cost Bioimpedance Measuring Instrument

in fig.6.14. However, in our study it differed little bit for the ease of the subjects. They were

made to rest for 10-15 minutes in a supine position. On the right and left forearms, Ag/AgCl electrodes were placed. Volunteers were told to lie down straight and remain still during measurement.

6.10 RESULTS

The test setup used to validate the instrument is similar to the setup used in impedance plethysmography for the measurement of cardiac output. Impedance is a measure of resistance. Plethysmography has become the gold standard for measuring blood volume changes in any part of the body based on electrical impedance changes [117]. It is also being used in the diagnosis of peripheral vascular diseases. In impedance plethysmography, values of instantaneous impedance (Z), basal impedance (Z_0), which is an average of calculated bioimpedance values and derivative of impedance with respect to time (dZ/dt) is used to calculate cardiac output parameters. Since the technique is a standard procedure, the values of basal impedance measured by this technique can be used to validate the instrument designed. The output of the demodulator is essentially the basal impedance of the section across which electrodes have been applied. The basal impedance values of forearm given in literature, [118] are used to validate the output signal of the instrument designed.

The output voltage signal of three sets of volunteers has been displayed in fig.6.15. The slight variations in the voltage values depict the variations in impedance (Z_0). The basal impedance is calculated using the constant voltage level. The calculated value of basal impedance and its comparison with values of basal impedance in literature has been shown in table 6.1. The comparison in table 6.1 shows that the values measured from the output of the instrument is in accordance with that of standard technique, which validates the design of the instrument.

TABLE 6.1: BASAL IMPEDANCE (FOREARM)

SET OF VOLUNTEERS [NOs]	MEASURED BY INSTRUMENT DESIGNED		STANDARD VALUES IN LITERATURE	
	A_V , AGE	A_V , $Z_0(\Omega)$	AGE GROUP	A_V , $Z_0(\Omega)$
A [5]	40	58.16	36-45	65.44 ±12.03
B [8]	48	71.57	46-55	67.50 ±6.38
C [12]	57	58.77	> 55	69.13 ±8.74

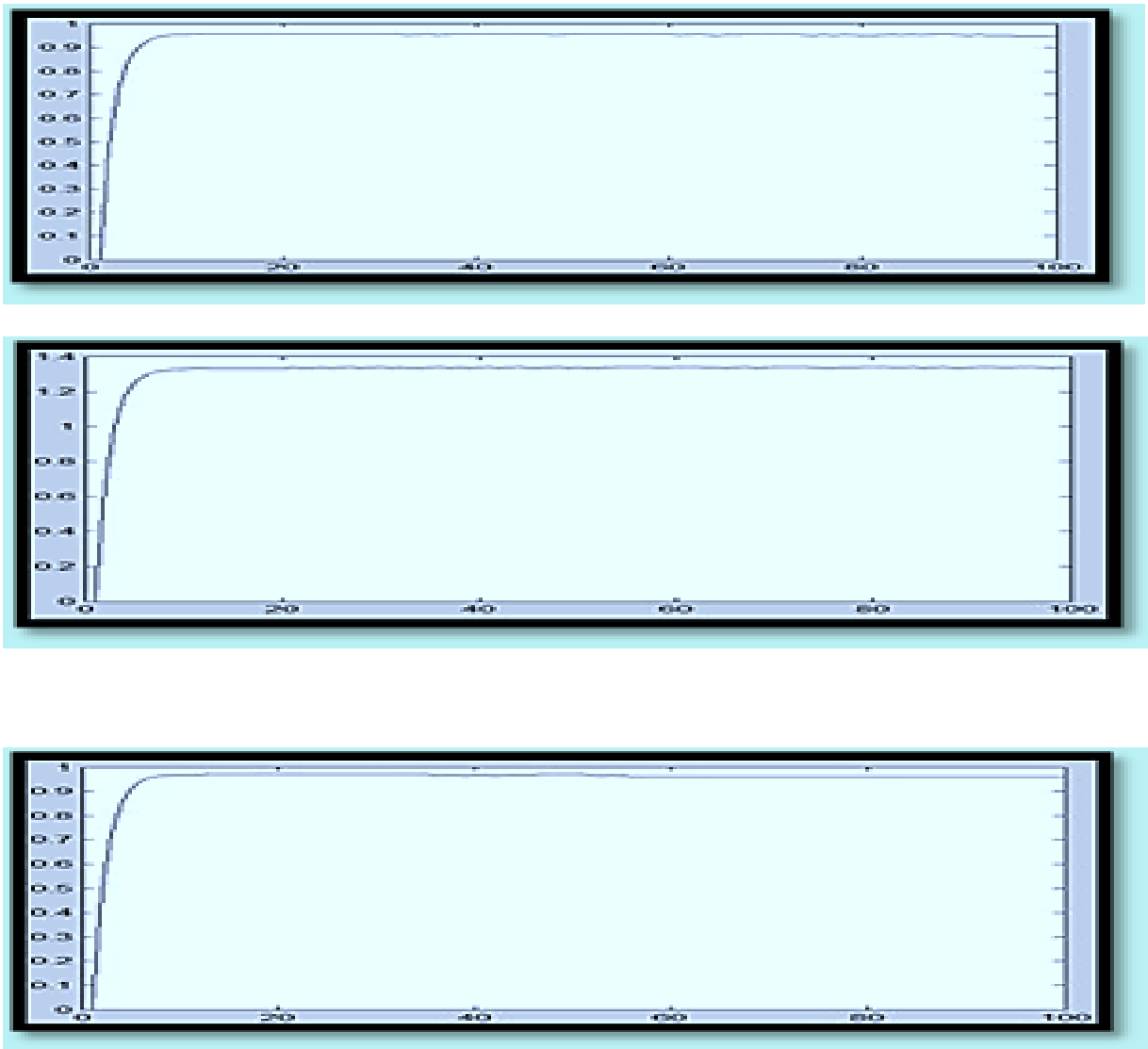


Fig.6.15 Output voltage signals measured using the instrument. (a) is the output signal of volunteer set-A (b) being the output signal of volunteer set-B and (c) is the output signal of volunteer set-C. The y-axis in each figure is the output voltage amplitude value and the x-axis represents number of samples.

6.11 SIGNIFICANT FINDINGS

A simple low cost bioimpedance measuring instrument has been designed using common electronic blocks. The results have been validated and have been found to be accurate and reliable. Each block of the instrument has been tested using simulation and verified experimentally. The method and device developed fulfills required specifications and can be used in clinical examinations. Bioimpedance measurement techniques can prove very useful for first hand diagnosis. The major problem for using this technique for diagnosis is that its results are not standardized. By standardized one means that just by looking the graph or using its results one can say whether the results correspond to a normal person or a patient suffering

from a disease. A large amount of analysis has to be done for a particular application of bioimpedance signals to enable the doctors to rely on results produced by bioimpedance analysis. The standardization of bioimpedance values for human body may be difficult due to variable ambient conditions, eating habits, lifestyle and anthropological background. So intensive and extensive research and in-depth analysis is required to be carried out towards normalization and standardization of the bioimpedance values.




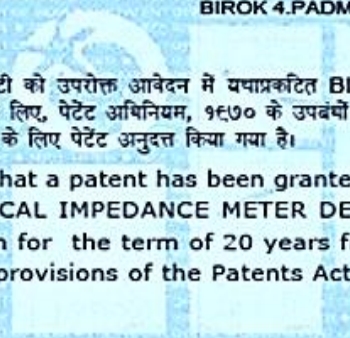

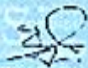
Physiological testing and health-monitoring systems can be benefitted greatly from this method. Devices must be compact, wearable, or even implantable for a wide variety of applications. As a result, the next generation of bioimpedance sensing systems must be designed to save energy and resources [119]. It's critical to consider the application as well as the type of cell or tissue culture to be monitored when selecting a bioimpedance measurement technique [119]. As a result, choosing the right electrode configuration is crucial. Future research should focus on the electrodes and the bioimpedance measurement method [119, 120]. Overall, this study describes a low-cost, bioelectrical impedance measurement system that has been successfully developed and tested and can be used effectively and efficiently for non-invasive health monitoring. The study also discussed some of the most important technological aspects and limitations of bioimpedance calculation and study. Finally, the theoretical dimensions, operating principles, implementations, benefits, disadvantages, and current research scenario, future developments, and challenges of bioimpedance analysis and calculation are all covered in great detail in this study.

This chapter is based on the following work:

Rajesh Birok & Rajiv Kapoor “Design of Low Cost Bioimpedance Measuring Instrument” International Journal of Advanced Computer Science and Applications, ISSN 21565570, 2158107X in Volume 13, No. 1 (2022). [SJR-0.193] [Published in ESCI]

PATENT AWARDED

BIOELECTRICAL IMPEDANCE METER DESIGN to 1. RAJIV KAPOOR 2. ABHISHEK GROVER 3. RAJESH BIROK 4. PADMA BATRA et al Vide Patent No.: 354875 [SL No: 011129756]; Application No.: 2169/DEL/2015

 INTELLECTUAL PROPERTY INDIA PATENTS DESIGNS TRADE MARKS GEOGRAPHICAL INDICATIONS	 भारत सरकार GOVERNMENT OF INDIA पेटेंट कार्यालय THE PATENT OFFICE पेटेंट प्रमाणपत्र PATENT CERTIFICATE (Rule 74 Of The Patents Rules)	क्रमांक : 011129756 SL No :	
पेटेंट सं. / Patent No.	:	354875	
आवेदन सं. / Application No.	:	2169/DEL/2015	
फाइल करने की तारीख / Date of Filing	:	17/07/2015	
पेटेटी / Patentee	:	1.RAJIV KAPOOR 2.ABHISHEK GROVER 3.RAJESH BIROK 4.PADMA BATRA et al.	
आविष्कारक (जहां लागू हो) / Inventor(s)	:	1.RAJIV KAPOOR 2.ABHISHEK GROVER 3.RAJESH BIROK 4.PADMA BATRA 5.AARCHISHYA KAPOOR	
<p>प्रमाणित किया जाता है कि पेटेटी को उपरोक्त आवेदन में यथाप्रकटित BIOELECTRICAL IMPEDANCE METER DESIGN नामक आविष्कार के लिए, पेटेंट अधिनियम, 1970 के उपबंधों के अनुसार आज तारीख 17th day of July 2015 से बीस वर्ष की अवधि के लिए पेटेंट अनुदत्त किया गया है।</p> <p>It is hereby certified that a patent has been granted to the patentee for an invention entitled BIOELECTRICAL IMPEDANCE METER DESIGN as disclosed in the above mentioned application for the term of 20 years from the 17th day of July 2015 in accordance with the provisions of the Patents Act,1970.</p>			
 INTELLECTUAL PROPERTY INDIA PATENTS DESIGNS TRADE MARKS GEOGRAPHICAL INDICATIONS			
			
अनुदान की तारीख : 30/12/2020 Date of Grant :			पेटेंट नियंत्रक Controller of Patent
<p>टिप्पणी - इस पेटेंट के नवीकरण के लिए फीस, यदि इसे बनाए रखा जाना है, 17th day of July 2017 को और उसके पश्चात प्रत्येक वर्ष में उसी दिन देय होगी। Note. - The fees for renewal of this patent, if it is to be maintained will fall / has fallen due on 17th day of July 2017 and on the same day in every year thereafter.</p>			

CHAPTER 7

CONCLUSIONS & FUTURE SCOPE

This chapter summarises the findings of this study based on theoretical and experimental contributions, as well as it specifies the future research plans.

7.1 CONCLUSIONS

In this study a new approach using higher order cumulants for the analysis of ECG signal has been proposed. Two new methods for ECG denoising namely 1) using ANN & CEEMD 2) Genetic Particle-Filter Improved Fuzzy-AEEMD have been proposed in this thesis. In addition to the above “Design of Low Cost Bioimpedance Measuring Instrument” has been discussed in depth as well. The brief summary of these proposed methods is as follows:

- The proposed method classifies dataset of ECG signals based upon higher order statistics i.e., using cumulants. This method is a comprehensive measure of non-linearity and gives better results in terms of time complexity. It provides a quality detection technique in comparison to the other methods used earlier in this research domain. The proposed method also compares this higher order statistics classification obtained using different classifiers such as SVM, Fuzzy-2 and DSNN to find the best classifier. In this classification of ECG, four classifiers as SVM & ANN, Fuzzy-2 and DSNN were used and DSNN is observed to be as the best classifier among these classifiers because of its repeated learning and analyzing ability. The results computed from DSNN classifier has the highest observed accuracy compared to the rest of the three classifiers and hence, DSNN is the best for using it for the ECG signals classification. In this proposed method, cumulants helps us to remove many divergences in the other type of ECG datasets. Therefore, the proposed method is used to detect this problem and address the issue very efficiently and accurately.

- For the ECG denoising:
 - The first method presents a novel approach for the filtering of low frequency artefacts of ECG signals by using Complete Ensemble Empirical Mode Decomposition (CEEMD) and Artificial Neural Networks (ANN), which removes most of the constituent noise while assuring no loss of information in

terms of the morphology of the ECG signal. The contribution of the method lies in the fact that it combines the advantages of both EEMD and ANN. The use of CEEMD ensures that the Neural Network does not get over fitted. It also significantly helps in building better predictors at individual frequency levels. The proposed method is compared with other state-of-the-art methods in terms of Mean Square Error (MSE), Signal to Noise Ratio (SNR) and Correlation Coefficient. The results show that the proposed method has better performance as compared to other state-of-the-art methods for low frequency artefacts removal from ECG.

- In terms of SNR & RMSE, the second approach offers de-noising of ECG signals using Genetic Particle Filter and Fuzzy Thresholding with the aid of AEEMD. This method outperforms EMD-based techniques and other existing noise removal methods. The AEEMD method is used to split the ECG signal into IMFs. The Adaptive Ensemble EMD (AEEMD) represents a significant advancement in noisy ECG signal filtering approach by providing adaptability, flexibility, versatility, and robustness. The AEEMD is superior than the EMD because it eliminates the signal's mode-mixing effect. Spectral Flatness is utilized to automatically discover the noisy Intrinsic Mode Functions using Fuzzy Thresholding. To achieve a clean ECG signal, the remaining noisy intrinsic mode functions are filtered using the Genetic Particle Filter. The Genetic Algorithm Particle Filter enhances the process of self-evolution and self-adaption. De-noising performance has been increased by combining the benefits of the AEEMD over EMD technology and the Genetic Particle Filter over the particle filter. Overall, the proposed method provides the better accuracy compared to other methods.
- A simple low cost bioimpedance measuring instrument has been designed using common electronic blocks. The results have been validated and have been found to be accurate and reliable. Each block of the instrument has been tested using simulation and verified experimentally. The method and device developed fulfills required specifications and can be used in clinical examinations. Primarily, it is based upon the low-cost component-level approach so that it can be easily used by researchers and investigators in the specific domain. The final measurement setup of instrument was tested on adult human subjects to obtain the impedance signal of the forearm which is

under investigation in this case. However, depending on the illness or activity under examination, the instrument can be used on any other part of the body. The current injected by the instrument is within the safe limits and the gain of the biomedical instrumentation amplifier is highly reasonable. The technique is easy and user-friendly, and it does not necessitate any special training, therefore it can be effectively used to collect bioimpedance data and interpret the findings for medical diagnostics. Moreover, in this design of low cost bioimpedance measuring instrument, several existing methods and associated approaches have been extensively explored, with in-depth coverage of their working principles, implementations, merits, and disadvantages, as well as focused on other technical aspects.

7.2 FUTURE RESEARCH SCOPE

Despite the suggested good performance approaches, several concerns have been identified, and these issues may lead to future research paradigms and scope:

The performance of proposed method for analysis of ECG signals using higher order cumulants can be further improved by employing various permutation and combinations of higher order cumulants on larger data set.

When examining the results, it is clear that simple ANN can produce excellent results at times, but their performance is inconsistent. The addition of CEEMD ensures that the system runs smoothly. The results show that the proposed method is clearly superior to other methods in the literature. The use of CEEMD has increased the filtration properties of ANN while also preventing overfitting. Furthermore, since the filtration will be conducted mainly at lower frequencies, any high frequency cardiac defects will not be filtered, which is an important consideration.

The suggested approach for de-noising ECG signals using a Genetic Particle Filter and Fuzzy Thresholding with AEEMD is computationally more difficult and requires real-time validation. As a future work, complexity can be reduced further by using more efficient algorithms for reducing number of iterations, thereby reducing the computation time. Whereas, validation can be improved by testing and training on large real time data set.

Bioimpedance measurement techniques can prove very useful for first hand diagnosis. The major problem for using this technique for diagnosis is that its results are not standardized. The standardization of bioimpedance values for human body may be difficult due to variable ambient conditions, eating habits, lifestyle and anthropological background. So intensive and

extensive research and in-depth analysis is required to be carried out towards normalization and standardization of the bioimpedance values.

In the future, investigation and research can be carried out for Bluetooth-enabled wireless instrumentation for Bio-Impedance Analysis [BIA] techniques. Moreover, in future studies Bluetooth-enabled wireless instrumentation for Electrochemical Impedance Spectroscopy (EIS) techniques could be investigated. Bioimpedance technology is becoming more prevalent as a result of an increasing number of healthcare monitoring applications. In the coming times the devices must be compact, wearable, or even implantable for a wide variety of applications. As a result, the next generation of bioimpedance sensing systems must be designed to save energy and resources.

REFERENCES

- [1] Netter F. H., Sharon Colacino Novartis, "Atlas of Human Anatomy", 2nd Edition, Rittenhouse Book Distributors Inc; 1997. [Google Scholar].
- [2] Ackmann, J.J., "Complex bioelectric impedance measurement system for the frequency range from 5 Hz to 1 MHz", *Ann Biomed Eng* 21, 135–146 (1993). <https://doi.org/10.1007/BF02367609> [PubMed] [Google Scholar]
- [3] Cha K, Chertow GM, Gonzalez J, Lazarus JM, Wilmore DW., "Multifrequency bioelectrical impedance estimates the distribution of body water", *J Appl Physiol* (1985). 1995 Oct;79(4):1316-9. doi: 10.1152/jappl.1995.79.4.1316. PMID: 8567578. [PubMed] [Google Scholar]
- [4] S. Grimnes and G. Martinsen, *Academic Press, "Bioimpedance & Bioelectricity Basics"*, 3rd edition; 2015, ISBN 978-0-12-411470-8 DOI 10.1016/C2012-0-06951-7
- [5] Lars Jodal, Medical Physicist, "Lecture notes on the electrical theory behind the measurement of body fluids with bioimpedance spectroscopy (BIS)", 2010
- [6] Miklavcic D, Pavselj N, Hart FX, "Electric Properties of Tissues", *Wiley Encyclopedia of Biomedical Engineering*. 2006 [Google Scholar]
- [7] H. P. Schwan, "Electrical properties of tissues and cell suspensions: mechanisms and models," *Proceedings of 16th Annual International Conference of the IEEE Engineering in Medicine and Biology Society*, 1994, pp. A70-A71 vol.1, doi: 10.1109/IEMBS.1994.412155.
- [8] Internet Article, Bodystat: Body Fat Analysers and Hydration Monitors. Bodystat Limited, USA, <http://www.bodystat.com/science>.
- [9] Pethig R, Kell DB. The passive electrical properties of biological systems: their significance in physiology, biophysics and biotechnology. *Phys Med Biol*. 1987 Aug;32(8):933-70. doi: 10.1088/0031-9155/32/8/001. PMID: 3306721.
- [10] Riu PJ. Comments on "Bioelectrical parameters of the whole human body obtained through bioelectrical impedance analysis". *Bioelectromagnetics*. 2004; 25:69–71. doi: 10.1002/bem.10190.
- [11] Gabriel C, Gabriel S, Corthout E. The dielectric properties of biological tissues: I. Literature survey. *Phys Med Biol*. 1996; 41:2231–49. doi: 10.1088/0031-9155/41/11/001. [PubMed] [CrossRef] [Google Scholar]
- [12] Martinsen G, Grimnes S, Schwan HP, "Interface phenomena and dielectric properties of biological tissue. *Encyclopedia of Surface and Colloid Science*". 2002; 20:2643–53. [Google Scholar]
- [13] Ojarand, Jaan, Land, Raul, Min, Mart and Rist, Marek. "How many frequencies to use in electrical bioimpedance measurements". *Impedance Spectroscopy: Advanced Applications: Battery Research, Bioimpedance, System Design*, edited by Olfa Kanoun, Berlin, Boston: De Gruyter, 2018, pp. 161-168. <https://doi.org/10.1515/9783110558920-016>
- [14] M. Sanaullah, "A Review of Higher Order Statistics and Spectra in Communication Systems", *Global Journal of Science Frontier Research Physics and Space Science Volume 13 Issue 4 Version 1.0 Year 2013*.
- [15] M. Signoretto, E. Olivetti, L. De Lathauwer and J. A. K. Suykens, "Classification of Multichannel Signals With Cumulant-Based Kernels," in *IEEE Transactions on Signal Processing*, vol. 60, no. 5, pp. 2304-2314, May 2012, doi: 10.1109/TSP.2012.2186443.
- [16] Dah-Chung Chang, Poh-Kuan Shih, "Cumulants-based modulation classification technique in multipath fading channels", *IET Comm.*, Vol. 9, Iss. 6, pp. 828–835, 2015. DOI: 10.1049/iet-com.2014.0773
- [17] Shivajirao M. Jadhav, L. Sanjay L. Nalbalwar, Ashok A. Ghatol, "ECG Arrhythmia Classification using Modular Neural Network Model", 2010. *IEEE EMBS Conference on Biomedical Engineering and Sciences (IECBES)*. DOI: 10.1109/IECBES.2010.5742200
- [18] Manab Kumar Das, Dipak Kumar Ghosh and Samit Ari, "Electrocardiogram (ECG) Signal Classification using S-transform, Genetic Algorithm and Neural Network", *IEEE 1st International Conference on Condition Assessment Techniques in Electrical Systems*, 2013. DOI: 10.1109/CATCON.2013.6737526
- [19] A. Kampouraki, G. Manis and C. Nikou, "Heartbeat Time Series Classification With Support Vector Machines," in *IEEE Transactions on Information Technology in Biomedicine*, vol. 13, no. 4, pp. 512-518, July 2009, doi: 10.1109/TITB.2008.2003323.
- [20] S. Edla, N. Kovvali and A. Papandreou-Suppappola, "Electrocardiogram Signal Modeling With Adaptive Parameter Estimation Using Sequential Bayesian Methods," in *IEEE Transactions on Signal Processing*, vol. 62, no. 10, pp. 2667-2680, May 15, 2014, doi: 10.1109/TSP.2014.2312316.
- [21] Kartik Audhkharsi, Osonde Osoba, Bart Kosko, 'Noise Benefits in Backpropagation and Deep Bidirectional Pre-training', 2013. *International Joint Conference on Neural Networks (IJCNN)*. DOI: 10.1109/IJCNN.2013.6707022
- [22] Kaiming He, Xiangyu Zhang, Shaoqing Ren, and Jian Sun, "Spatial Pyramid Pooling in Deep Convolutional Networks for Visual Recognition", *IEEE Transactions On Pattern Analysis And Machine Intelligence*, Vol. 37, No. 9, September 2015
- [23] I.A. Hameed, C.G. Sorensen, O. Green, "Building an intelligent controller using simple genetic type-2 fuzzy logic system". 'Fuzzy controllers, theory and applications', 1st ed. Grigorie, L. ISBN:978-953-307-543-3, pp. 148–162, February, 2011.
- [24] A. Halder et al., "General and Interval Type-2 Fuzzy Face-Space Approach to Emotion Recognition," in *IEEE Transactions on Systems, Man, and Cybernetics: Systems*, vol. 43, no. 3, pp. 587-605, May 2013, doi: 10.1109/TSMCA.2012.2207107.
- [25] Chia-Feng Juang and Po-Hsuan Wang, "An Interval Type-2 Neural Fuzzy Classifier Learned Through Soft Margin Minimization and its Human Posture Classification Application", *IEEE Transactions on Fuzzy Systems*. Volume: 23, Issue: 5, Oct. 2015. doi: 10.1109/TFUZZ.2014.2362547
- [26] S. Graja and J. -. Boucher, "Hidden Markov tree model applied to ECG delineation," in *IEEE Transactions on Instrumentation and Measurement*, vol. 54, no. 6, pp. 2163-2168, Dec. 2005, doi: 10.1109/TIM.2005.858568.
- [27] Ahmadian, S. Karimifard, H. Sadoughi and M. Abdoli, "An Efficient Piecewise Modeling of ECG Signals Based on Hermitian Basis Functions", in *Proc. IEEE EMBS*, pp. 3180-3183, 2007.
- [28] V. Sharmila, E. HariKrishna, K.N. Reddy, K.A. Reddy, "A New Method for Enhancement of ECG Signals Using Cumulant Based AR Modeling", *Proc. of IEEE Conference on Information and Communication Technologies*, 2013.
- [29] Liang-Yu Shyu, Ying-Hsuan Wu, and WeichihHu, "Using Wavelet Transform and Fuzzy Neural Network for VPC Detection From the Holter ECG", *IEEE Transactions On Biomedical Engineering*, Vol. 51, No. 7, July 2004.
- [30] Mahesh S. Chavan, R A. Agarwala, M.D.Uplane, "Application of the Chebyshev Type II Digital Filter For Noise Reduction In ECG Signal" *Proceedings of the 5th WSEAS Int. Conf. on Signal Processing, Computational Geometry & Artificial Vision, Malta, September 15-17, 2005* (pp1-8).
- [31] Mahesh S. Chavan, R A. Agarwala, M.D.Uplane, "Digital Elliptic Filter Application For Noise Reduction In ECG Signal" *4th WSEAS International Conference on Electronics, Control and Signal Processing, Miami, Florida, USA, 17-19 November, 2005* (pp.58-63).
- [32] Dr. K. L. Yadav and Sachin Singh, "Performance evaluation of different adaptive filters for ECG signal processing", *International Journal On Computer Science and Engineering*, vol. 40, no. 5, pp. 1880-1883, 2010.

- [33] Muhammad Zia-Ur-Rahman, Rafi Ahamed Shaik and D.V.RamaKoti Roddy, "Efficient sign based normalized adaptive filtering techniques for cancelation of artifacts in ECG signals: Application to wireless biotelemetry", *Journal of signal processing*, vol.91, no. 2, pp. 225-239, February 2011.
- [34] Ching-Haur Chang, Kang-Ming Chang and Hsien-Ju Ko, "Cancellation of high frequency noise in ECG signals using Adaptive filter without external reference", *Proceedings of International Conference on Biomedical Engineering and Informatics*, pp. 787-790, Yantai, October 2010.
- [35] DL Donoho. "Denoising by soft thresholding", *IEEE Trans Inform Theory*, 14(3),1995, pp 612-627.
- [36] M Alfaouri and K Daqrouq, "Electrocardiogram (ECG) Signal denoising by Wavelet Transform thresholding", *American Journal of Applied Sciences*, Vol. 5 Issue 3pp.no 276-281,2008.
- [37] M Kania, M Fereniec, R Maniewski, "Wavelet Denoising for Multilead High resolution Electrocardiogram (ECG) Signals", *Measurement Science Review*, Volume 7, Section 2, No.4, pp no. 30-33, 2007.
- [38] L Chmelka and J Kozumpik, "Wavelet Based Wiener Filter for Electrocardiogram signal denoising", *IEEE computers in cardiology*, 2005, pp no. 771-774, 2005.
- [39] D.T luong, "Study on the limitations of removal of Baseline noise from electro cardiography signal in measurement using wavelet analysis", *IEEE, ICUFN*, 2013.
- [40] C.Y-F Ho, B..W.-K, Ling, T.R-L. Wong, A.Y.-P chan. .P.-K.-S.Tam, "Fuzzy rule based multi-wavelet Electrocardiogram (ECG) denoising", *Fuzzy Systems, IEEE international Conference*,pp.no 1064-1068, 2008
- [41] N. E. Huang, Z. Shen, S. R. Long, M. C. Wu, H. H. Shih, Q. Zheng, N.-C. Yen, C. C. Tung, and H. H. Liu. "The Empirical Mode Decomposition and Hilbert Spectrum for Nonlinear and Nonstationary Time Series Analysis". *Proceedings of the Royal Society London A.*, 454:903-995, 1998. <https://doi.org/10.1098/rspa.1998.0193>
- [42] A.O Boudraa, J C cexus, "EMD Based signal filtering", *IEEE Transactions on Instrumentation and Measurement*, vol 56, no. 6, pp 2196-2202, 2007.
- [43] Anil Chacko and Samit Ari, "Denoising of ECG signals using Empirical Mode Decomposition based technique" *IEEE-International conference on Advances in Engineering, Science and Management (ICAESM -2012)* March 30,31, 2012 pg no 6-9.
- [44] B. Pradeep Kumar, S Balambigai and R Asokan, "ECG denoising based on Hybrid Technique", *IEEE- International conference on Advances in Engineering, Science and Management (ICAESM -2012)*, pp no. 285-290.
- [45] Changnian Zhang, XiaLi and Mengmeng Zhang, "A novel ECG signal denoising method based on Hilbert Huang Transform", *2010 International Conference on Computer and Communication Technologies in Agriculture Engineering, CCTAE-2010*, pg no 284-287.
- [46] Zhi-Dong Zhao, Yu-Quen Chen, "A new method for Removal of Baseline Wander and Power Line Interference in ECG signals", *Proceedings in the Fifth International Conference on Machine Learning and Cybernetics, Dalian, 13-16 August 2006*,pg no. 4342-4347.
- [47] Na Pan, vai MingI, Mai Peng Un and Pun Sio hang, "Accurate removal of baseline wander in ECG using EMD", *proceedings of NFSI & ICFBI'2007 China*, pg no 177-180
- [48] Kumar, Shailesh & Panigrahy, Damodar Sahu, & Prasanna. (2018). "Denoising of Electrocardiogram (ECG) signal by using Empirical Mode Decomposition (EMD) with Non-Local Mean (NLM) technique". *Biocybernetics and Biomedical Engineering* 38(2). DOI: 10.1016/j.bbe.2018.01.005
- [49] X. Wang, Y. Zhou, M. Shu, Y. Wang and A. Dong, "ECG Baseline Wander Correction and Denoising Based on Sparsity", in *IEEE Access*, vol. 7, pp. 31573-31585, 2019, doi: 10.1109/ACCESS.2019.2902616.
- [50] Dengyong Zhang, Shanshan Wang, Feng Li, Shang Tian, Jin Wang, Xiangling Ding, Rongrong Gong, "An Efficient ECG Denoising Method Based on Empirical Mode Decomposition, Sample Entropy, and Improved Threshold Function", *Wireless Communications and Mobile Computing*, vol. 2020, Article ID 8811962, 11 pages, 2020. <https://doi.org/10.1155/2020/8811962>
- [51] Z. Wu and N. E. Huang, "Ensemble Empirical Mode Decomposition: A noise-assisted data analysis method," *Advances in Adaptive Data Analysis*, vol. 1, no. 1, pp. 1-41, 2009.
- [52] M. E. Torres, M. A. Colominas, G. Schlotthauer and P. Flandrin, "A complete ensemble empirical mode decomposition with adaptive noise," *2011 IEEE International Conference on Acoustics, Speech and Signal Processing (ICASSP)*, 2011, pp. 4144-4147, doi: 10.1109/ICASSP.2011.5947265.
- [53] G. Singh, G. Kaur and V. Kumar, "ECG denoising using adaptive selection of IMFs through EMD and EEMD," *2014 International Conference on Data Science & Engineering (ICDSE)*, 2014, pp. 228-231, doi: 10.1109/ICDSE.2014.6974643.
- [54] Krishna Tejal, Rahul Tiwari and Satish Mohanty "Adaptive denoising of ECG using EMD, EEMD and CEEMDAN signal processing techniques", , Published under licence by IOP Publishing Ltd. *Journal of Physics: Conference Series*, Volume 1706, First International Conference on Advances in Physical Sciences and Materials 13-14 August 2020, Coimbatore, India Citation Krishna Teja et al 2020 *J. Phys.: Conf. Ser.* 1706 012077
- [55] Rui Rodrigues and Paula Couto "A Neural Network Approach to ECG Denoising", *Computational Engineering, Finance, and Science (cs.CE); Neural and Evolutionary Computing (cs.NE)*. arXiv:1212.5217 [cs.CE].
- [56] Nibedit Dey, Tripada Prasad Dash and Sriram Dash, "ECG signal denoising by Functional Link Artificial Neural Network (FLANN)", *International Journal of Biomedical Engineering and Technology*, Volume 7, Issue 4
- [57] Lean Yu , , Shouyang Wang, Kin Keung Lai, "Forecasting crude oil price with an EMD-based neural network ensemble learning paradigm", *Energy Economics*, Volume 30, Issue 5, September 2008, Pages 2623-2635
- [58] Zhenhai Guoa, Weigang Zhaob, Haiyan Luc, Jianzhou Wangb, "Multi-step forecasting for wind speed using a modified EMD-based artificial neural network model", *Renewable Energy*, Volume 37, Issue1.
- [59] M. S. Choudhry, A. Puri and R. Kapoor, "Removal of baseline wander from ECG signal using cascaded Empirical Mode Decomposition and morphological functions," *2016 3rd International Conference on Signal Processing and Integrated Networks (SPIN)*, 2016, pp. 769-774, doi: 10.1109/SPIN.2016.7566803.
- [60] H. Shi, R. Liu, C. Chen, M. Shu and Y. Wang, "ECG Baseline Estimation and Denoising With Group Sparse Regularization," in *IEEE Access*, vol. 9, pp. 23595-23607, 2021, doi: 10.1109/ACCESS.2021.3056459.
- [61] B. Pradeep Kumar, S. Balambigai and R. Asokan, "ECG de-noising based on hybrid technique," *IEEE-International Conference On Advances In Engineering, Science And Management (ICAESM -2012)*, 2012, pp. 285-290.
- [62] V. N. P. Raj and T. Venkateswarlu, "ECG signal denoising using Undecimated Wavelet Transform," *2011 3rd International Conference on Electronics Computer Technology*, 2011, pp. 94-98, doi: 10.1109/ICECTECH.2011.5941808.
- [63] Z. Liu, J. Wang and B. Liu, "ECG Signal Denoising Based on Morphological Filtering," *2011 5th International Conference on Bioinformatics and Biomedical Engineering*, 2011, pp. 1-4, doi: 10.1109/icbbe.2011.5780239.
- [64] Changnian Zhang, Xia Li and Mengmeng Zhang, "A novel ECG signal denoising method based on Hilbert-Huang Transform," *2010 International Conference on Computer and Communication Technologies in Agriculture Engineering*, 2010, pp. 284-287, doi: 10.1109/CCTAE.2010.5544365.
- [65] Xiang J, Zhong Y, "A fault detection strategy using the enhancement ensemble empirical mode decomposition and random decrement technique", *Microelectron Reliab.* Volume 75, August 2017, Pages 317-326

- [66] A. Chacko and S. Ari, "Denoising of ECG signals using Empirical Mode Decomposition based technique," IEEE-International Conference On Advances In Engineering, Science And Management (ICAESM -2012), 2012, pp. 6-9.
- [67] N. Nikvand, H. Bagherzadeh Rafsanjani and M. A. Khalilzadeh, "ECG signal denoising using noise invalidation," 2010 17th Iranian Conference of Biomedical Engineering (ICBME), 2010, pp. 1-4, doi: 10.1109/ICBME.2010.5704917.
- [68] Tracey BH, Miller EL. "Nonlocal means denoising of ECG signals". IEEE Trans Biomed Eng. 2012 Sep;59(9):2383-6. doi: 10.1109/TBME.2012.2208964. Epub 2012 Jul 17. PMID: 22829361.
- [69] A. Sanyal, A. Baral and A. Lahiri, "Application of S-transform for removing baseline drift from ECG," 2012 2nd National Conference on Computational Intelligence and Signal Processing (CISP), 2012, pp. 153-157, doi: 10.1109/NCCISP.2012.6189697.
- [70] N. Nikolaev, Z. Nikolov, A. Gotchev and K. Egiastian, "Wavelet domain Wiener filtering for ECG denoising using improved signal estimate," 2000 IEEE International Conference on Acoustics, Speech, and Signal Processing. Proceedings (Cat. No.00CH37100), 2000, pp. 3578-3581 vol.6, doi: 10.1109/ICASSP.2000.860175.
- [71] S. L. Joshi, R. A. Vatti and R. V. Tornekar, "A Survey on ECG Signal Denoising Techniques," 2013 International Conference on Communication Systems and Network Technologies, 2013, pp. 60-64, doi: 10.1109/CSNT.2013.22.
- [72] Arijit Roy., et al., "An experimental method of bioimpedance measurement and analysis for discriminating tissues of fruit or vegetable." in *AIMS Biophysics*, March 2020, Volume 7, Issue 1: 41-53. DOI: 10.3934/biophy.2020004.
- [73] E. Louaroudi, B. Sanchez, "On the correct use of stepped-sine excitations for the measurement of time-varying bioimpedance," in *Physiological Measurement*, IOP Publishing 2017 Feb;38(2): N73-N80. doi: 10.1088/1361-6579/aa556d.
- [74] Haslett, J.W.; Rao, M.K.N., "A High Quality Controlled Current Source," in *Instrumentation and Measurement*, IEEE Transactions on, vol.28, no.2, pp.132-140, June 1979
- [75] Annus, P.; Krivoshei, A.; Min, M.; Parve, T., "Excitation Current Source for Bioimpedance Measurement Applications: Analysis and Design," in *Instrumentation and Measurement Technology Conference Proceedings*, 2008. IMTC 2008. IEEE, vol., no., pp.848-853, 12-15 May 2008
- [76] Pallas-Areny, Ramon, and John G. Webster, "Analog Signal Processing / 1st ed, ISBN-10:0471125288, Wiley
- [77] Electrical Cardiometry" Wikipedia, Author: Wikipedia contributors, Publisher: Wikipedia, Page Version ID: 1095430476
- [78] Amit K. Gupta, "Respiration rate measurement based on impedance pneumography application report", SBAA1811-February 2011, Texas Instruments
- [79] O. G. Martinsen, S. Clausen, J. B. Nysaether and S. Grimnes, "Utilizing Characteristic Electrical Properties of the Epidermal Skin Layers to Detect Fake Fingers in Biometric Fingerprint Systems—A Pilot Study," in *IEEE Transactions on Biomedical Engineering*, vol. 54, no. 5, pp. 891-894, May 2007, doi: 10.1109/TBME.2007.893472.
- [80] David Naranjo-Hernández, Javier Reina-Tosina, Mart Min, "Fundamentals, Recent Advances, and Future Challenges in Bioimpedance Devices for Healthcare Applications", *Journal of Sensors*, vol. 2019, Article ID 9210258, 42 pages, 2019. <https://doi.org/10.1155/2019/9210258>
- [81] P. S. H. Jose, K. Rajasekaran, P. Rajalakshmy and B. Jebastina, "A Non-Invasive Method for Measurement of Blood Glucose using Bio Impedance Technique," 2019 2nd International Conference on Signal Processing and Communication (ICSPC), 2019, pp. 138-142, doi: 10.1109/ICSPC46172.2019.8976732.
- [82] V. Sharmila, E. HariKrishna, K. N. Reddy and K. A. Reddy, "A new method for enhancement of ECG signals using cumulant based AR modeling," 2013 IEEE Conference on Information & Communication Technologies, 2013, pp. 634-637, doi: 10.1109/CICT.2013.6558171.
- [83] R. J. Martis, U. R. Acharya, A. K. Ray and C. Chakraborty, "Application of higher order cumulants to ECG signals for the cardiac health diagnosis," 2011 Annual International Conference of the IEEE Engineering in Medicine and Biology Society, 2011, pp. 1697-1700, doi: 10.1109/IEMBS.2011.6090487.
- [84] F. Bovolo, L. Bruzzone and L. Carlin, "A Novel Technique for Subpixel Image Classification Based on Support Vector Machine," in *IEEE Transactions on Image Processing*, vol. 19, no. 11, pp. 2983-2999, Nov. 2010, doi: 10.1109/TIP.2010.2051632.
- [85] Moody GB, Mark RG. The impact of the MIT-BIH Arrhythmia Database. *IEEE Eng in Med and Biol* 20(3):45-50 (May-June 2001). (PMID: 11446209) <https://physionet.org/content/mitdb/1.0.0>, DOI:<https://doi.org/10.13026/C2F305>
- [86] Muris Mujagic, "Characterization of ECG Noise Source", *Science, Health Science, Cardiology*
- [87] H. Shi, R. Liu, C. Chen, M. Shu and Y. Wang, "ECG Baseline Estimation and Denoising With Group Sparse Regularization," in *IEEE Access*, vol. 9, pp. 23595-23607, 2021, doi: 10.1109/ACCESS.2021.3056459.
- [88] Christos Stergiou and Dimitrios Siganos, "Neural Networks", Pacific Northwest National Laboratory
- [89] Hao Yu, Bogdan M. Wilamowski, "Levenberg-Marquardt Training", 2010, Auburn University
- [90] Albrecht P. S-T segment characterization for long-term automated ECG analysis. M.S. thesis, MIT Dept. of Electrical Engineering and Computer Science, 1983. MIT-BIH ST change Database , DOI:<https://doi.org/10.13026/C2ZW2H>, physiobank.org
- [91] Moody GB, Muldrow WE, Mark RG. A noise stress test for arrhythmia detectors. *Computers in Cardiology* 1984; 11:381-384. MIT BIH Noise Stress Test Database, DOI:<https://doi.org/10.13026/C2HS3T> physiobank.org
- [92] Tabrizi AA, Garibaldi L, Fasana A, Marchesiello S, "Performance improvement of ensemble empirical mode decomposition for roller bearings damage detection", *Shock Vib*. 2015;1-10. *Experimental Shock and Vibration Analysis*. Volume 2015 |Article ID 964805 | <https://doi.org/10.1155/2015/964805>
- [93] Zhang L, Chen H, Li J, Chen W, "New method to solve the end effect of empirical mode decomposition", Paper presented at 2nd International Congress on Image and Signal Processing; Oct 17-19; 2009, Tianjin, China. DOI: 10.1109/CISP.2009.5304936
- [94] Üstündağ, M., Gökbulut, M., Şengür, A. et al. "Denoising of weak ECG signals by using wavelet analysis and fuzzy thresholding. *Netw Model Anal Health Inform Bioinforma* 1,135-140(2012).<https://doi.org/10.1007/s13721-012-0015-5>
- [95] G. Li, X. Zeng, J. Lin and X. Zhou, "Genetic particle filtering for denoising of ECG corrupted by muscle artifacts," 2012 8th International Conference on Natural Computation, 2012, pp. 562-565, doi: 10.1109/ICNC.2012.6234530.
- [96] Zhang D, Cai C, Chen S, Ling L. 2019. An improved genetic algorithm for optimizing ensemble empirical mode decomposition method. *Syst Sci Control Eng*. 7(2):53-63.
- [97] Fabien Soulier., et al., "Very Low Resource Digital Implementation of Bioimpedance Analysis." in *Sensors (Basel)*, MDPI, 2019 Aug 1; 19(15):3381. doi: 10.3390/s19153381
- [98] Jaan Ojarand., et al., "How many frequencies to use in electrical bioimpedance measurements." in book: *Impedance Spectroscopy. Advanced Applications: Battery Research, Bioimpedance, System Design* (pp.161-168), December 2018, Publisher: Walter de Gruyter
- [99] Khalil SF, Mohktar MS, Ibrahim F. "The theory and fundamentals of bioimpedance analysis in clinical status monitoring and diagnosis of diseases". *Sensors (Basel)*. 2014 Jun 19;14(6):10895-928. doi: 10.3390/s140610895. PMID: 24949644; PMCID: PMC4118362.
- [100] R Kusche et al., "Dry electrodes for bioimpedance measurements – Design, characterization and comparison." in *Biomedical Physics & Engineering Express*, IOP, Volume 5, Number 1, October-2018, DOI: 10.1088/2057-1976/aaea59.

- [101] Kalvøy H, Frich L, Grimnes S, Martinsen OG, Hol PK, Stubhaug A. "Impedance-based tissue discrimination for needle guidance". *Physiol Meas*. 2009 Feb;30(2):129-40. doi: 10.1088/0967-3334/30/2/002. Epub 2009 Jan 9. PMID: 19136732.
- [102] Yufera A, Rueda A. "A method for bioimpedance measure with four- and two-electrode sensor systems". *Annu Int Conf IEEE Eng Med Biol Soc*. 2008;2008:2318-21. doi: 10.1109/IEMBS.2008.4649662. PMID: 19163165.
- [103] Xiaoqiu Huang, Duc Nguyen, D. W. Greve and M. M. Domach, "Simulation of microelectrode impedance changes due to cell growth," in *IEEE Sensors Journal*, vol. 4, no. 5, pp. 576-583, Oct. 2004, doi: 10.1109/JSEN.2004.831302.
- [104] I. Gjaever and C. R. Keese, "Use of Electric Fields to Monitor the Dynamical Aspect of Cell Behavior in Tissue Culture," in *IEEE Transactions on Biomedical Engineering*, vol. BME-33, no. 2, pp. 242-247, Feb. 1986, doi: 10.1109/TBME.1986.325896.
- [105] Carvalho TS, Fonseca AL, Coutinho ABB, Jotta B, Pino AV, Souza MN. "Comparison of bipolar and tetrapolar techniques in bioimpedance measurement". *XXIV Congresso Brasileiro de Engenharia Biomédica – CBEB; 2014* [Google Scholar]
- [106] Geddes, L.A., Roeder, R. "Criteria for the Selection of Materials for Implanted Electrodes". *Annals of Biomedical Engineering* 31, 879–890 (2003). <https://doi.org/10.1114/1.1581292>
- [107] Kalvøy H, Johnsen GK, Martinsen OG, Grimnes S. "New method for separation of electrode polarization impedance from measured tissue impedance". *Open Biomed Eng J*. 2011;5:8-13. doi: 10.2174/1874120701105010008. Epub 2011 Feb 4. PMID: 21625369; PMCID: PMC3102312.
- [108] Wang, J. , Hu, W. , Kao, T. , Liu, C. and Lin, S. (2011) "Development of forearm impedance plethysmography for the minimally invasive monitoring of cardiac pumping function". *Journal of Biomedical Science and Engineering*, 4, 122-129. doi: 10.4236/jbise.2011.42018.
- [109] Adel S. Sedra, Kenneth C. Smith, "Microelectronic Circuits", 5th edition Oxford International Student addition.
- [110] Bioelectrical impedance analysis in body composition measurement: National Institutes of Health Technology Assessment Conference Statement. *Am J Clin Nutr*. 1996 Sep;64(3 Suppl):524S-532S. doi: 10.1093/ajcn/64.3.524S. PMID: 8780375.
- [111] G. B. Clayton, "88 Practical Opamp Circuits", 5th edition Oxford International Student addition.
- [112] ICL 8038 datasheet
- [113] Nazanin Neshatvar., et al., "Analog Integrated Current Drivers for Bioimpedance Applications: A Review." in *Sensors (Basel)*, *Pub Med*. 2019 Feb 13;19(4): 756.DOI: 10.3390/s19040756
- [114] Kim, Sun I., and Tae S. Suh. "Current Source for Wideband Electrical Bioimpedance Spectroscopy Based on a Single Operational Amplifier." *World Congress of Medical Physics and Biomedical Engineering 2006 August 27 - September 1, 2006COEX Seoul, Korea. Berlin Heidelberg: Springer-Verlag., 2007.*
- [115] Biopotential Amplifiers in "The Biomedical Engineering Handbook" (2000) by Joachim H. Nagel edited by Joseph D. Bronzino
- [116] Qu, Minghai; Zhang, Yujian; Webster, J.G.; Tompkins, Willis J., "Motion Artifact from Spot and Band Electrodes During Impedance Cardiography," in *Biomedical Engineering, IEEE Transactions on*, vol.BME-33, no.11, pp.1029-1036, Nov. 1986.
- [117] "25 years of impedance plethysmography" *BARC Newsletter No.236*, September 2003
- [118] Divyesh L Prajapati, Chintan V Parmar, Pradnya A Gokhale, Hemant B Mehta, Chinmay J Shah, "Non-Invasive Assessment of Blood Flow Index In Healthy Volunteers Using Impedance Plethysmography". *International Journal of Medical and Health Sciences* ISSN 2277-4505
- [119] Tushar Kanti Bera, "Bioelectrical Impedance Methods for Non-invasive Health Monitoring: A Review." in *J Med Eng*. 2014; 2014: 381251. Published online 2014 Jun 17. doi: 10.1155/2014/381251. PMCID: PMC4782691, PMID: 27006932
- [120] M. Amini, 1,* J. Hisdal,2 and H. Kalvøy3, "Applications of Bioimpedance Measurement Techniques in Tissue Engineering." in *J. Electrical Bioimpedance*. 2018 Jan; 9(1): 142–158. doi: 10.2478/joeb-2018-0019.

AUTHOR'S BIOGRAPHY



RAJESH BIROK,
Associate Professor,
Department of Electronics & Communication Engineering,
Delhi Technological University, Delhi, India
Email: rbirok@dtu.ac.in

RAJESH BIROK received his Bachelor of Technology (B. Tech) and Master of Technology (M. Tech) in Electronics and Communication Engineering both from Regional Engineering College, Kurukshetra (Now National Institute of Technology-Kurukshetra), Haryana, India in the years 1995 and 2000 respectively. Presently, he is working as Associate Professor, in the Department of Electronics & Communication Engineering, Delhi Technological University, Delhi, India-110042 since December-2009. His research interests include Biomedical Signal Measurement and Analysis, Communication Systems, Wireless Communication etc.

